# THESIS APPROVAL

## GRADUATE SCHOOL, KASETSART UNIVERSITY

Master of Science (Chemistry)
**DEGREE**

Chemistry                                Chemistry
**FIELD**                                **DEPARTMENT**

**TITLE:**   A Study of Relationship between the Ca/Si Ratio and
             Structural Properties of Calcium Silicate Hydrate (C-S-H) Gel

**NAME:**   Mr. Chutrin  Arunruviwat

**THIS  THESIS  HAS  BEEN  ACCEPTED  BY**

_____**THESIS  ADVISOR**
(       Assistant Professor Surachai  Thachepan, Ph.D.       )

_____**DEPARTMENT  HEAD**
(     Associate Professor Waraporn  Parasuk, Dr.rer.nat.     )

**APPROVED  BY  THE  GRADUATE  SCHOOL  ON**  _____

_____ **DEAN**
(  Associate Professor Gunjana  Theeragool, D.Agr.  )

THESIS

A STUDY OF RELATIONSHIP BETWEEN THE Ca/Si RATIO AND
STRUCTURAL PROPERTIES OF CALCIUM SILICATE HYDRATE (C-S-H) GEL

CHUTRIN  ARUNRUVIWAT

A Thesis Submitted in Partial Fulfillment of
the Requirements for the Degree of
Master of Science (Chemistry)
Graduate School, Kasetsart University
2015

Chutrin Arunruviwat 2015: A Study of Relationship between the Ca/Si Ratio and Structural Properties of Calcium Silicate Hydrate (C-S-H) Gel. Master of Science (Chemistry), Major Field: Chemistry, Department of Chemistry. Thesis Advisor: Assistant Professor Surachai Thachepan, Ph.D. 81 pages.

The present study investigated a relationship between Ca/Si ratio and structural properties of calcium silicate hydrate (C-S-H) gels. The structure of C-S-H was characterized by fourier transform infrared (FTIR) spectroscopy, X-ray diffraction (XRD) and $^{29}$Si magic angle spinning nuclear magnetic resonance ($^{29}$Si MAS-NMR) spectroscopy. FTIR analysis revealed that the type of silicate species in the C-S-H gel depended on the Ca/Si ratio. The results suggested that the structure of the C-S-H synthesized at low Ca/Si ratio was similar to silica gel, whereas the sample synthesized at high Ca/Si ratio contained high proportion of silicate chains. Both XRD and $^{29}$Si MAS-NMR confirmed phase and structure of the synthesized samples which were consisted of different silicate structures of C-S-H gel, namely, $Q^1$, $Q^2$, $Q^3$ and $Q^4$. The structure of magnesium silicate hydrate (M-S-H) gel was studied. The results showed that the structure of the M-S-H was similar to C-S-H, but no $Q^1$ silicate species was observed in its structure at high Mg/Si ratio. Furthermore, mixed silicate species between C-S-H and M-S-H were observed in the sample synthesized by using mixed hydroxides of calcium and magnesium. Finally, the FTIR analysis of the hydrated cement showed the component of calcium and magnesium in its structure. The results suggested the significant role of cation in advancing the formation of silicate chains, which could be of general interest in understanding the formation behavior of silicate species in cement and related materials.

_____     _____     ___ / ___ / ___
     Student's signature              Thesis Advisor's signature

# ACKNOWLEDGEMENTS

I wish to express my sincere gratitude to my advisor, Assistant Professor Dr. Surachai Thachepan for his unwavering support and continuously valuable guidance throughout the duration of my graduate study and research. I would not have achieved this if I did not get the support that I have always received from him. I also wish to express my appreciation to Professor Dr. Supapan Saraphin and Assistant Professor Dr. Songwut Suramitr for worthy suggestions. Additionally, I am also appreciated to Mr. Thammanoon Thaweechai, a graduate student in Physical chemistry field, for the advantageous suggestion on my research.

Finally, I wish to express my great appreciation and my gratitude to my family for their hard work, advice, encouragement, understanding and the financial assistance, which made my graduate study possible and I would like to thank all of my friends who make through both happiness and difficulties together.

Chutrin Arunruviwat

March, 2015

# TABLE OF CONTENTS

**Page**

# LIST OF TABLES

# LIST OF FIGURES

# LIST OF FIGURES (Continued)

# LIST OF FIGURES (Continued)

# LIST OF FIGURES (Continued)

# LIST OF FIGURES (Continued)

# LIST OF ABBREVIATIONS

| | | |
|---|---|---|
| a.u. | = | Atomic unit |
| TEOS | = | Tetraethyl orthosilicate |
| DI water | = | Deionized Water |
| C-S-H | = | Calcium silicate hydrate |
| M-S-H | = | Magnesium silicate hydrate |
| FTIR | = | Fourier transform infrared spectroscopy |
| XRD | = | X-ray diffraction |
| $^{29}$Si MAS-NMR | = | $^{29}$Si magic angle spinning nuclear magnetic resonance spectroscopy |
| XANES | = | X-ray absorption near edge spectroscopy |
| SEM | = | Scanning electron microscopy |
| TEM | = | Transmission electron microscopy |
| $Q^0$ | = | Silicate ($SiO_4^{2-}$) monomer |
| $Q^1$ | = | 1 atom of Si form bond with the silicate ($SiO_4^{2-}$) |
| $Q^2$ | = | 2 atom of Si form bond with the silicate ($SiO_4^{2-}$) |
| $Q^3$ | = | 3 atom of Si form bond with the silicate ($SiO_4^{2-}$) |
| $Q^4$ | = | 4 atom of Si form bond with the silicate ($SiO_4^{2-}$) |
| Å | = | Angstrom (unit of length) |
| nm | = | Nanometer |
| $cm^{-1}$ | = | Reciprocal centimeter or inverse centimeter |
| rpm | = | Revolutions per minute |
| $^o$C | = | Celsius |

# A STUDY OF RELATIONSHIP BETWEEN THE Ca/Si RATIO AND STRUCTURAL PROPERTIES OF CALCIUM SILICATE HYDRATE (C-S-H) GEL

## INTRODUCTION

Cement is one of the cheapest and most common construction-materials that has been widely used in the building and construction industry. Nowadays, with an increasing global population and economic growth there is more and more demand for food, drugs, and habitat. So, the cement industry has increased manufacture of its product to meet the demand. The synthesis cement production process requires a lot of energy to create the cement powder. $CO_2$ is also emitted during cement production; for every ton of Portland cement manufactured, approximately one ton of $CO_2$ release (Lodeiro *et al.*, 2009). Current and future research is focused on developing the manufacturing process of cement and improving the composition of cement. There are several ways that can be done such as developing and increasing efficiency in the cement production process, studying the factors affect to strength and composition structure of cement for developing clinker and searching for new additives to improve properties and enhance quality of cement. This research is study the factors that affect to cement structure, leading to the development of environmental friendly cement with less carbon loading in the future.

Cement consists of 3 major parts as clinker, gypsum and additives. All components are blended and heated to high temperature. The process of heating releases $H_2O$ and $CO_2$ and then causes other reactions between solids, including partial melting. The clinkers are essential for a good cement production, but the cement manufacture is used a widely variety of minerals, including calcium oxide, silica, alumina, iron oxide, magnesium oxide, titanium dioxide, and others. However, the most important minerals in cement product are calcium oxide and silica.

The cement paste was created from a mixing of cement powder and water. However it might simple to prepared, the cement hydration process have complex chemical reactions, which are still not understand this mechanism (Odler, 1998). Cement hydration reaction have affected by many factors such as the composition of the clinker, the ion species, the surface of the mixture, the initial water/cement powder ratio, the temperature, and the additives (Odler, 1998; Jackson, 1998). The main component after hydration is calcium silicate hydrate (C-S-H), constituting 60-70% of hydrated cement (Dolado *et al.*, 2007). The stoichiometric composition of C-S-H usually depends on various factors such as the starting materials, calcium/silicon (Ca/Si) ratio, pH and temperature. It is also believed that the continuous formation of C-S-H phases during hydration is responsible for impressive strength and properties of hardened cement. The C-S-H consists of calcium, silicon, oxygen and other elements such as magnesium and aluminum which are the most important to the structure of cement product, but it are not confirm the exact ratio of Ca/Si or other element in cement. Generally, the Ca/Si ratio of C-S-H gel in Portland cement is accepted in the range around 0.7-2.3 which depends on the type and amount of precursors used in the preparation of cement (Cong and Kirkpatrick, 1996; Dolado *et al.*, 2007). The natural structure of C-S-H such as tobermorite and jennite have been used extensively as a model for study the molecular structure of C-S-H in the cement (Figure 1). These minerals are characterized by layers of polymerized silicon oxide cross-linked with calcium or calcium hydroxide.
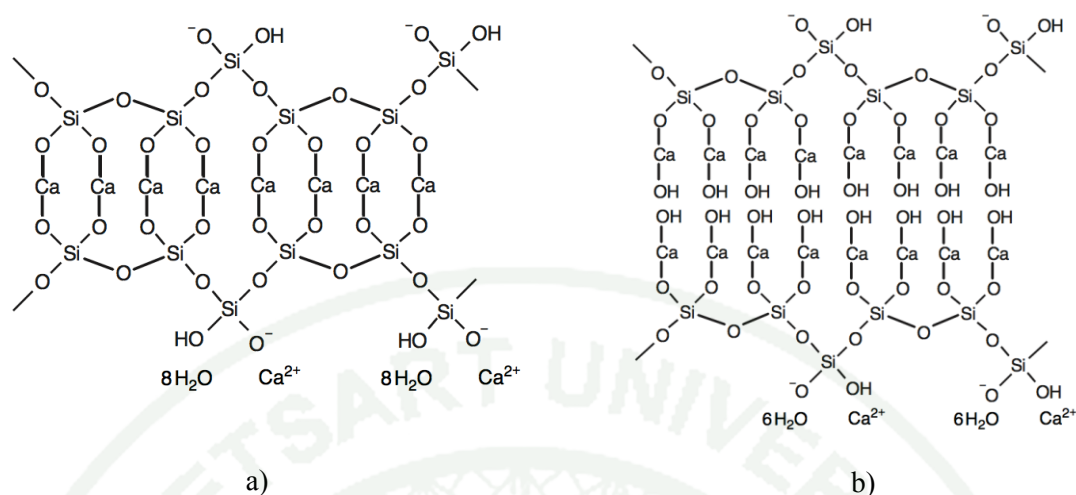
**Figure 1** Structure of calcium silicate hydrate a) Tobermorite and b) Jennite

**Source:** MacLaren *et al.* (2003)

The structures of tobermorite and jennite contain layers of silicate chains and calcium oxide (tobermorite) or calcium hydroxide (jennite) as shown in Figure 1. The calcium layer of tobermorite and jennite suggested that both amount and type of calcium components has affected to the C-S-H structure, which the calcium oxide layer of tobermorite showed the amount of calcium ion in the structure less than the calcium hydroxide layer of jennite. Besides, C-S-H structure shows the silicon tetrahedral unit $((SiO_4)^{4-})$ connected with the layers of $Ca^+$ or $Ca(OH)_2$ while the basic structure of silica gel shows the silicon tetrahedral unit, connecting with the other unit as a network structure.

The objective of this work presented in my thesis is the synthesis and characterization of silica gel and C-S-H. Silica gel was synthesized under acidic and basic condition via dehydration and condensation reaction. C-S-H sample was synthesized by using silicon and calcium as a starting material via the same reaction with silica gel. Tetraethyl orthosilicate (TEOS) and sodium metasilicate ($Na_2SiO_3$) was used a silicon source, and calcium hydroxide ($Ca(OH)_2$) and magnesium hydroxide ($Mg(OH)_2$) was used calcium and cation source. Additionally, this work studied the relationship between the ratio of cation/silicon and the C-S-H structure. The changes in

molecular structure associated with changing in starting materials and Ca/Si ratio or cation/silicon ratio are analyzed by various techniques. The primary technique of characterization is Fourier transform infrared (FTIR) spectroscopy, X-ray diffraction (XRD), and $^{29}$Si magic angle spinning nuclear magnetic resonance ($^{29}$Si MAS-NMR) spectroscopy.

# OBJECTIVES

There are three main objectives of this work which were

1. To prepare and characterize calcium silicate hydrate (C-S-H) and magnesium silicate hydrate (M-S-H) gel

2. To study the relationship between the (Ca or Mg)/Si ratio and the structure of calcium silicate hydrate (C-S-H) and magnesium silicate hydrate (M-S-H) gel

3. To study the effect of cation species between calcium and magnesium ions on the structure

# LITERATURE REVIEW

This section mentioned a review of works done by some previous researchers on preparation methods and characterization techniques of calcium silicate hydrate (C-S-H) gel.

The main component of Portland cement is calcium hydroxide, aluminates and unhydrated clinker. When the cement powder is mixed with water, the crystalline portlandite and amorphous nanostructured hydration product called calcium silicate hydrate gel or C-S-H gel were obtained. The chemical composition and molecular structure of C-S-H gel are important for many properties of concrete. The C-S-H structure has been studied extensively since the first structural models were presented in 1952 (Richardson, 2008) but the structure has been difficult to characterize. However, more advanced techniques such as Fourier transform infrared (FTIR) spectroscopy, X-ray diffraction (XRD) spectroscopy, and $^{29}$Si magic angle spinning nuclear magnetic resonance ($^{29}$Si MAS-NMR) spectroscopy have aided much in studying the structure of C-S-H.

Several models for the molecular structure of C-S-H have been proposed, which widely portray it as a non-crystalline calcium oxide layer and silicate chains (Richardson, 2008). These models behave in ways that resemble naturally occurring tobermorite and jennite. The structure of C-S-H gel is silicate chains attached to a calcium oxide layer, which is a similar to the layered structure of clay (Figure 2). So it is evident that the major factors affecting the strength of the structure is a long chain of silicate and layer of calcium oxide.
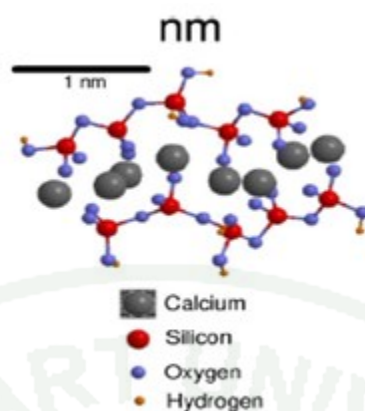
**Figure 2** The structure of C-S-H gel at the nanometer scale, which is a chain of
silicate with calcium oxide layers was inserted

**Source:** Ayuela *et al.* (2007)

The variability of the Ca/Si ratio in C-S-H gel has produced many slightly
different models. It has been suggested that the Ca/Si ratio of tobermorite and jennite
are 0.83 and 1.5, respectively. Hydrated cement has Ca/Si ratio between 1.2 and 2.1
(Richardson, 1999). Taylor *et al*. (1956) suggested that the Ca/Si ratio of tobermorite
model can be raised above 0.88 by the removal of bridging silica tetrahedral and
replacement by calcium ions in the interlayer. Taylor (1986) continued to develop his
earlier work in modeling the structure of C-S-H by proposing a model that is composed
of structural components of jennite and 1.4 nm tobermorite. The range in the Ca/Si ratio
was explained by removal of the bridging silicate tetrahedral, and was linearly
proportional to the reciprocal of the silicate chain length. Cong and Kirkpatrick (1996)
proposed a defect of tobermorite structure similar to 1.4 nm tobermorite. These defects
stem from the removal of the bridging silica tetrahedra and it being displaced and
rotated relative to the Ca-O layer.

Ayuela *et al.* (2007) proposed a model of C-S-H by simulations with quantum
chemical methods and studied the silicate chain. The results showed that the ionic
species in the structure has an important role in the generating chain silicates and then
the silicate chain as a stabilized structure will consist of m atoms of Si by m = 3n - 1

when n = 1, 2, 3, ... So, The possibility of creating cement higher performance exists by adding silica nanoparticles.

Allen *et al.* (2007) studied the composition and density of nanoscale calcium silicate hydrate (C-S-H) gel in cement and suggested the chemical formula of C-S-H particle is $(CaO)_{1.7}(SiO_2)(H_2O)_{1.80}$ including density is 2.604 Mg m$^{-3}$ by using techniques of small-angle neutron, X-ray scattering and hydrogen/deuterium neutron isotope effect studied the composition. After that using this results study to describe the chemically active surface area in cement, and distribution of water in the nanoscale structure of C-S-H gel particle (Figure 3).
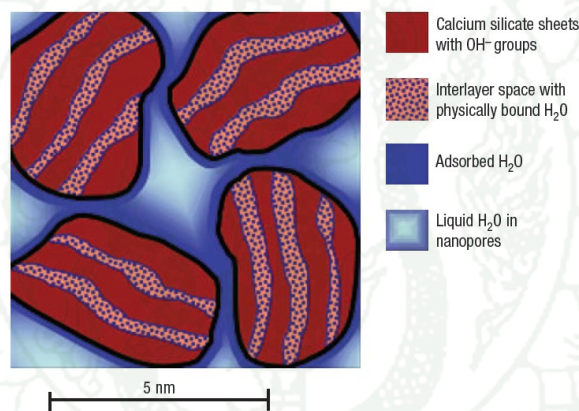


**Figure 3** The schematic diagram of the nanoscale structure of C-S-H gel particle

The Ca/Si ratio has an effect on the structure of C-S-H will consider the change in the Ca/Si ratio by omitting bridging silica tetrahedral and adding interlayer of $Ca^{2+}$ when the Ca/Si ratio is increased (Richardson, 2007). Grutzeck *et al.* (1989) synthesized C-S-H sample with Ca/Si ratios between 0.00 and 1.31 via reaction of fumed silica and calcined $CaCO_3$ in water. At lower Ca/Si ratios (below 0.12), the samples consisted of $Q^3$ and $Q^4$ silicate species at -100.7 ppm and 114.5 ppm as measured by using $^{29}$Si magic angle spinning nuclear magnetic resonance ($^{29}$Si MAS-NMR) spectroscopy. For the sample at the 0.12 Ca/Si ratio, $Q^3$ and $Q^4$ silica tetrahedral were still present and appeared a new peak at -85.0 ppm which was assigned to $Q^2$ silicate species. At 0.91

Ca/Si ratio showed a small shoulder attributed to $Q^1$ silicate species, indicating the end of a silicate chain. At higher Ca/Si ratios (above 1.07), the samples contained only peaks attributable to $Q^2$ and $Q^1$ silicate species.

Faucon *et al.* (1997) used the molecular dynamics simulations and $^{29}$Si MAS-NMR spectroscopy for study structure of C-S-H. The C-S-H sample was synthesized by vary ratio of Ca/Si from 0.66 to 0.83. The result of synthesized C-S-H with Ca/Si ratio at 0.83 showed that about 15% of $Q^1$ silicate species in structure and Si-Ca distance is much shorter than sample with Ca/Si ratio at 0.66 because the oxygen atoms that bonded to the bridging silica tetrahedral of sample with Ca/Si ratio at 0.66 were hydroxylated. The Ca/Si ratio at 0.83, $Ca^{2+}$ in the interlayer creates a charge deficit with the oxygen atoms that bonded to the bridging silica tetrahedral which oxygen atoms that were not shared with other tetrahedral. So, this is a result of the rupture of the silicate chain, subsequent hydroxylation of the silica tetrahedral, and formation of $Q^1$ environments in the structure of C-S-H.

Kirkpatrick *et al.* (1997) studied the structure of C-S-H by Raman spectroscopy. The Raman spectra of C-S-H sample showed the peaks of Si-O stretching, Si-O-Si bending, internal deformation of the Si-O tetrahedral and Ca-O polyhedral, and some characteristic peaks at lower frequencies. The spectra of jennite and 14Å tobermorite were quite similar by confirmed the result from NMR which showed $Q^2$ silicate species in the structure. For synthesized C-S-H with Ca/Si ratios between 0.88 and 1.45, Raman spectra were consistent with a defect tobermorite model which corresponded with NMR result. In addition, The Raman spectra of synthesized C-S-H with Ca/Si ratios below 1.0 were very similar to those of 14Å tobermorite. At Ca/Si ratios above 1.0, C-S-H samples showed substantial concentrations of both $Q^1$ and $Q^2$ silicate species, indicating the possible presence of jennite environments. The results also confirmed that the structure of jennite was dominated by silicate tetrahedral with $Q^2$ silicate species.

Khouchaf *et al.* (2009) reported medium- and short-range orders change of amorphous silica as a result of chemical degradation. Structural changes were studied by X-ray absorption near edge structure (XANES), $^{29}$Si MAS-NMR spectroscopy, and

controlled pressure scanning electron microscope (CP-SEM). The depolymerization of amorphous $SiO_2$ compounds mainly induced the formation of $Q^3$ silicate species and appear the diffusion of calcium and potassium inside the structure. XANES and NMR result showed that $SiO_2$ tetrahedrons, which formed the starting silica network, were mostly affected. Micro-XANES spectra showed the presence of a mixture of silicon environments with four oxygen atoms and lower than four atoms. NMR results showed that $Q^3$ and $Q^2$ silicate species were principally formed after the depolymerization of the $Q^4$ silicate species that presented in the starting amorphous $SiO_2$.

Dolado *et al.* (2007) studied the molecular dynamics simulations of C-S-H by varying Ca/Si ratio between 0.7 and 2.0. It was found that the presence of $Ca^{2+}$ atoms decreases the rate of polymerization of the silica chain corresponding with the number of $Q^0$ silicate species decreases more slowly when the Ca/Si ratio is increased. The simulation of C-S-H with Ca/Si ratio at 0.7 showed 15% of $Q^3 + Q^4$ silica tetrahedral environments and that proportion decreased when increasing the Ca/Si ratio. C-S-H with Ca/Si ratio at 0.79 showed that the ($Q^3+Q^4$) decreases linearly when the Ca/Si ratio is increased. Whereas, the nonlinear forms of C-S-H with Ca/Si ratio at 2.0 were disappeared. Thus, these results indicate that the calcium ions were concluded to enforce the formation of linear structures in the polymerization of $Si(OH)_4$.

Lodeiro *et al.* (2012) synthesized C-S-H sample with Ca/Si ratios between 0.39 and 1.54 by using double decomposition of sodium silicate and calcium nitrate. All samples showed that substantial carbonation occurred except for those with Ca/Si ratio at 1.02 and 1.54. The samples with Ca/Si ratio between 0.65 and 0.65 showed $^{29}Si$ MAS-NMR signal at -83 ppm which was assigned to the $Q^2$ silicate species. At higher Ca/Si ratios, samples also showed intensity in this range, and a peak could be identified due to overlap peaks of $Q^2$ and $Q^1$ silicate species at -85 and -78 ppm, respectively. In the two samples were not appear the carbonated, and showed that the mean chain length (MCL) of the silicate chain was 4.68 and 3.02 silica tetrahedral for Ca/Si ratios of 1.02 and 1.54, respectively.

Kim *et al.* (2013) synthesized C-S-H sample with Ca/Si ratios between 0.9 and 1.5 by extracting calcium oxide (CaO) from calcium carbonate ($CaCO_3$) and mixed with silica ($SiO_2$) and deionized water. The stoichiometric formula of the synthesized C-S-H were approximated as $C_{0.7}SH_{0.6}$, $C_{1.0}SH_{0.8}$ and $C_{1.2}SH_{2.4}$ for Ca/Si ratios at 0.9, 1.2 and 1.5 respectively. The synthesized C-S-H powders were dried and characterized by X-ray diffraction (XRD) and $^{29}Si$ MAS-NMR spectroscopy. The results suggested that the silicate polymerization of C-S-H increased when decreasing the Ca/Si ratio moreover the C-S-H synthesized at high Ca/Si ratio ($C_{1.2}SH_{2.4}$) showed the high water content in structure. The structure of synthesized C-S-H with varying the Ca/Si ratio indicated the relationship the role of water in enabling good compaction with affect the stiffness of C-S-H

Lodeiro *et al.* (2009) studied the effect of $Na_2O$ on the structure of C-S-H gels by using Fourier transform infrared (FTIR) spectroscopy. The C-S-H samples were synthesized by using calcium nitrate as a calcium source and sodium silicate as a silicon source. The C-S-H samples were control the pH of the solution by using NaOH. At high pH, the precursor transformed to C-S-H gel in the very short term (72 hours). The FTIR result of all synthesized C-S-H showed the $Q^2$ silicate species was the main structure, but the peak attributed to carbonates (calcite) was also found when the synthesized sample with $Na_2O/SiO_2$ ratio was $\geq 4$. Besides, the structure of C-S-H gels showing enhanced carbonation by the amount of alkali and alkali-induced modification of the original C-S-H gel. He continued to study the compatibility between the main product of Portland cement hydration and the main product of the alkali activation of fly ash, C-S-H and N-A-S-H gels, respectively. Both gels were synthesized with laboratory reagents at different pH values. Mixes of the two were synthesized as well, using the sol-gel process. The gels synthesized with this procedure were shown to precipitate together with a silica-rich gel. In addition, the pH level was found to play a determining role in both C-S-H and N-A-S-H gel synthesis. The C-S-H gel was the major phase formed at pH > 11 and N-A-S-H gel for pH > 12.5. The results relating to the joint synthesis of the two (C-S-H and N-A-S-H) gels were not conclusive.

Lodeiro *et al.* (2010) used techniques of Fourier transform infrared (FTIR) spectroscopy, Transmission electron microscopy (TEM) and X-ray diffraction (XRD) to characterize the impacts of alkali and aluminum on cement synthesizing process. The synthesized C-S-H sample (pH value over 13) were mixed with different concentrations of aluminum nitrate and sodium hydroxide. The results showed that both alkali and aluminum increased the degree of silicate polymerization in the C-S-H gels and precipitated a crystalline calcium aluminosilicate phase. The structures of C-S-H gels were similar to those previously observed for alkali-activated slag. These systems had sufficient calcium availability to produce aluminate-substituted C-S-H and an enhanced degree of cross-linking facilitated by aluminates at high pH. However, this enhanced cross-linking appeared to be limited. No silicate connectivity higher than $Q^2$ (possibly $Q^3$) were indicated in the present study.

Mostafa *et al.* (2010) studied the structure of tobermorite samples by using X-Ray diffraction (XRD), Scanning electron microscopy (SEM) and Fourier transform infrared (FTIR) spectroscopy. The samples were synthesized from calcium silicate hydrates with $Fe^{3+}$ and $Mg^{2+}$ substitution under hydrothermal conditions at 175 °C. The results indicated that $Fe^{3+}$ and $Mg^{2+}$ ions played a role in crystallinity, morphology, and structure of synthesized tobermorite. $Mg^{2+}$ ions increased the crystallinity of tobermorite and changed the morphology from platy-shape at 4 hours curing time to lamellar-shape at longer curing times. $Fe^{3+}$ ions increased the imperfection of tobermerite at short curing time. However, they increased the crystallinity at a longer curing time and the morphology of tobermorite changed dramatically from reticulated-shape to fiber-shape. The FTIR result proved that $Fe^{3+}$ and $Mg^{2+}$ increased polymerization of silicate chain and chain cross-linkage consisting of tobermorite lamellar and fiber morphology that grew parallel to the b-axis (along the silicate chains). The cation exchange capacity (CEC) of $Fe^{3+}$ and $Mg^{2+}$ substituted tobermorites was lower than unsubstituted tobermorite. Cross-linkage in the silicate chains was found to cause a reduction in cation exchange capacity.

Pardal *et al.* (2009) synthesized the structure of Al-substituted C-S-H (C-A-S-H) by varying Al/Si and Ca/(Al+Si) ratio. The samples were synthesized from C-S-H (Ca/Si ratio at 0.66 and 0.95) at different weight concentrations in a solution that prepared from the hydration of tricalcium aluminate ($Ca_3Al_2O_6$) in water. XRD and EDX (TEM) analysis showed that the result of pure C-A-S-H was obtained only for calcium hydroxide concentrations below 4.5 mmol/l or Ca/Si ratio of the initial C-S-H is below 1. Otherwise, calcium carboaluminate is also present in the structure. The kinetic of the formation of C-A-S-H was a fast reaction which typically less than a few hours.

Puertas *et al.* (2011) studied the structure of C-A-S-H gel forming in alkali-activated slag (AAS) pastes and compared with the C-S-H gel forming in a Portland cement paste by Fourier transform infrared (FTIR) spectroscopy, $^{29}$Si and $^{27}$Al magic angle solid nuclear magnetic resonance (MASNMR) and Back-scattering scanning electron microscopy (BSE/EDX). The $^{29}$Si NMR result indicated that the structure of C-S-H from hydration of Portland cement was dominated by $Q^1$ silicate species and had a mean chain length (MCL) of 3.80. The C-A-S-H activated with NaOH had high $Q^2$ and low $Q^3$ silicate species contents and showed a MCL of 8.00. In the C-A-S-H activated with waterglass ($Na_2O \cdot nSiO_2 \cdot mH_2O$ + NaOH) had a high amounts of $Q^3$ silicate species and showed a MCL increase to 12.71. In addition, it showed the large amounts of aluminum in the structure. The use of waterglass added silicon to the system had an effect to decrease of Ca/Si ratio of the C-S-H.

Minet *et al.* (2006) synthesized the hybrid organic-inorganic calcium silicate hydrate (C-S-H) gel via a sol-gel process. The C-S-H samples were obtained by precipitation of a mixture of trialkoxysilane (ethyltriethoxysilane, *n*-butyltrimethoxysilane or 3-aminopropyltriethoxysilane) and tetraethoxysilane diluted in $CaCl_2$ ethanol-water solution. The XRD pattern showed an increase of the basal distance of C-S-H with the content of trialkoxysilane which suggested the incorporation of organic moieties in the interlayer. $^{29}$Si NMR result confirmed that trialkoxysilanes such as ethyl- or aminopropylsilane were incorporated in the silicate chains of the C-S-H structure. In the case of highly hydrophobic trialkoxysilanes such as n-

butyltrimethoxysilane, the results suggested that a separation occured between silicates and trialkoxysilanes. This simple approach might offer new opportunities to design new cement based nano- composites by covalently bonding monomer molecules into the interlayer of C-S-H and then proceeding to in-situ polymerization.

The studies reviewed here indicate the possibility of improving the properties of cement for the better by studying the relationship between the structure of C-S-H gel at the nanometer scale with the properties of the cement to be able to predict and design the structure of C-S-H gel as needed, then adjusting the properties of the cement by reducing or adding some elements. This project will study the factors that affect the stability of the C-S-H gel nanostructure and that affect the strength properties of cement. The work of this study covers a variety of factors, including the length of the chain silicate and the layers of calcium oxide and of ionic species. The samples were synthesized in the laboratory to get quality materials and then were tested for their properties.

# MATERIALS AND METHODS

## 1. Chemicals

- Tetraethyl orthosilicate ($Si(OC_2H_5)_4$, Sigma Aldrich)
- Sodium metasilicate ($Na_2SiO_3 \cdot H_2O$, BDH laboratory supplies)
- Sodium hydroxide (NaOH, Carlo Erba)
- Hydrochloric (HCl, Labscan)
- Calcium hydroxide ($Ca(OH)_2$, UNIVAR)
- Magnesium hydroxide ($Mg(OH)_2$, UNILAB)
- De-ionized (DI) water
- Cement powder

## 2. Apparatus

### 2.1  Fourier transform infrared (FTIR) spectroscopy

FTIR was performed using a PERKIN ELMER Spectrum one FTIR spectrometer and KBr disk method. Samples for FTIR were finely ground with desiccated KBr and hydraulically pressed. FTIR spectra were recorded from 4000 to 400 $cm^{-1}$ at a resolution of 4 $cm^{-1}$.

### 2.2  X-Ray Diffraction (XRD)

XRD was performed to identify crystalline phases and observe changes in the unit cell dimensions in the structure. This technique used a BRUKER A8 Advance A25 powder diffractometer with Cu-K$\alpha$ radiation in the theta/theta configuration for measurements. The diffractometer was operated at 40 kV and 40 mA. Measurements were made from 10° to 60° 2θ at a rate of 2 second time/step with a step size of 0.02.

2.3 $^{29}$Si Magic Angle Spinning Nuclear Magnetic Resonance ($^{29}$Si MAS-NMR) spectroscopy

Solid state magic angle spinning nuclear magnetic resonance was performed on samples to characterize the local atomic structure of $^{29}$Si. The $^{29}$Si MAS-NMR technique used a Varian Unity Inova spectrometer operating at 500MHz. Cross-polarization and magic angle spinning (CP/MAS) solid probe and Nano probe were used. Chemical shifts were measured relative to 4,4-Dimethyl-4-silapentane-1-sulfonate acid (DSS).

2.4 Deconvolution

Analysis and deconvolution of FTIR and NMR spectra were performed using the computer program. Spectra were phase and baseline corrected. The deconvolution method was conducted through a computer program used to separating a complex curve into individual curves. The following parameters were adjusted to achieve a good fitting.

## 3. Synthesis

3.1 Silica gel

Silica gel was synthesized either acidic or basic conditions via hydrolysis and condensation reaction. Both reactions have been used primarily for silica synthesis. For the acidic condition, 0.024 mol of tetraethyl orthosilicate (TEOS) was mixed with 1.0M 8.84 ml. of hydrochloric (HCl). The mixture was stirred at room temperature for 24 hours. A clear gel was obtained by vacuum filtration of the reaction mixture, washed repeatedly with de-ionized (DI) water until the obtained filtrate achieved neutral pH, and was dried in an oven at 40°C for 24 hours. For the basic condition, the sample was synthesized similarly to the acid condition, but 1.0M HCl was replaced by 1.0M sodium hydroxide (NaOH).

## 3.2  Calcium Silicate Hydrate (C-S-H) gel

C-S-H samples were synthesized by using tetraethyl orthosilicate (TEOS) as a silicon source and calcium hydroxide (Ca(OH)$_2$) as a calcium source. In a typical synthesis, a stoichiometric amount of the silicon source and calcium source were mixed with de-ionized (DI) water in a closed Teflon reactor under a nitrogen atmosphere (Figure 4). The calcium to silicon (Ca/Si) ratio was varied between 0.1 and 2.0. The silicon source to water molar ratio was kept constant at 20 (Table 1). The reaction mixture was magnetically stirred at 600 rpm at room temperature for 24 hours. Subsequently, the white precipitate products were obtained by vacuum filtration of the reaction mixture, washed repeatedly with DI water until the obtained filtrate achieved neutral pH, and dried in an oven at 40˚C for 24 hours. In addition, another C-S-H sample series were synthesized by using sodium metasilicate (Na$_2$SiO$_3$) as a silicon source replacing TEOS. In synthesis method used the same previously method by varied Ca/Si ratio between 0.1 and 2.0, and Si/Water molar ratio was kept constant at 20 (Table 2).

## 3.3  Magnesium silicate hydrate (M-S-H) gel

M-S-H samples were synthesized by using tetraethyl orthosilicate (TEOS) as a silicon source and magnesium hydroxide (Mg(OH)$_2$) as a magnesium source. The synthesis M-S-H method was like a synthesis method of C-S-H. The amount of TEOS and Mg(OH)$_2$ were mixed with de-ionized (DI) water in a closed Teflon reactor under a nitrogen atmosphere (Figure 4). The Mg/Si ratio was varied between 0.1 and 1.5, and Si/water molar ratio was kept constant at 20 (Table 3). The reaction mixture was magnetically stirred at 600 rpm at room temperature for 24 hours. After that, the white precipitate products were obtained by vacuum filtration of the reaction mixture, washed repeatedly with DI water until the obtained filtrate achieved neutral pH, and dried in an oven at 40˚C for 24 hours.

3.4  Synthesis C-S-H gel by varying the amount of magnesium replaced calcium

The samples were synthesized using TEOS, $Ca(OH)_2$ and $Mg(OH)_2$ as a silicon, calcium and magnesium source, respectively. The method used a same method as C-S-H with Si/Ca ratio at 1.0 but varying % $Mg(OH)_2$ instead $Ca(OH)_2$ from 0% to 100% (Table 4). The mixture was stirred at 600 rpm at room temperature for 24 hours in a closed Teflon reactor under a nitrogen atmosphere (Figure 4). After that, the white precipitate products were obtained by vacuum filtration of the reaction mixture, washed repeatedly with DI water until the obtained filtrate achieved neutral pH, and dried in an oven at 40°C for 24 hours.

**Table 1**  The amount of calcium hydroxide ($Ca(OH)_2$) used for the preparation of C-S-H ratios at Ca/Si ratio between 0.1 and 2.0 by mixing with 0.0240 mole of tetraethyl orthosilicate (TEOS), and 0.4800 mole of de-ionized (DI) water

| Ca/Si | $Ca(OH)_2$ | |
|---|---|---|
| | mole | g. |
| 0.1 | 0.0024 | 0.1778 |
| 0.2 | 0.0048 | 0.3556 |
| 0.4 | 0.0096 | 0.7113 |
| 0.5 | 0.0120 | 0.8891 |
| 0.6 | 0.0144 | 1.0669 |
| 0.8 | 0.0192 | 1.4225 |
| 1.0 | 0.0240 | 1.7782 |
| 1.5 | 0.0360 | 2.6672 |
| 2.0 | 0.0480 | 3.5563 |

**Table 2** The amount of calcium hydroxide (Ca(OH)$_2$) used for the preparation of C-
S-H ratios at Ca/Si ratio between 0.1 and 2.0 by mixing with 0.0240 mole of
sodium metasilicate (Na$_2$SiO$_3$·5H$_2$O,) and 0.4800 mole of de-ionized (DI)
water

| Ca/Si | Ca(OH)$_2$ | |
|---|---|---|
| | mole | g. |
| 0.1 | 0.0024 | 0.1778 |
| 0.2 | 0.0048 | 0.3556 |
| 0.4 | 0.0096 | 0.7113 |
| 0.5 | 0.0120 | 0.8891 |
| 0.6 | 0.0144 | 1.0669 |
| 0.8 | 0.0192 | 1.4225 |
| 1.0 | 0.0240 | 1.7782 |
| 1.5 | 0.0360 | 2.6672 |
| 2.0 | 0.0480 | 3.5563 |

**Table 3** The amount of magnesium hydroxide (Mg(OH)$_2$) used for the preparation of
M-S-H ratios at Mg/Si ratio between 0.1 and 1.5 by mixing with 0.0240 mole
of tetraethyl orthosilicate (TEOS), and 0.4800 mole of de-ionized (DI) water

| Mg/Si | Mg(OH)$_2$ | |
|---|---|---|
| | mole | g. |
| 0.1 | 0.0024 | 0.1400 |
| 0.2 | 0.0048 | 0.2800 |
| 0.4 | 0.0096 | 0.5600 |
| 0.5 | 0.0120 | 0.7000 |
| 0.6 | 0.0144 | 0.8400 |
| 0.8 | 0.0192 | 1.1199 |
| 1.0 | 0.0240 | 1.3999 |
| 1.5 | 0.0360 | 2.0999 |

**Table 4** The amount of calcium hydroxide ($Ca(OH)_2$) and magnesium hydroxide
($Mg(OH)_2$) used for the preparation of C-S-H by magnesium instead calcium
from 0% to 100% by mixing with 0.0240 mole of tetraethyl orthosilicate
(TEOS), and 0.4800 mole of de-ionized (DI) water

| %Mg | $Ca(OH)_2$ | | $Mg(OH)_2$ | |
|---|---|---|---|---|
| | mole | g. | mole | g. |
| 0 | 0.0240 | 1.7782 | 0.0000 | 0.0000 |
| 25 | 0.0180 | 1.3336 | 0.0060 | 0.3500 |
| 50 | 0.0120 | 0.8891 | 0.0120 | 0.7000 |
| 100 | 0.0000 | 0.0000 | 0.0240 | 1.3999 |

N₂ inflow

Open/Close

Cation sources

N₂ outflow

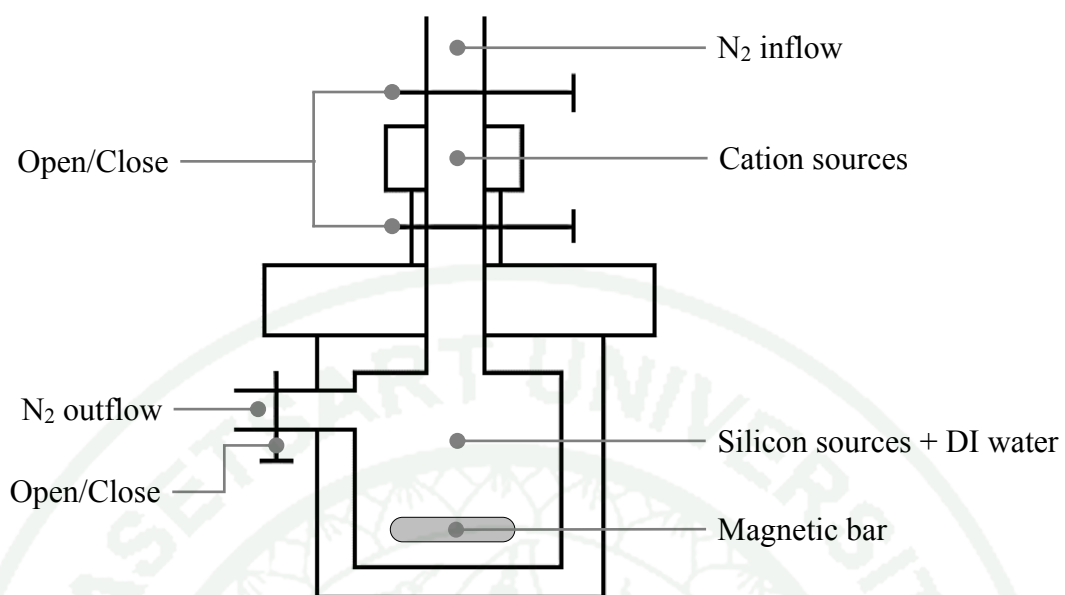Silicon sources + DI water

Open/Close

Magnetic bar

**Figure 4**  Model of Teflon reactor used to synthesize the C-S-H and M-S-H sample

# RESULTS AND DISCUSSION

## 1. Silica gel

The silica gel was synthesized either basic or acidic condition. In basic condition, the addition of sodium hydroxide (NaOH) with stirring to tetraethyl orthosilicate (TEOS) produced a white gel and another sample, the mixture of hydrochloric acid (HCl) and tetraethyl orthosilicate produced a translucent gel when over 24 hour (Figure 5). Upon air drying, both gels turned white and opaque and their volume reduced by approximately 50% due to the loss of water. FTIR analysis of both gels (Figure 6, Table 5) showed similar characteristic absorption bands at 3450, 1645, 1180, 1100, 960, 800 and 467 $cm^{-1}$. The strong and broad peak centered at 1100 $cm^{-1}$ with a shoulder at about 1180 $cm^{-1}$ corresponded to Si-O-Si asymmetric stretching. The peak at 960 $cm^{-1}$ could be assigned to Si-O stretching of the silanol (Si-OH) group. The bands at 800 and 467 $cm^{-1}$ were assigned to Si-O symmetric stretching and O-Si-O bending, respectively. (Olejniczak *et al.*, 2005; Al-Oweini and Ei-Rassy, 2009). The broad band at 3450 $cm^{-1}$ and medium band at 1645 $cm^{-1}$ were due to O-H stretching and H-O-H bending of water molecules, respectively (Al-Oweini and Ei-Rassy, 2009).

Furthermore, the XRD pattern of the samples synthesized under acidic and basic conditions were very similar. Both patterns clearly showed a broad peak at 2theta of 20-30 degree, indicating the amorphous nature of silica sample (Figure 7). The XRD results were consistent with the previous report, which showed similar broad XRD peak for amorphous silica (Musić *et al.*, 2010).
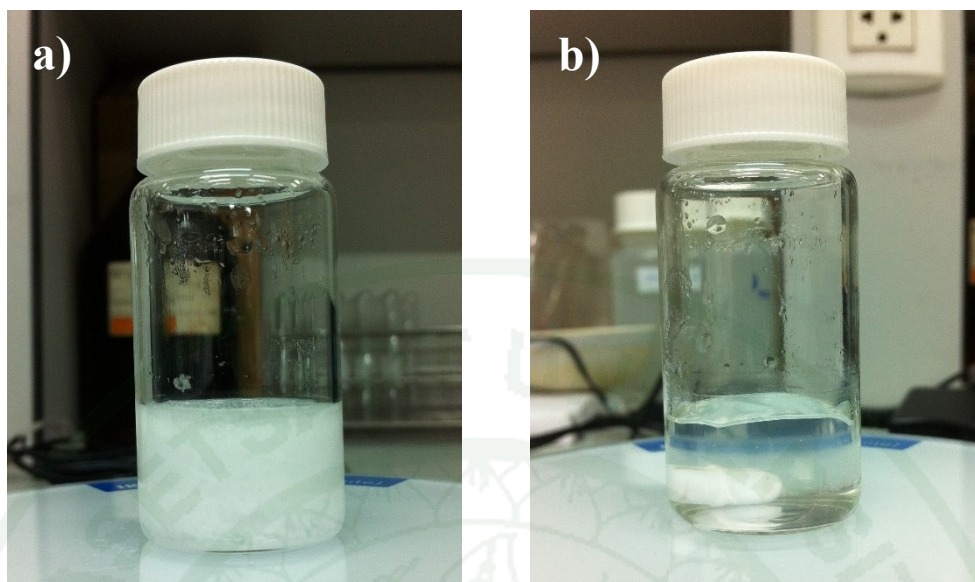
**Figure 5** Images of silica gels synthesized under a) basic and b) acidic condition
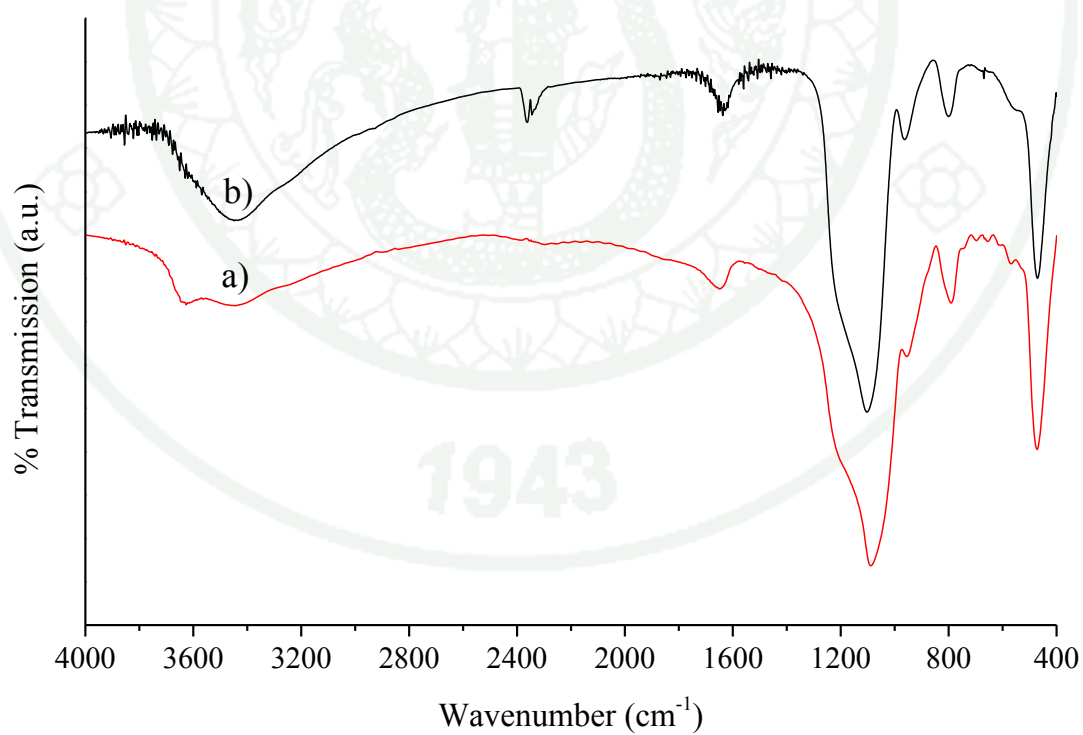


**Figure 6** FTIR spectra of silica gels synthesized under a) basic and b) acidic
condition

**Table 5**  Assignments of the FTIR band of silica gel

| Wavenumber (cm$^{-1}$) | Mode of vibration |
|---|---|
| 3450 | O-H stretching |
| 1645 | H-O-H bending |
| 1180 | Si-O-Si stretching |
| 1100 | Si-O-Si stretching |
| 960 | Si-OH stretching |
| 800 | Si-O stretching |
| 467 | Si-O bending |

**Sources:**  Al-Oweini *et al*. (2009)
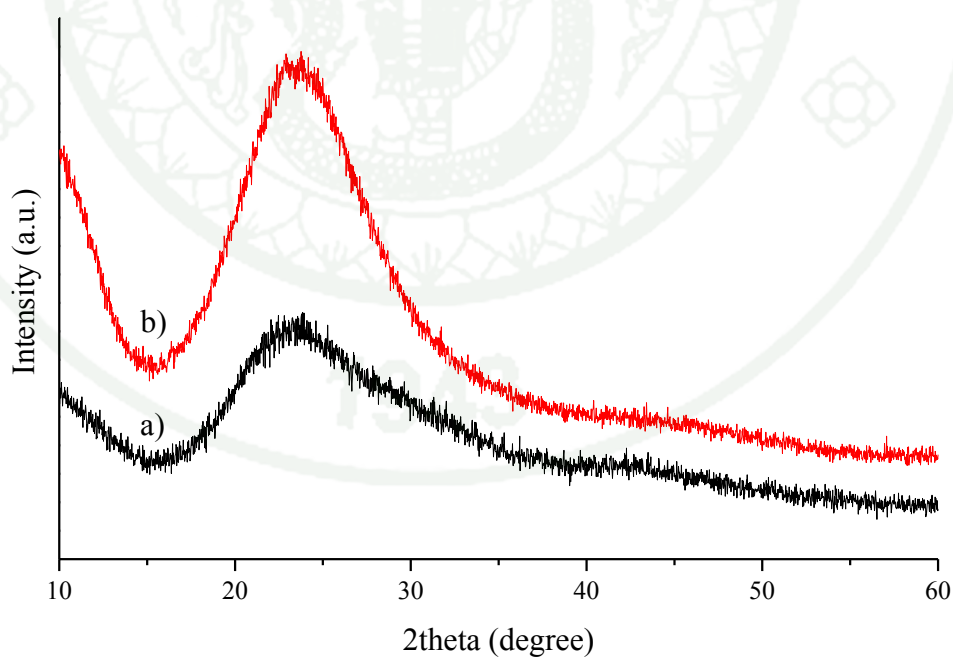


**Figure 7**  XRD patterns of the silica gels synthesized under a) basic and b) acidic condition

## 2. Calcium silicate hydrate (C-S-H) gel

The C-S-H samples were synthesized using tetraethyl orthosilicate (TEOS) as a silicon source and calcium hydroxide ($Ca(OH)_2$) as a calcium source at initial Ca/Si ratios between 0.1 and 2.0. After 24 hours of reaction, the samples become white gel when over 24 hours. Upon air drying, the gel turned white crumbly powder. The amount of each sample will depend on the initial Ca/Si ratio (Figure 8).
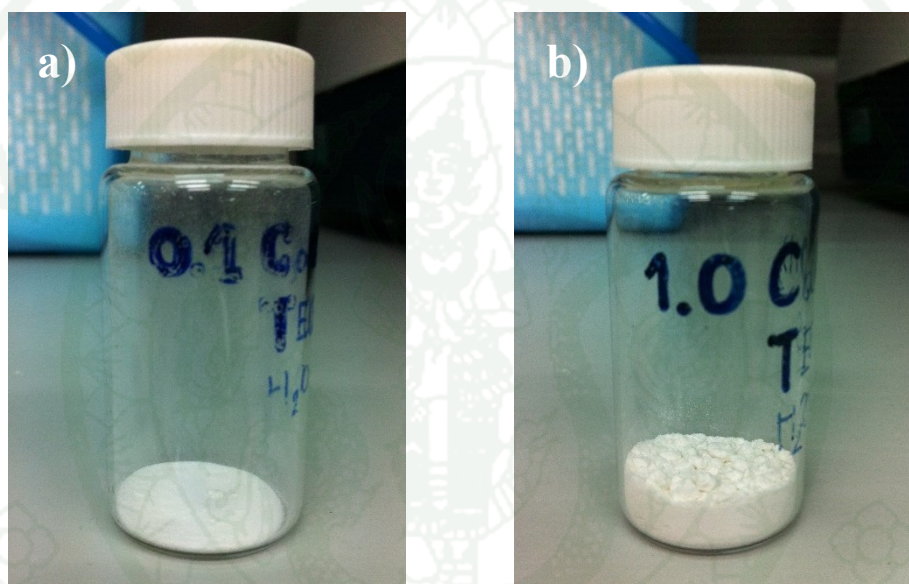


**Figure 8** Images of the C-S-H samples synthesized at Ca/Si ratio of a) 0.1 and b) 1.0

In general, all spectra exhibited similar characteristic absorption signatures of silanol (Si-OH) and siloxane (Si-O-Si) bonds of silicates. FTIR spectra of the C-S-H sample synthesized at the Ca/Si ratio between 0.1 and 2.0 were shown in Figure 9. The absorption bands in the region of 400-800 cm$^{-1}$ were attributed to Si-O bending vibrations ($\delta$) due to the deformation of $SiO_4^{2-}$ tetrahedral. The spectra showed some absorption features differently developed in the region between 400 and 800 cm$^{-1}$ as the Ca/Si ratio increased. The Si-O bending band was observed at 459 cm$^{-1}$ for the C-S-H samples with a very low Ca/Si ratio (0.1-0.2). This band shifted to 455 cm$^{-1}$ for the samples with an intermediate Ca/Si ratio (0.4-0.8) and to 449 cm$^{-1}$ for those with a high

Ca/Si ratio (1.0-2.0), together with a shoulder developed at about 486 cm$^{-1}$. In addition, the intensity of the shoulder at 665 cm$^{-1}$ for the sample with a very low Ca/Si ratio (0.1-0.2) was progressively higher as the Ca/Si ratio increased. Furthermore, the band at 790 cm$^{-1}$ for the sample with a very low Ca/Si ratio (0.1-0.2) decreased in intensity and disappeared at the Ca/Si ratio of approximately 0.4. The concurrent development of the band at 665 cm$^{-1}$ and the disappearance of the band at 790 cm$^{-1}$ as the Ca/Si ratio increased indicated that the C-S-H gel was preferably formed particularly at high Ca/Si ratio.

The absorptions in the range 800-1300 cm$^{-1}$ comprised symmetric and asymmetric Si-O stretching ($\nu$) modes that were overlapped. The complicated broad peak was a result of the structure and vibrational energies of the silicate species. The symbol $Q^n$ ($Q^1$, $Q^2$ …) has been designated for the silicate species, where n is the number of Si atoms, forming bond with the silicate ($SiO_4^{2-}$). The structures of the $Q^n$ silicate species was illustrated in Figure 10 and the corresponding vibrational absorption were tabulated in Table 6.

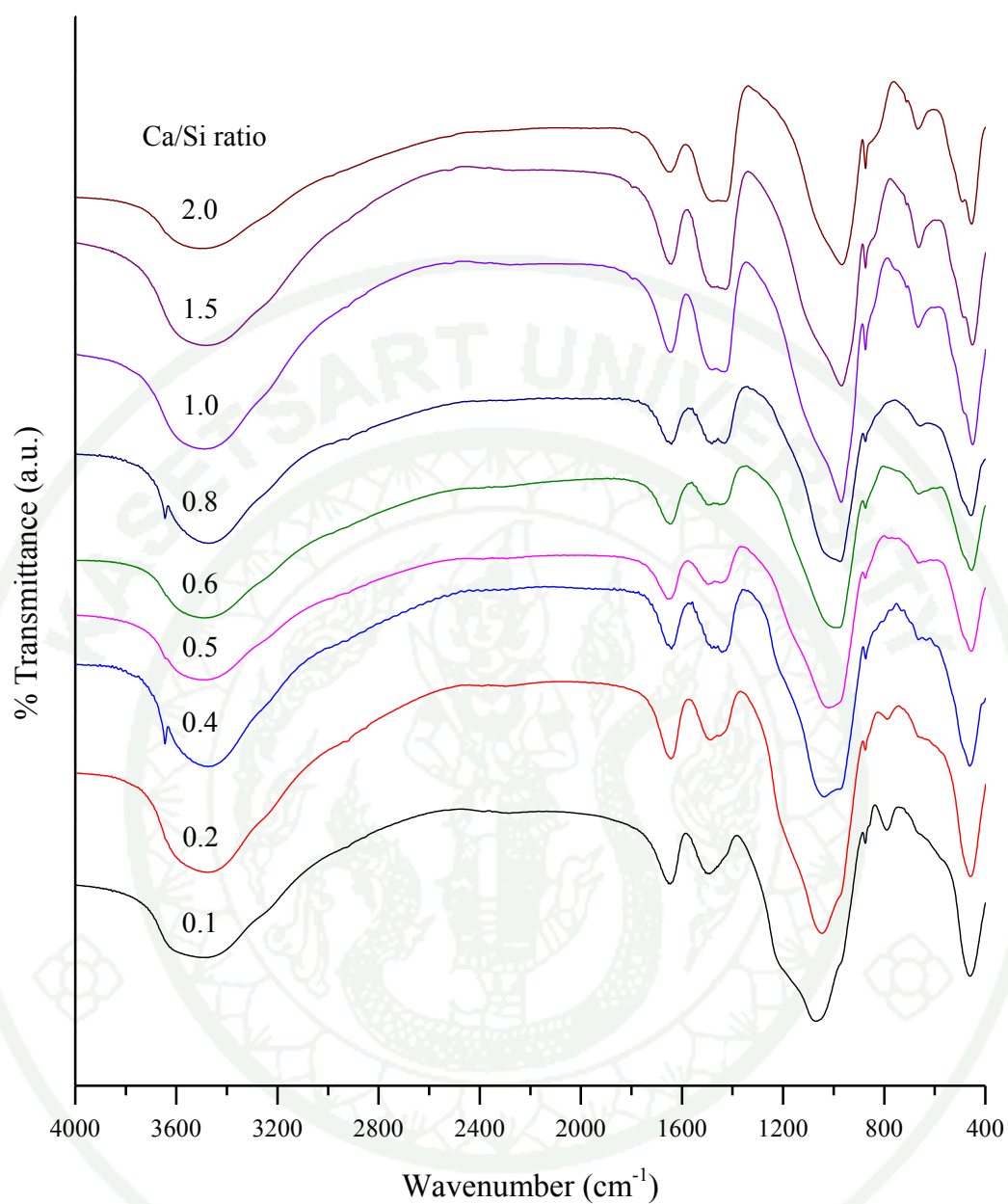**Figure 9** FTIR spectra of the C-S-H samples synthesized with the initial Ca/Si ratio
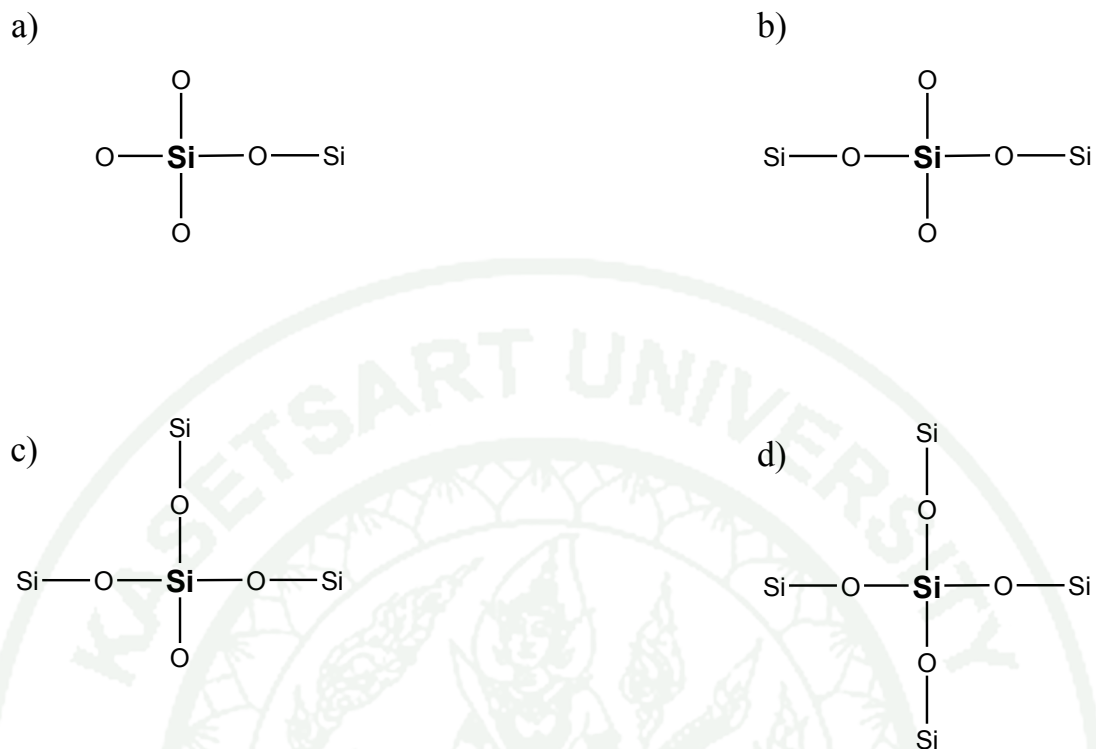between 0.1 and 2.0

a)

b)

c)

d)



**Figure 10**  The structure of the $Q^n$ silicate species a) $Q^1$, b) $Q^2$, c) $Q^3$ and d) $Q^4$

**Source:**  MacLaren *et al.* (2003)

**Table 6** Assignments of the FTIR band of Calcium silicate hydrate (C-S-H) gel

| Absorption (cm$^{-1}$) | Silicate species |
| --- | --- |
| 3450 | O-H stretching |
| 1645 | H-O-H bending |
| 1400-1500 | C-O stretching |
| 1095-1205 | Si-O-Si stretching ($Q^4$) |
| 1030-1060 | Si-O-Si stretching ($Q^3$) |
| 950-970 | Si-O-Si stretching ($Q^2$) |
| 875 | C-O bending |
| 830-860 | Si-O-Si stretching ($Q^1$) |
| 800 | Si-O stretching |
| 467 | Si-O bending |

Detailed analysis of the absorption spectra in the range of 800-1300 cm$^{-1}$ gave fruitful structural information of the silicate species formed. The spectral examination revealed that the characteristic band attributed to the Si-O-Si asymmetric stretching, shifted from 1070 to 970 cm$^{-1}$ as the Ca/Si ratio was increased from 0.1 to 1.0. No further shift of this band was observed for the C-S-H samples with Ca/Si ratio exceeded 1.0, suggesting the resemblance of their structure and Si-O bonding in the C-S-H gels. In order to gain thorough understanding about the bonding in the silica gel and C-S-H, the absorption in this region was deconvoluted and the results were depicted in Figures 11-20. The peak area of the $Q^n$ silicate species obtained from the deconvoluted spectra was listed in Table 7. Apart from the C-O stretching of the carbonate at 860-875 cm$^{-1}$, there were essentially 4 components centred at approximately 830-860, 950-970, 1030-1060 and 1095-1205 cm$^{-1}$, which could be assigned to the Si-O stretching vibrations of the $Q^1$, $Q^2$, $Q^3$ and $Q^4$ silicates, respectively. The fundamentally characteristic $Q^1$ and $Q^2$ components of the silicate chain were typically observed in the

C-S-H. In contrast, the $Q^3$ and especially $Q^4$ were used as evidences to determine the extent of silicate polymerization. A large amount of $Q^4$ indicated a higher degree of structural order for the silicate tetrahedral and the formation of silica gel.

Deconvolution method could be used as a tool to classify the component of the overlapping peak. According to the results from the deconvolution method, the synthesized C-S-H samples could be categorized into two groups, the C-S-H gels with Ca/Si ratio below 0.6 and those with the ratio above 0.6. $Q^1$, $Q^2$, $Q^3$ and $Q^4$ silicate species were found for the C-S-H gels with low Ca/Si ratios (below 0.6). The peak of $Q^3$ silicate species and showed the highest intensity, suggesting that the main structure in this sample. In contrast, the C-S-H gels with a high Ca/Si ratio (above 0.6) showed the $Q^2$ silicate species as a main components but did not show the $Q^4$ silicate species (Figure 21). The deconvolution method efficiently differentiated the $Q^1$, $Q^2$, $Q^3$ and $Q^4$ silicate species in the structure of the C-S-H samples. The missing of the $Q^4$ signal suggested that the decrease of polymerization occurred at high Ca/Si ratio because Si atoms were increasingly replaced by Ca atoms thus the silicate ions could not condense to silicate network. The C-S-H sample with a high Ca/Si showed the $Q^1$ silicate species. In contrast, the C-S-H sample at low Ca/Si showed the $Q^4$ silicate species but not the $Q^1$ species. $^{29}$Si MAS NMR could be used to examine the $Q^n$ silicate species in C-S-H samples because the number of $(SiO_4)^{4-}$ units bonded to each Si center produced a different electron density around the central Si atom. This leads to a more negative chemical shift, relative to tetramethylsilane (TMS). The results of $^{29}$Si NMR were in accordance with the results of FTIR. The signals of $SiO_2$ sample at around -90, -100 and -108 ppm could be assigned to $Q^2$, $Q^3$ and $Q^4$, respectively, indicating a silica network in the structure (Figure 22). While increasing the Ca/Si ratios, the intensity of the $Q^1$ signal at around -80 increase but the intensity of the $Q^3$ and $Q^4$ decreased, suggesting that the condensation to form $Q^3$ and $Q^4$ decrease (MacLaren *et al.,* 2003).

Generally, the hydrolysis and condensation reaction of silicon alkoxide with an acid or a base catalyst yield silica gel ($SiO_2$). The structure of the silica gel can be viewed as a silicon bonded to four oxygen atoms in a tetrahedral unit. When the gel reaction is complete and the silicon atoms become $Q^4$ silicate species. However, the

silica gel possess an imperfect silica network, The $Q^3$ and $Q^2$ silicate species are typically found in the structures.

In the present work, the samples were synthesized using TEOS as a silicon source and the basic sodium hydroxide. The TEOS underwent hydrolysis and condensation to form silica gel. The FTIR results indicated that the samples were mostly composed of $Q^4$, $Q^3$ and $Q^2$ silicate species. The C-S-H samples were synthesized from reaction between TEOS as the silicon source and $Ca(OH)_2$ as the calcium source. The FTIR results showed the differences between the structures of the synthesized silica gel and C-S-H samples and indicated that the structure changed when changing the Ca/Si ratio. Calcium ions appeared to affect the condensation of the silica gel in a way that the influence of the negative charge of the silicate ions formed during the reaction was reduced. As a result, less condensation between the silicate ions occurred. The result from this condensation was a gel with lower structural integrity. Under this condition, the intensity of the signal from the $Q^4$ silicate species decreased but the intensity of the signal from $Q^3$, $Q^2$ and $Q^1$ silicate species increased. Especially when the proportion of calcium increased, the peak area of the signal from the $Q^1$ silicate species became higher compared to experiments without calcium ions.
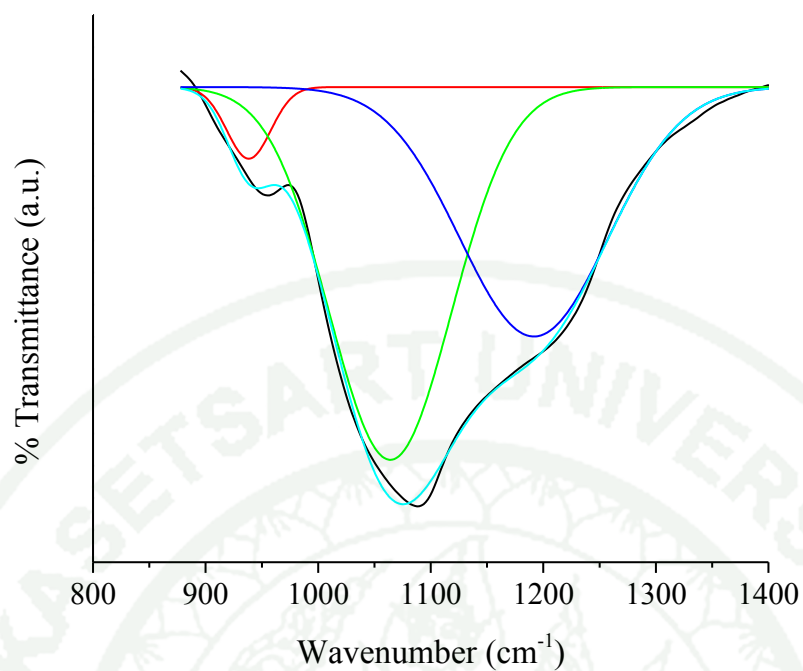
**Figure 11** Deconvoluted spectra of the synthesized $SiO_2$ under basic condition



**Figure 12** Deconvoluted spectra of the synthesized C-S-H with the Ca/Si ratio at 0.1

**Figure 13** Deconvoluted spectra of the synthesized C-S-H with the Ca/Si ratio at 0.2
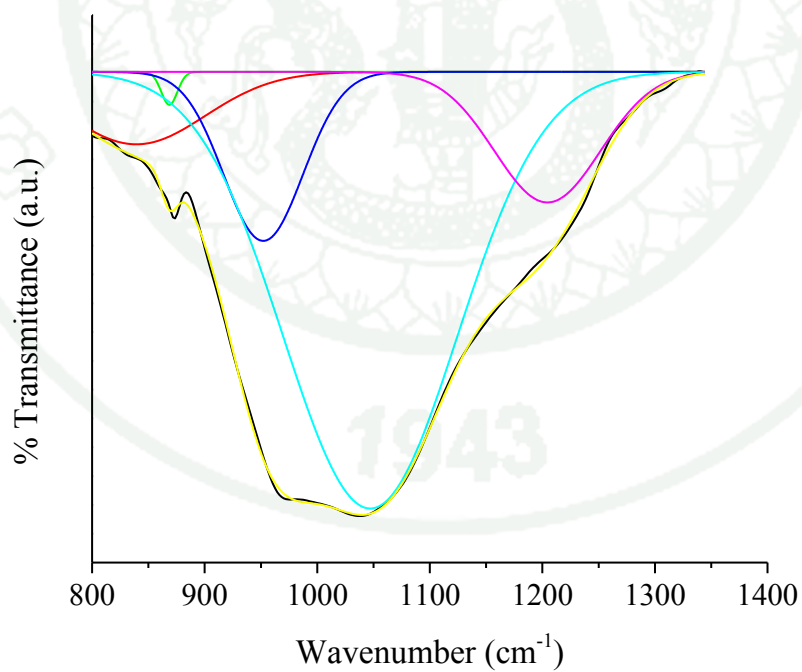


**Figure 14** Deconvoluted spectra of the synthesized C-S-H with the Ca/Si ratio at 0.4

**Figure 15** Deconvoluted spectra of the synthesized C-S-H with the Ca/Si ratio at 0.5



**Figure 16** Deconvoluted spectra of the synthesized C-S-H with the Ca/Si ratio at 0.6
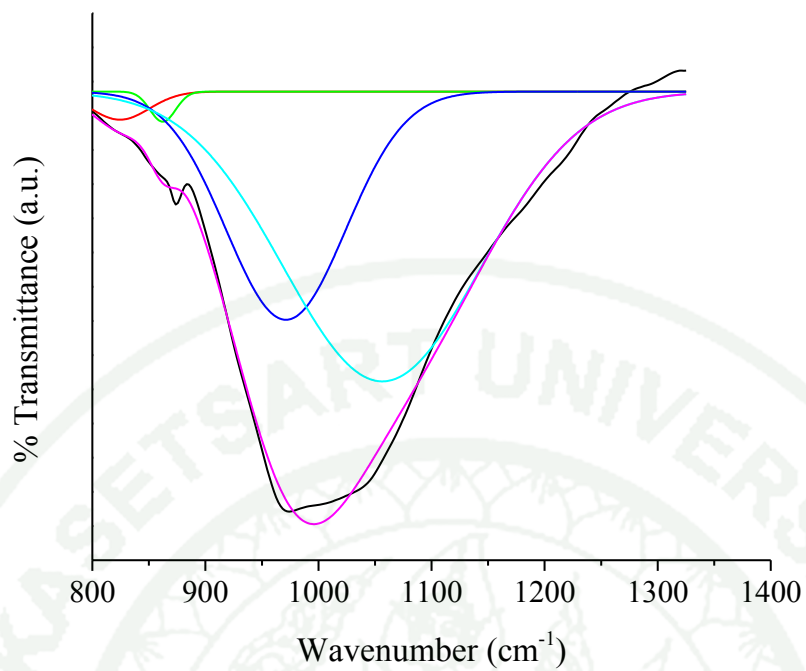
**Figure 17** Deconvoluted spectra of the synthesized C-S-H with the Ca/Si ratio at 0.8
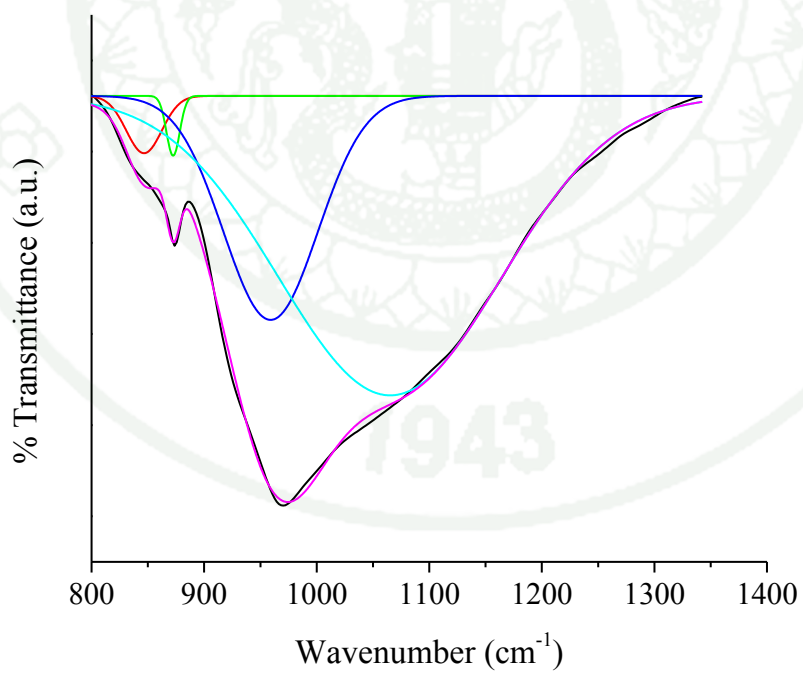


**Figure 18** Deconvoluted spectra of the synthesized C-S-H with the Ca/Si ratio at 1.0
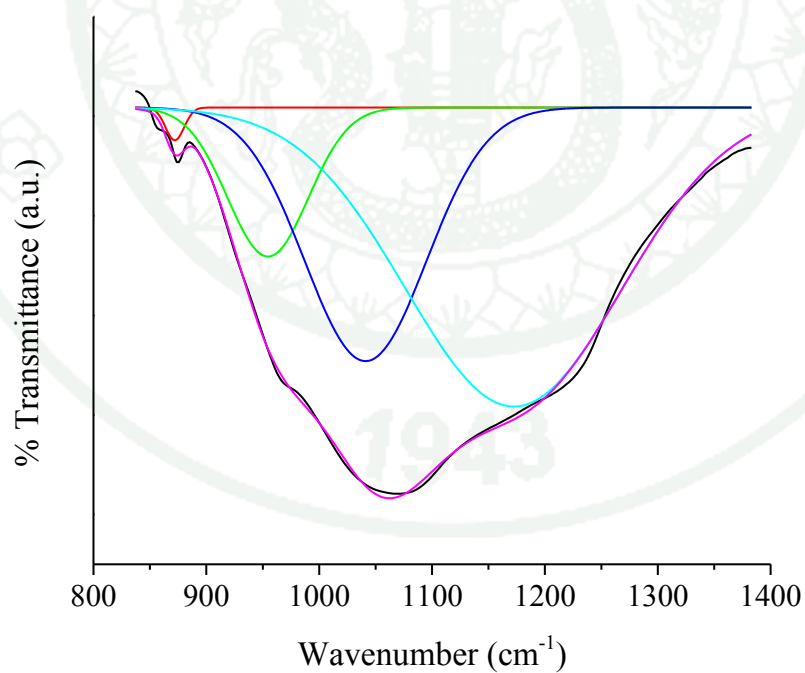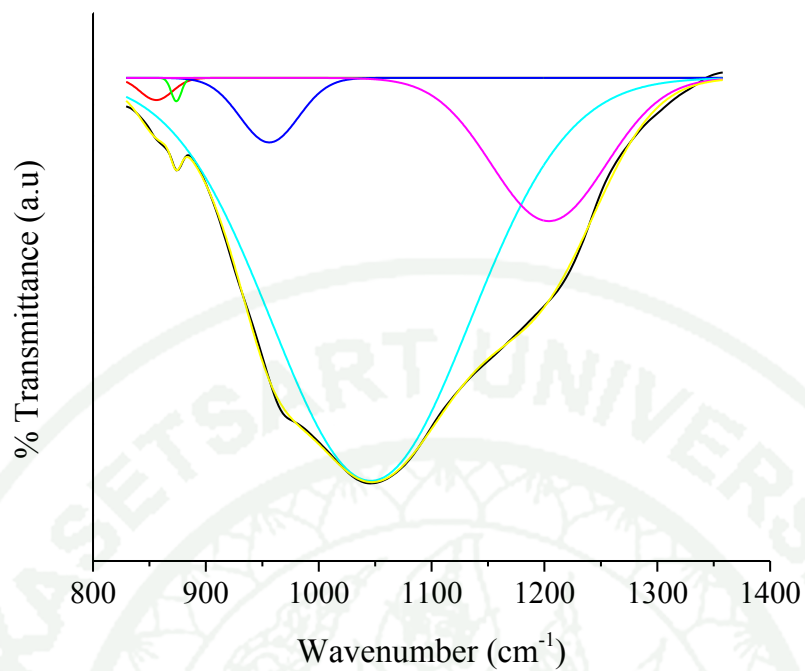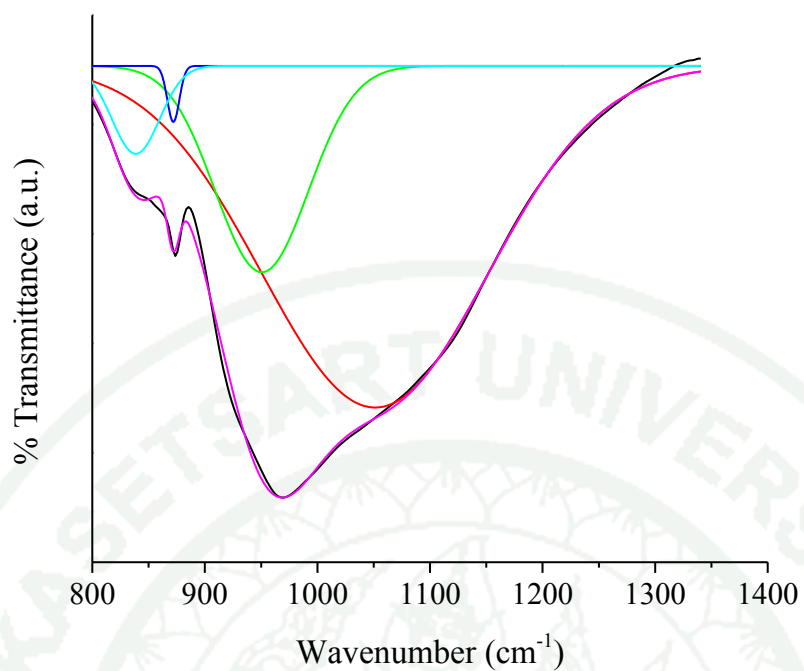
**Figure 19** Deconvoluted spectra of the synthesized C-S-H with the Ca/Si ratio at 1.5
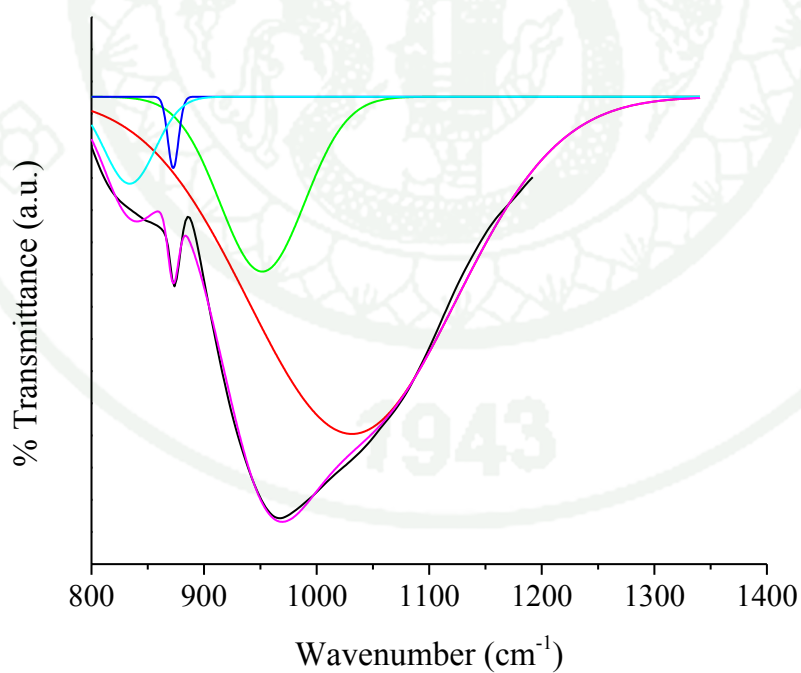


**Figure 20** Deconvoluted spectra of the synthesized C-S-H with the Ca/Si ratio at 2.0
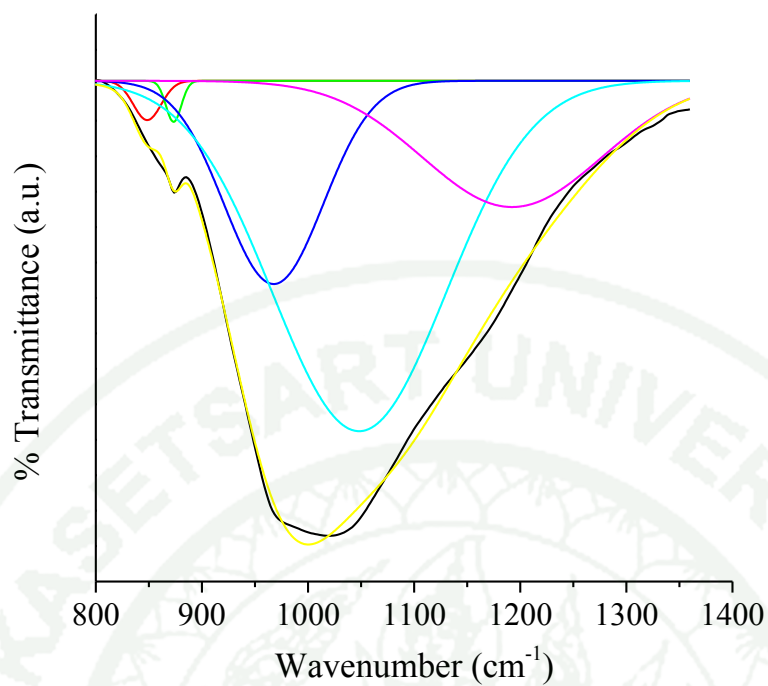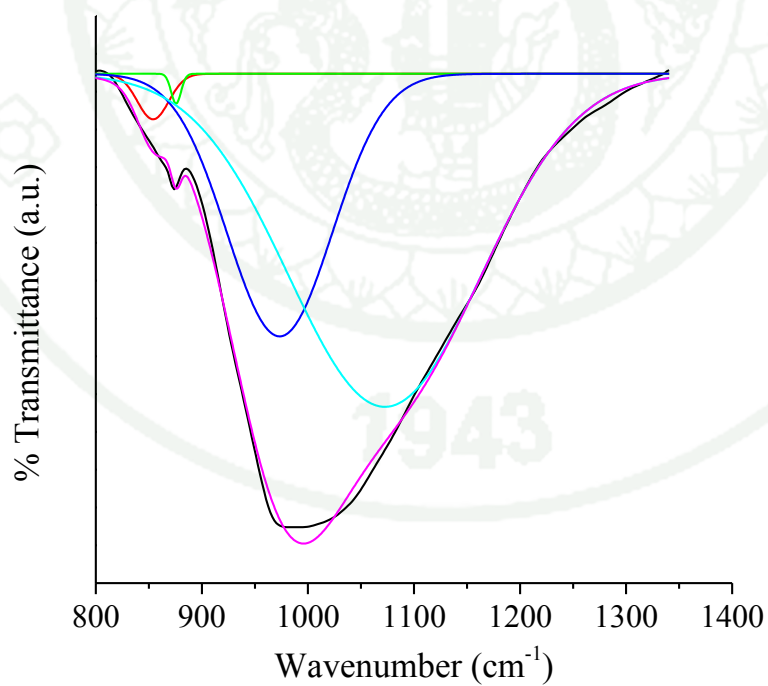
**Table 7** Peak area from the deconvolution FTIR spectra of the synthesized calcium
silicate hydrate (C-S-H) gel (Figure 11-20)

| Ca/Si ratio | Silicate species | | | |
|---|---|---|---|---|
| | $Q^1$ | $Q^2$ | $Q^3$ | $Q^4$ |
| 0.0 | | 0.04 | 0.53 | 0.43 |
| 0.1 | | 0.11 | 0.29 | 0.60 |
| 0.2 | 0.01 | 0.04 | 0.79 | 0.16 |
| 0.4 | 0.09 | 0.12 | 0.67 | 0.12 |
| 0.5 | 0.01 | 0.21 | 0.57 | 0.21 |
| 0.6 | 0.02 | 0.30 | 0.69 | |
| 0.8 | 0.02 | 0.32 | 0.66 | |
| 1.0 | 0.02 | 0.24 | 0.74 | |
| 1.5 | 0.04 | 0.19 | 0.77 | |
| 2.0 | 0.05 | 0.17 | 0.78 | |
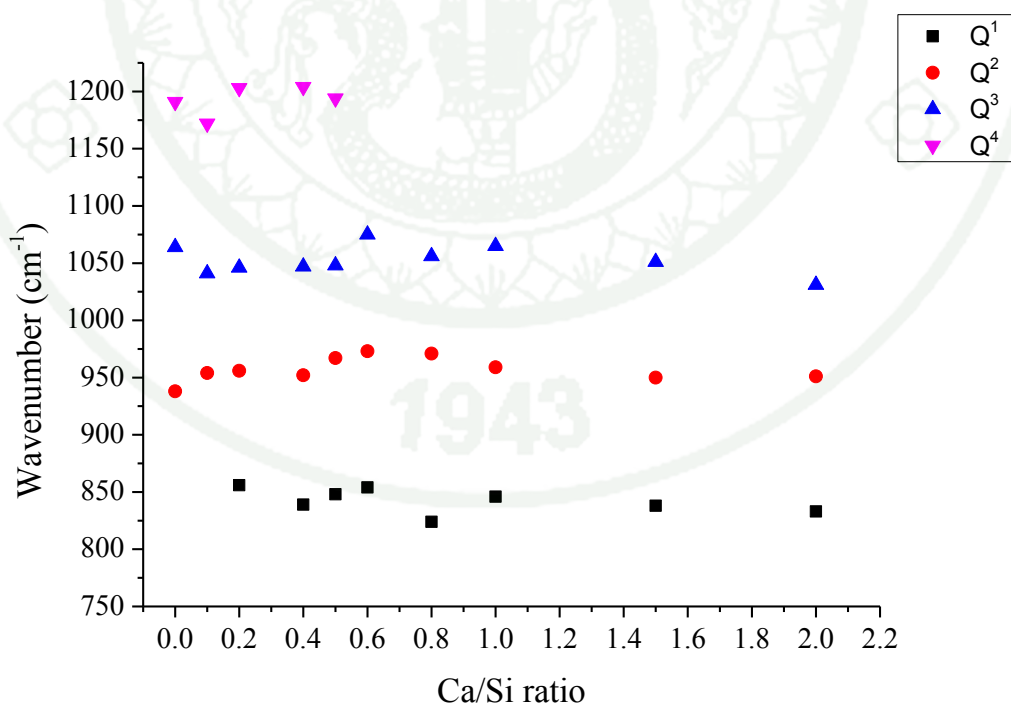


**Figure 21** Composition-dependent shift of deconvoluted components of synthesized
C-S-H sample with initial Ca/Si ratio between 0.1 and 2.0
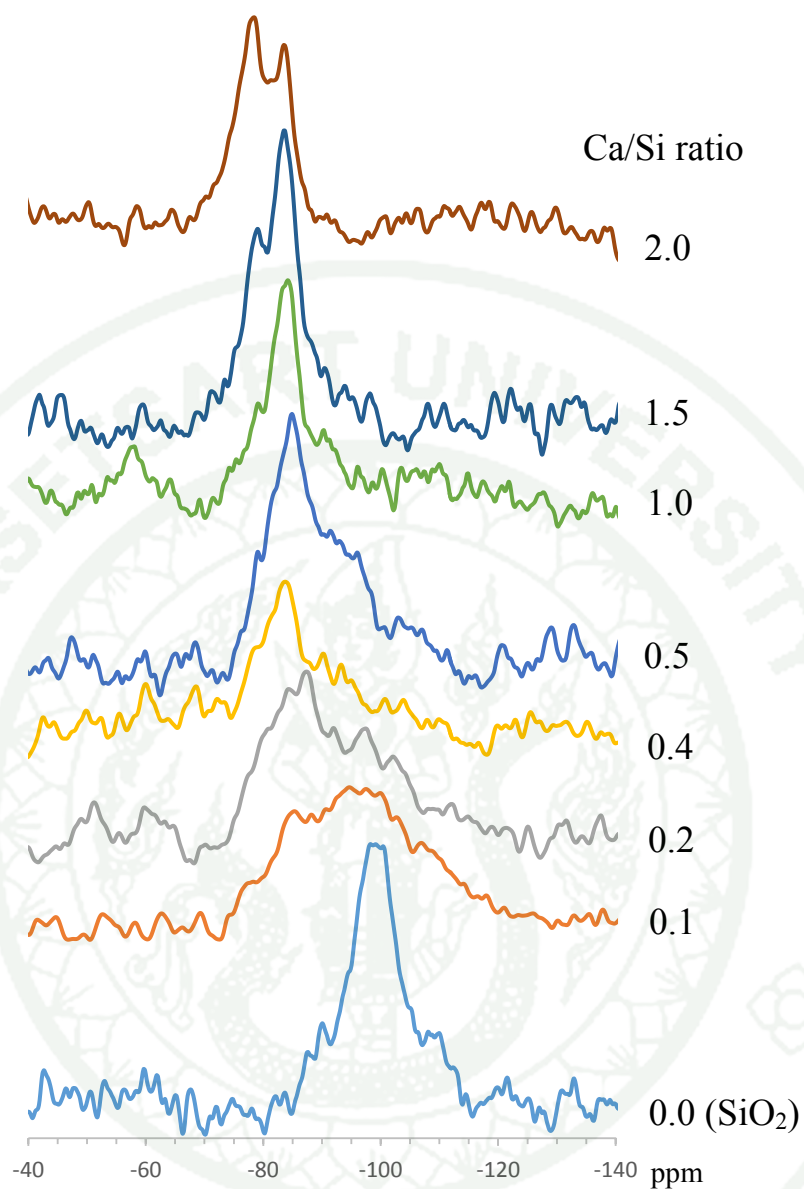
**Figure 22** $^{29}$Si MAS NMR spectra of $SiO_2$ and C-S-H samples synthesized with
initial Ca/Si ratio between 0.1 and 2.0

The absorption in the range 3300-3600 $cm^{-1}$ was a result of the O-H stretching vibration of the $H_2O$ molecules at the surface or in the structure of the C-S-H. The signal of $H_2O$ molecules could be confirmed by an absorption at 1650 $cm^{-1}$. The absorption in this range could be the result of the O-H bond of Si-OH group which were located at the surface of the product or the hydroxyl group of $Ca(OH)_2$ because the absorptions were in the same range. The sharp band at 3650 $cm^{-1}$ was assigned to the stretching vibration of bulk O-H group of calcium hydroxide. The strong band between 1400-1500 $cm^{-1}$ and the sharp band at 875 $cm^{-1}$ were ascribed to asymmetric stretching and out-of-plane bending of carbonate, respectively. The appearance of the carbonate indicated that the carbonation process readily occurred despite the use of deionized and decarbonated water and the inert nitrogen atmosphere during the synthesis. The carbonation possibly occurred during the washing process, which was carried ambient temperature and pressure.

The XRD technique is a popular technique used to characterize the property of crystal. XRD pattern of silicate gel clearly showed a broad peak at 2theta around 20-30 degree, demonstrating the amorphous phase of silica. XRD pattern of the synthesized C-S-H showed similar sharps peak and positions (Figure 23), suggesting the same crystallinity of sample. The pattern were consisted of calcium silicate hydrate (C-S-H) peaks overlapped with the calcium hydroxide and calcium carbonate peaks. The calcium carbonate could be occur from reaction of excess calcium and carbon dioxide. The XRD pattern of synthesized C-S-H at 29, 32 and 50 degree were consistent with the XRD database of calcium silicate hydrate (C-S-H) in the JCPDS card of 33-0306, supporting with the FTIR result. Moreover, the small broad peak around 20-30 degree of amorphous silica appeared in the C-S-H sample and decreased when Ca/Si ratio was increased. It indicated that the possibility of the higher crystallinity of the synthesized sample when the $Q^4$ silicate species reduced but the $Q^2$ silicate species increased. In addition, the XRD results exhibited the peak of $CaCO_3$ at 23, 29, 36, 39, 43 and 47 degree and $Ca(OH)_2$ at 18, 34, 47 and 51 degree.
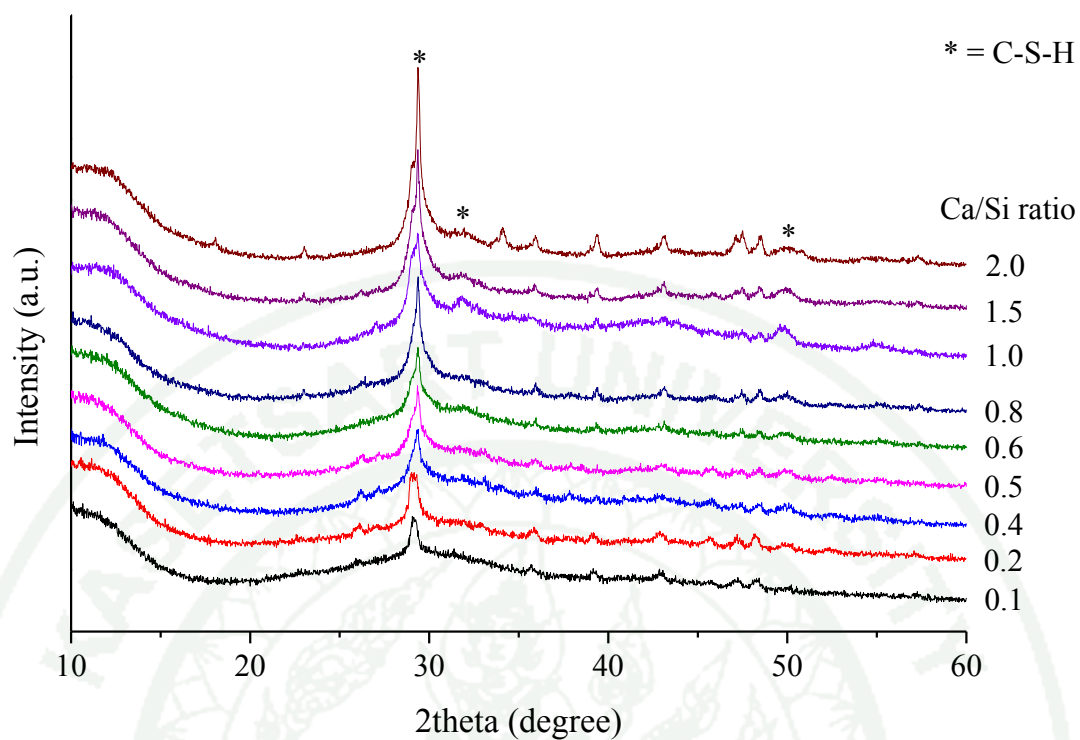
**Figure 23** XRD patterns of C-S-H samples synthesized with initial Ca/Si ratio
between 0.1 and 2.0

**3. Calcium silicate hydrate (C-S-H) by using sodium metasilicate as a silicon source and calcium hydroxide as a calcium source**

The C-S-H sample was synthesized with the same method in previous section but using sodium metasilicate ($Na_2SiO_3$) as a silicon sources instead in order to study the effect of changing a silicon source on the formation silicate. The synthesized C-S-H were white gel in 24 hours and changed to white crumbly powder when dried. The amount of sample will depend on the initial Ca/Si ratio which was similar to the C-S-H synthesized using TEOS (Figure 24).

Analysis of the synthesized C-S-H at the Ca/Si ratio between 0.1 and 2.0 by FTIR techniques (Figure 25) showed that the characteristic absorption bands were almost similar to the C-S-H synthesized using TEOS. The absorption range of 400-800 cm$^{-1}$ were attributed to Si-O bending vibrations ($\delta$) of $SiO_4^{2-}$ tetrahedral. When increasing the Ca/Si ratio, the absorption at 500 cm$^{-1}$ separated into two peak at 450 and 500 cm$^{-1}$. The peak at 670 cm$^{-1}$ was due to the symmetric stretching vibration of Si-O-Si.



**Figure 24**  Images of the C-S-H samples synthesized using $Na_2SiO_3$ at Ca/Si ratio a) 0.1 and b) 1.0

**Figure 25** FTIR spectra of the C-S-H samples synthesized using $Na_2SiO_3$ with the initial Ca/Si ratio between 0.1 and 2.0

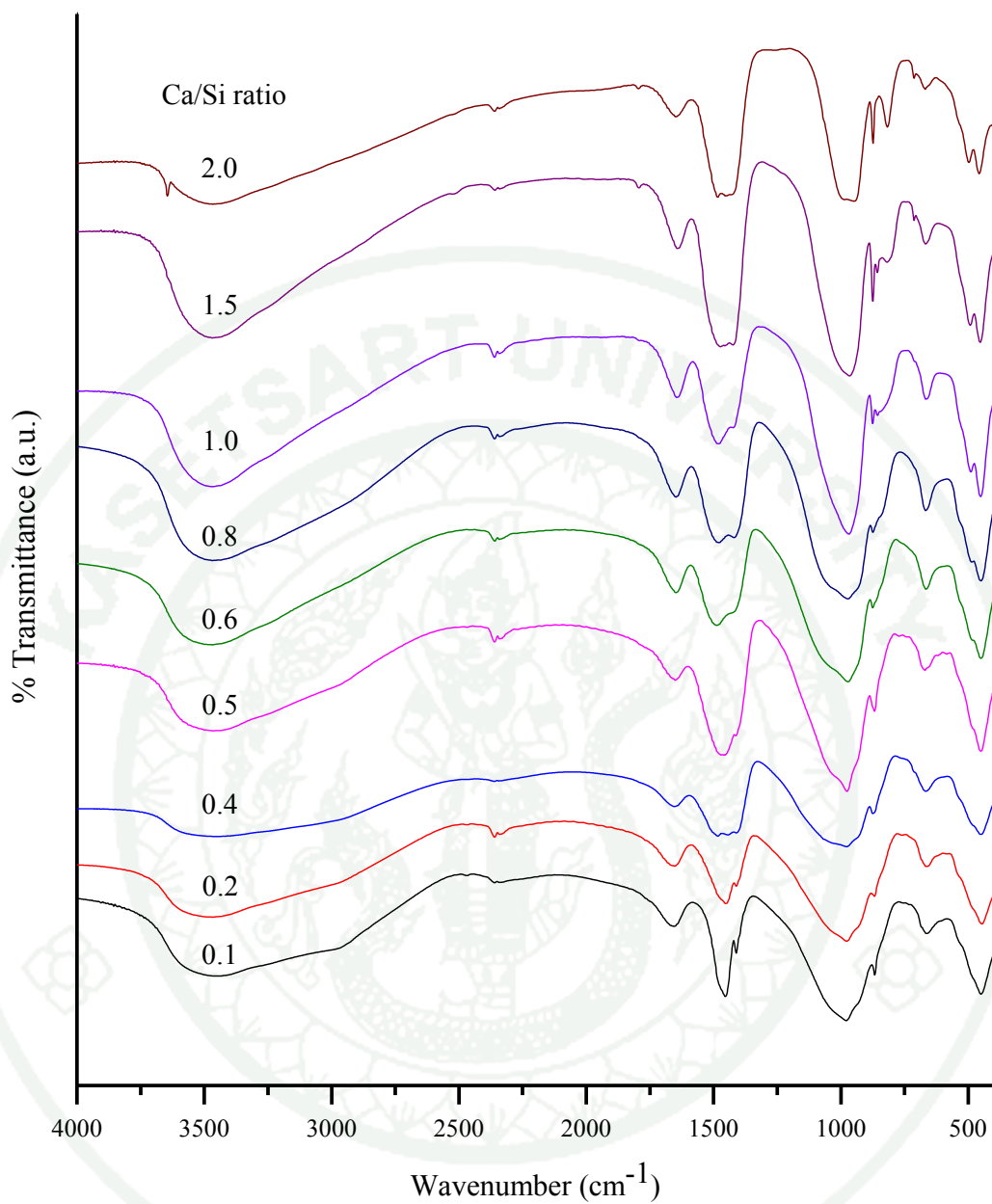The absorption in the range at 800-1300 $cm^{-1}$ typically showed the overlapping of both symmetric and asymmetric Si-O stretching ($v$) vibrations. The signals appearing at about 870 $cm^{-1}$ corresponded to C-O stretching ($v$) vibrations of the calcium carbonate. In order to gain thorough understanding about the Si-O bonding in the $Na_2SiO_3$ and C-S-H, the spectra in this region were deconvoluted (Figures 26-35). The peak area of the $Q^n$ silicate species obtained from the deconvolution method was listed in Table 8 and the deconvolution spectra were shown in Figure 36.

The complex absorption band was deconvoluted into its relevant components. The synthesized C-S-H samples could be categorized into two groups, the C-S-H gels with Ca/Si ratio below 1.0 and those with the ratio above 1.0. The $Q^3$ and $Q^2$ silicate species in the structure of $Na_2SiO_3$ precursor could be hydrolyzed into $Q^2$, $Q^1$ and $Q^0$ silicate species and condensed into $Q^3$ and $Q^4$ silicate species. So, the peak of all silicate species appeared in the synthesized C-S-H sample with Ca/Si ratio below 1.0. The high peak of $Q^3$ silicate species was a main structure in this sample, indicating the high $SiO_2$ content and more polymerization. Whereas, $Q^1$, $Q^2$ and $Q^3$ silicate species were observed for those with Ca/Si ratio above 1.0 and showed the peak of $Q^1$ and $Q^2$ silicate species increased when increasing Ca/Si ratio. The missing of the $Q^4$ signal of the synthesized C-S-H at high Ca/Si ratio (above 1.0) suggested that the negative charge of silicate ion was reduced by cation while the substrate was hydrolyzed and condensation. As a result, the intensity of the signal from the $Q^4$ silicate species decreased whereas the intensity of the signal from $Q^2$ and $Q^1$ silicate species increased. The $Q^1$ peak was the evidence for progressive decrease of silicate polymerization.

Moreover, the sodium ion was able to reduce the influence of the negative charge of the silicate ions similar to the calcium ion. In the case of silica gel, sodium hydroxide (NaOH) was used to synthesize silica under basic condition. FTIR spectra appeared the peak of $Q^4$, $Q^3$ and $Q^2$ silicate species in the structure but showed the different intensity peak of silicate species when compared with the synthesized silica under acid condition. The spectra were deconvoluted to classify and describe the intensity of silicate species. The deconvoluted spectra of the synthesized silica gel under basic condition showed the peak area of $Q^2$ silicate species more than the synthesized

silica gel under acid condition in Figure 37, suggesting the effect of sodium ion. In the case of C-S-H synthesized by using sodium metasilicate ($Na_2SiO_3$) as the silicon source, FTIR spectra showed the $Q^4$, $Q^3$, $Q^2$ and $Q^1$ silicate species in the structure, but C-S-H synthesized by tetraethyl orthosilicate (TEOS) as a silicon source only showed the $Q^4$, $Q^3$ and $Q^2$ silicate species at low Ca/Si ratio. The appearance of $Q^1$ silicate species in the sample derived from $Na_2SiO_3$ showed the effect to reducing the negative charge of the silicate ions of $Na^+$ ion. When increasing Ca/Si ratio above 0.8, the $Q^4$ signal of the sample derived from $Na_2SiO_3$ disappeared while that of the sample derived from TEOS disappeared at Ca/Si ratio of 0.6. The basic solution, the silicate ion could be combined to $Q^4$ silicate species via condensation reaction. In addition, the $Na_2SiO_3$ precursor was consist of the $Q^3$ silicate species as a main structure, which could be condensed to $Q^4$ silicate species. So, the sample derived from $Na_2SiO_3$ showed the $Q^4$ signal at Ca/Si ratio higher than those synthesized from TEOS.
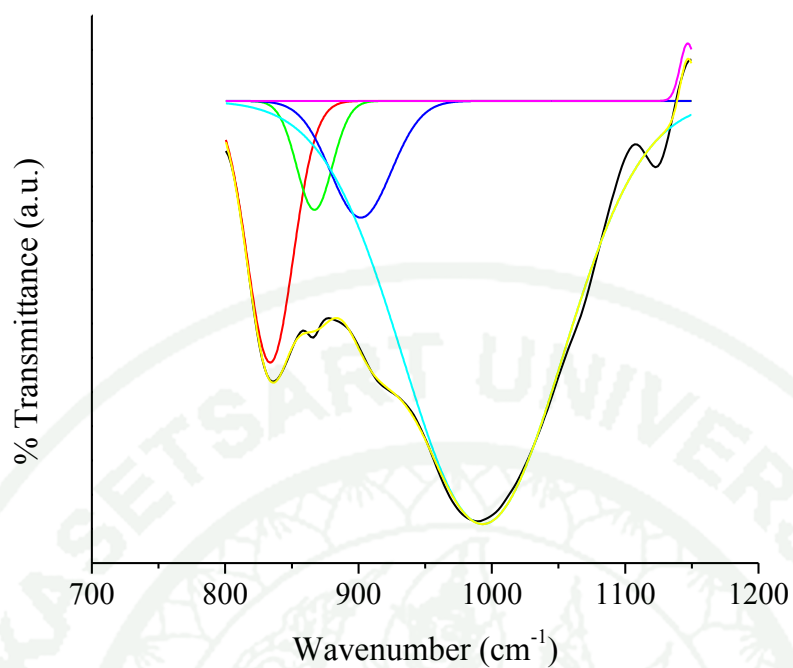
**Figure 26** Deconvoluted spectra of Na$_2$SiO$_3$ precursor



**Figure 27** Deconvoluted spectra of the synthesized C-S-H derived from Na$_2$SiO$_3$
with the Ca/Si ratio at 0.1

**Figure 28**  Deconvoluted spectra of the synthesized C-S-H derived from $Na_2SiO_3$ with the Ca/Si ratio at 0.2



**Figure 29**  Deconvoluted spectra of the synthesized C-S-H derived from $Na_2SiO_3$ with the Ca/Si ratio at 0.4
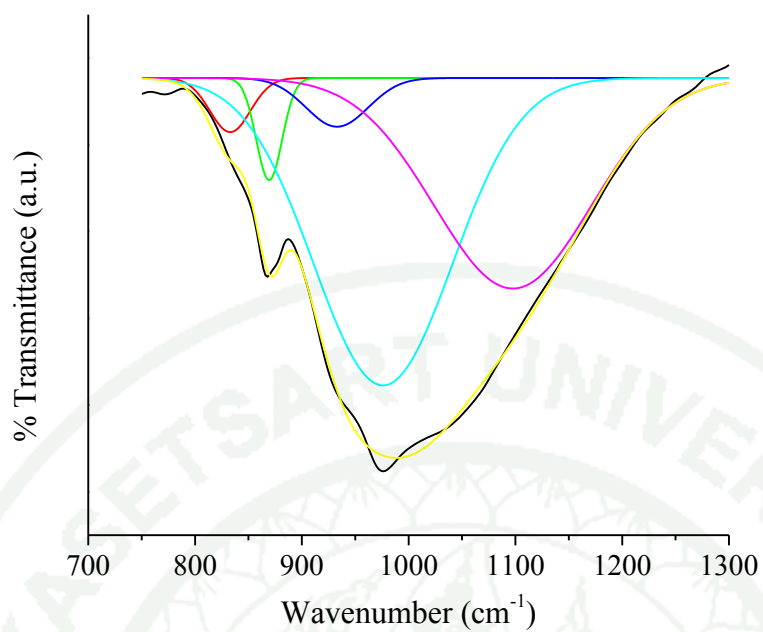
**Figure 30**  Deconvoluted spectra of the synthesized C-S-H derived from $Na_2SiO_3$
with the Ca/Si ratio at 0.5
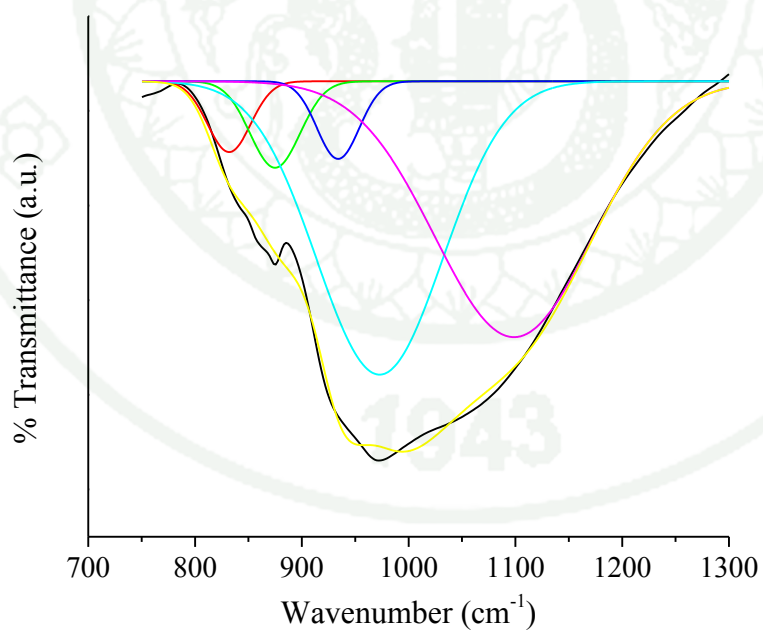


**Figure 31**  Deconvoluted spectra of the synthesized C-S-H derived from $Na_2SiO_3$
with the Ca/Si ratio at 0.6
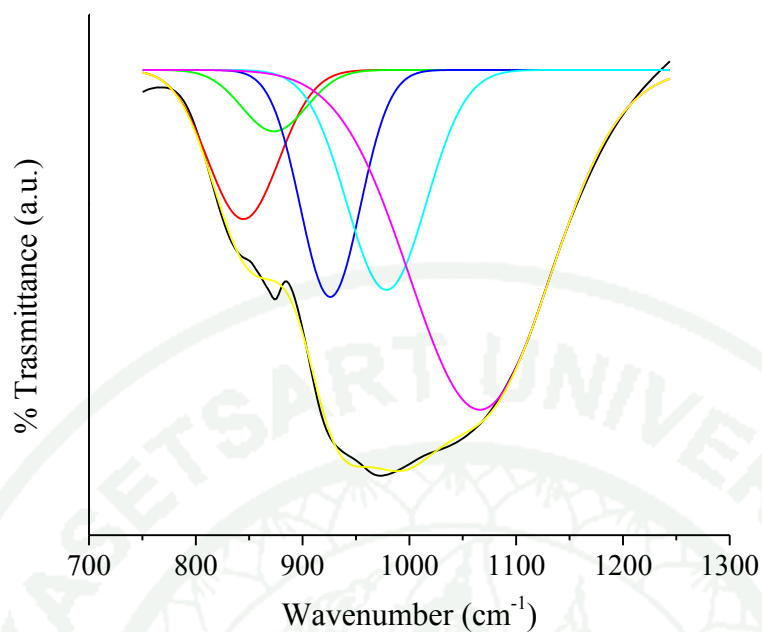
**Figure 32**  Deconvoluted spectra of the synthesized C-S-H derived from $Na_2SiO_3$ with the Ca/Si ratio at 0.8
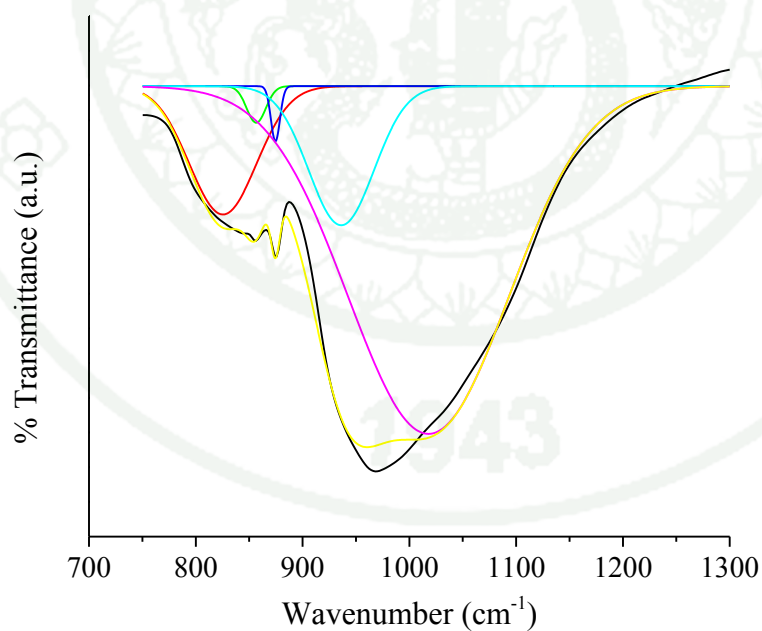


**Figure 33**  Deconvoluted spectra of the synthesized C-S-H derived from $Na_2SiO_3$ with the Ca/Si ratio at 1.0
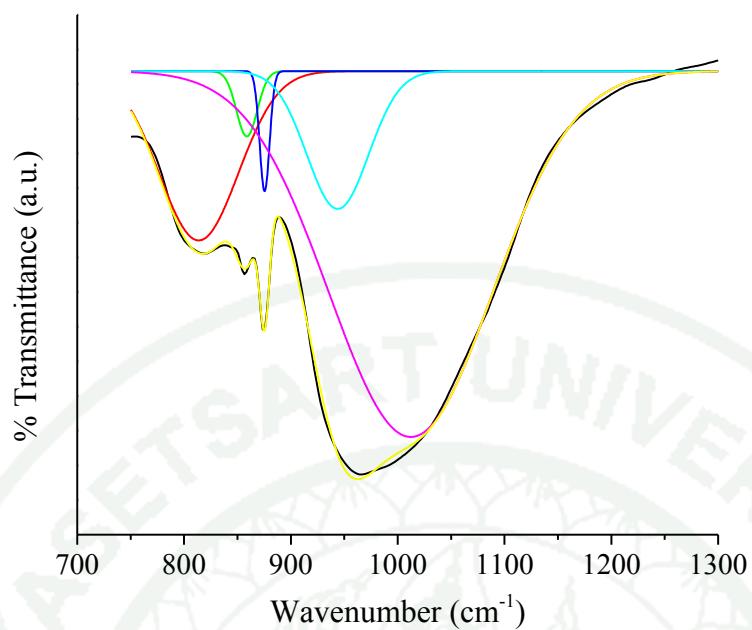
**Figure 34** Deconvoluted spectra of the synthesized C-S-H derived from $Na_2SiO_3$ with the Ca/Si ratio at 1.5
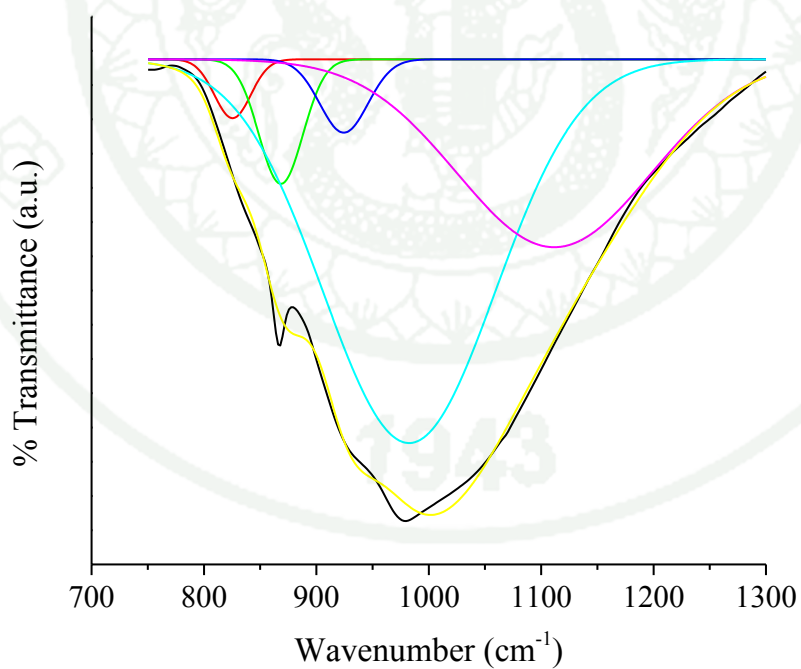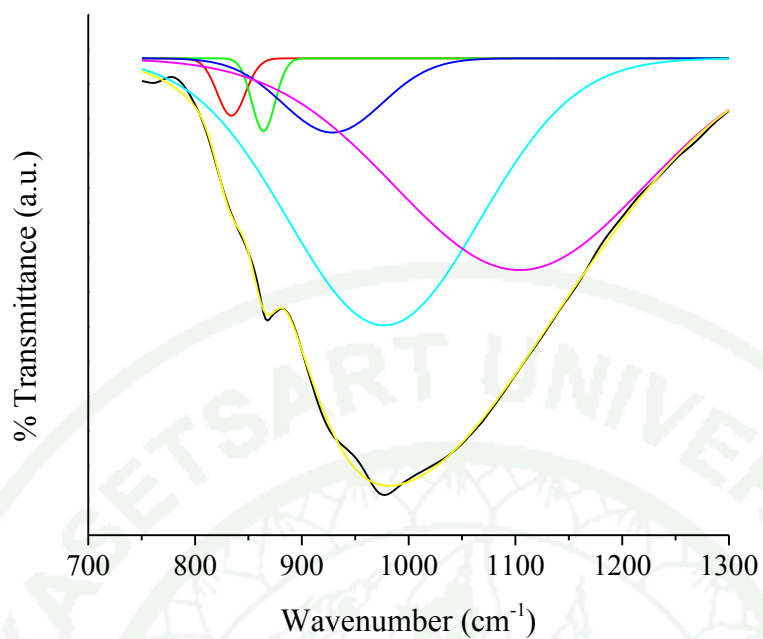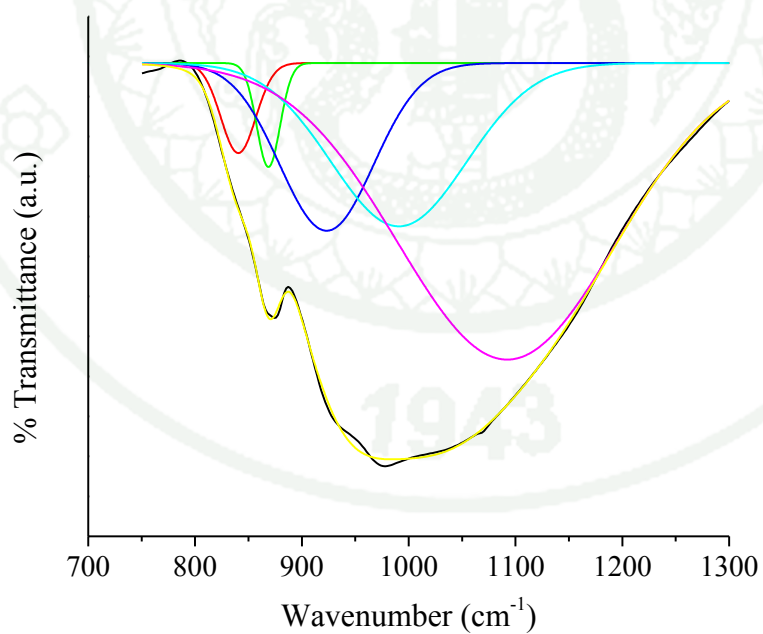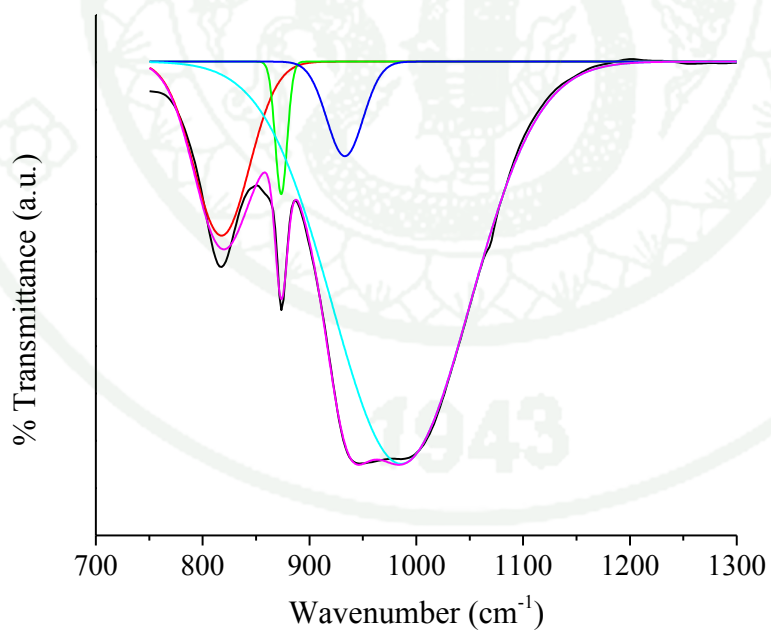


**Figure 35** Deconvoluted spectra of the synthesized C-S-H derived from $Na_2SiO_3$ with the Ca/Si ratio at 2.0

**Table 8** Peak area from the deconvolution FTIR spectra of the synthesized calcium
silicate hydrate (C-S-H) gel (Figure 26-35)

| Ca/Si ratio | Silicate species | | | |
|---|---|---|---|---|
| | $Q^1$ | $Q^2$ | $Q^3$ | $Q^4$ |
| 0.1 | 0.02 | 0.03 | 0.61 | 0.34 |
| 0.2 | 0.01 | 0.07 | 0.45 | 0.47 |
| 0.4 | 0.03 | 0.15 | 0.21 | 0.61 |
| 0.5 | 0.03 | 0.04 | 0.53 | 0.41 |
| 0.6 | 0.04 | 0.04 | 0.44 | 0.48 |
| 0.8 | 0.12 | 0.15 | 0.19 | 0.54 |
| 1.0 | 0.11 | 0.12 | 0.76 | |
| 1.5 | 0.02 | 0.12 | 0.86 | |
| 2.0 | 0.14 | 0.05 | 0.81 | |
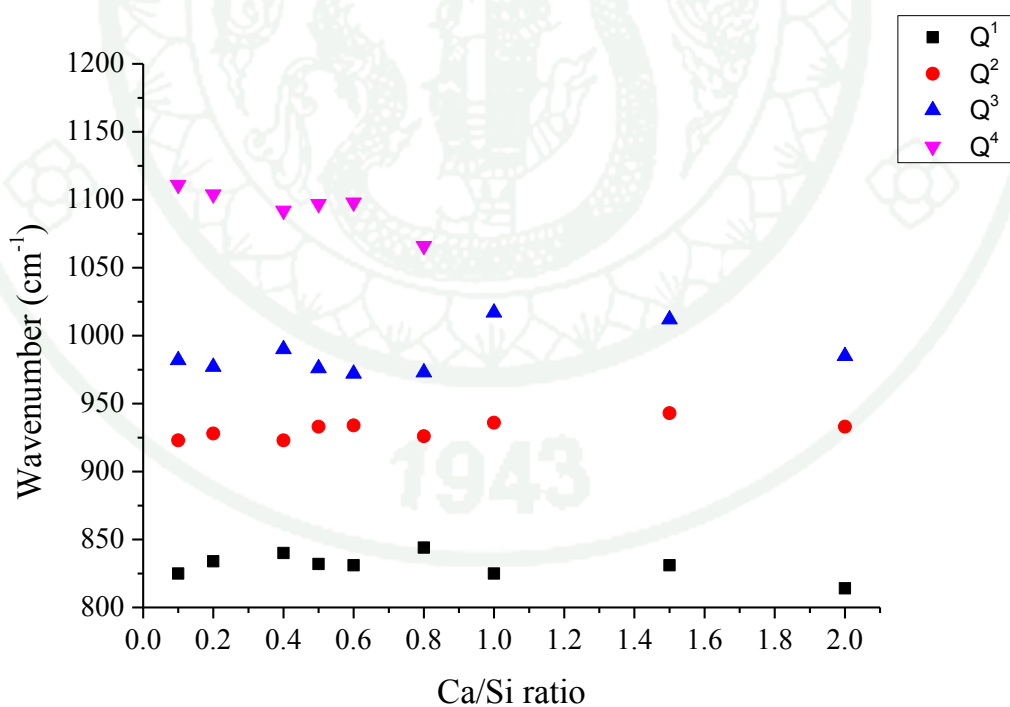


**Figure 36** Composition-dependent shift of deconvoluted components of synthesized
C-S-H sample derived from $Na_2SiO_3$ with initial Ca/Si ratio between 0.1
and 2.0
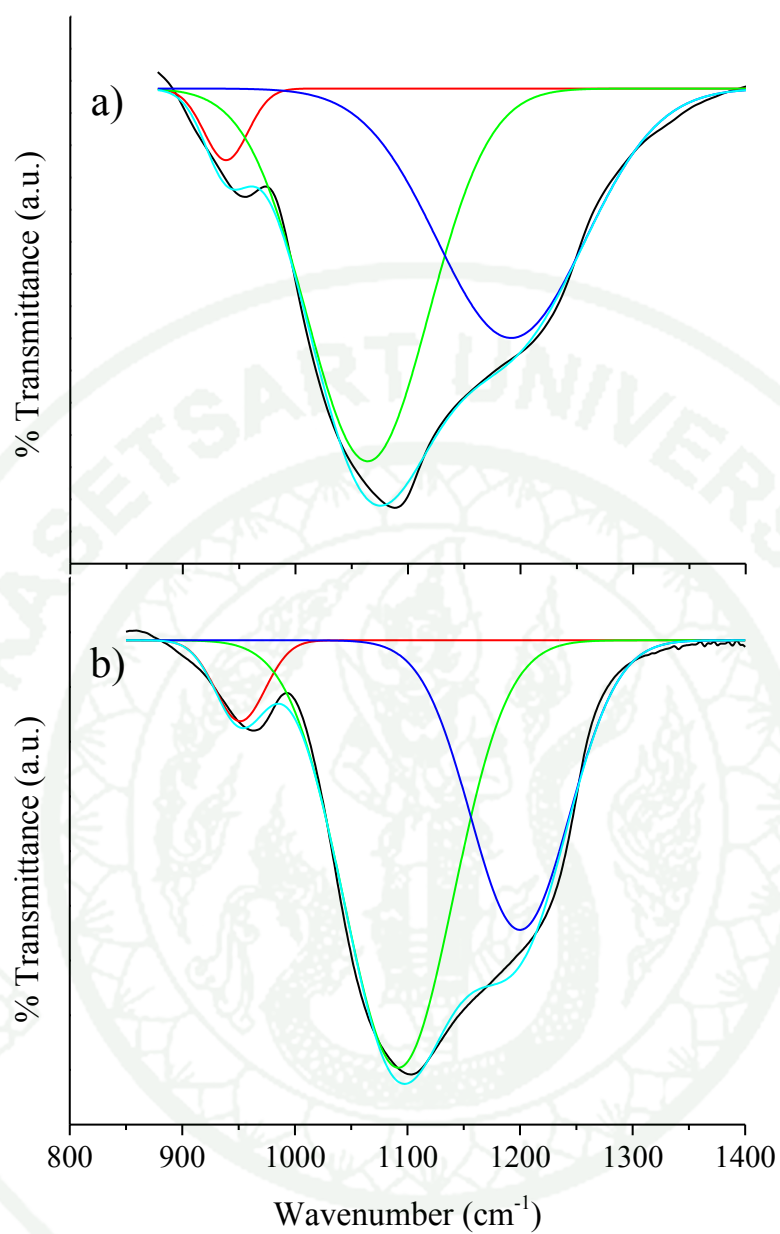
**Figure 37** Deconvoluted spectra of the synthesized silica gel under a) basic and b) acidic condition

The appearance of the strong band between 1400-1500 cm$^{-1}$ and the sharp peak at 875 cm$^{-1}$ could be ascribed to asymmetric stretching and out-of-plane bending of carbonate ($CO_3^{2-}$). The absorption in the range 3300-3600 cm$^{-1}$ was a result of the vibration of the O-H bond, caused by either the $H_2O$ molecules at the surface or the OH in the structure of the C-S-H sample and also corresponded to the absorption peak around 1650 cm$^{-1}$. The sharp peak at 3650 cm$^{-1}$ was assigned to stretching vibration of bulk OH group of calcium hydroxide. XRD patterns exhibited calcium silicate hydrate (C-S-H) peak overlapped with those of $CaCO_3$ and $Ca(OH)_2$ (Figure 38). The peak of C-S-H appeared at 2theta of 29, 32 and 50 degree, which could be clearly seen in the pattern of the synthesized sample with higher Ca/Si ratio. Besides, the XRD results showed the overlap peak of $CaCO_3$ at 23, 29, 36, 39, 43 and 47 degree and $Ca(OH)_2$ at 18, 34, 47 and 51 degree, corresponding to FTIR result.
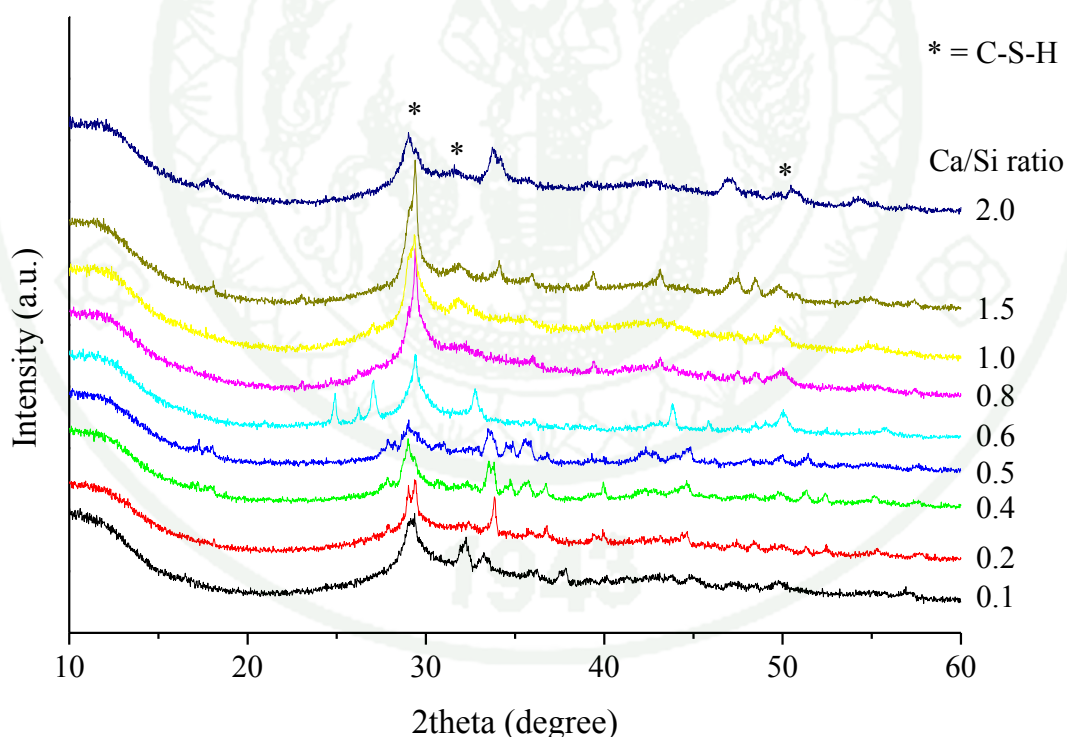


**Figure 38** XRD patterns of C-S-H samples synthesized with initial Ca/Si ratio
between 0.1 and 2.0

## 4. Magnesium silicate hydrate (M-S-H) gel

The magnesium silicate hydrate (M-S-H) samples were synthesized using magnesium hydroxide ($Mg(OH)_2$) instead of calcium hydroxide ($Ca(OH)_2$) in order to study the effects of changing type of cation and increasing Mg/Si ratio on the formation of silicates. The synthesized product appeared as a white gel within 24 hours and changed to white crumbly powder when dried. (Figure 39). The amount of sample will increase when increasing magnesium.



**Figure 39**  Images of the M-S-H synthesized using Mg/Si ratio at a) 0.1 and b) 1.0

Analysis of the synthesized M-S-H using Mg/Si ratio between 0.1 and 1.5 by FTIR technique (Figure 40) showed that were almost similar to the synthesized C-S-H sample. The vibrational spectra of the M-S-H sample showed an asymmetric stretching band of $CO_3^{2-}$ at 1490-1410 cm$^{-1}$ and a bending band of $H_2O$ molecule at 1637 cm$^{-1}$. The stretching vibration of O-H group in $H_2O$ or hydroxyls appeared as a broad band at 3442-3441 cm$^{-1}$. The sharp absorption near 3700 cm$^{-1}$ corresponded to Mg-OH group of $Mg(OH)_2$. The characteristic absorption of silicate at 900-1300 cm$^{-1}$ were analyzed using the deconvolution method. The results were depicted in Figure 41-48 and the peak area of the $Q^n$ silicate species obtained from the deconvoluted spectra were listed

in Table 9. The synthesized M-S-H with Mg/Si ratio below 0.4 exhibited the peak of $Q^3$ as the main structure and also a broad peak of $Q^4$ silicate species around 1060 cm$^{-1}$ and 1190 cm$^{-1}$, respectively. The structure of M-S-H appeared to be similar to the structure of C-S-H sample at Ca/Si ratio below 0.4, which contained high $SiO_2$ content. When increasing Mg/Si ratio, the intensity of the signal of $Q^4$ silicate species decreased and disappeared at Mg/Si ratio above 0.4 (Figure 49). In the same way, The $Q^2$ silicate species appeared in the structure and showed the high intensity when increased the Ma/Si ratio, indicating the decrease of silicate polymerization. The magnesium ion had an effect to the decrease of polymerization by magnesium ions in solution perhaps reducing the influence of the negative charge of the silicate ions formed during the reaction.

The C-S-H and M-S-H samples were synthesized using TEOS as the silicon source but using different cations, $Ca(OH)_2$ for C-S-H and $Mg(OH)_2$ for M-S-H. Both cations could reduce the influence of the negative charge of the silicate ions formed during the reaction, thus reduce the silicate polymerization. The effect was increasingly pronounced as the concentration of the cation increased. At low cation (below 0.2), the samples showed the $Q^3$ as the main structure and also the $Q^4$ silicate species. When increasing amount of cation, the peak area of the signal from $Q^4$ silicate species decreased, but the peak area of the signal from $Q^2$ silicate species increased. The structure of C-S-H and M-S-H were mainly consisted of $Q^2$ silicate species. In the case of C-S-H, the $Q^1$ silicate species appeared in the structure of synthesized sample at Ca/Si ratio above 0.2, but did not show in structure of synthesized M-S-H sample. The $Mg(OH)_2$ has the solubility of 0.00069/100 g. $H_2O$ which is lower than that of $Ca(OH)_2$ (0.160/100 g. $H_2O$). So, the synthesized sample solution of M-S-H had a lower cation than that of C-S-H.
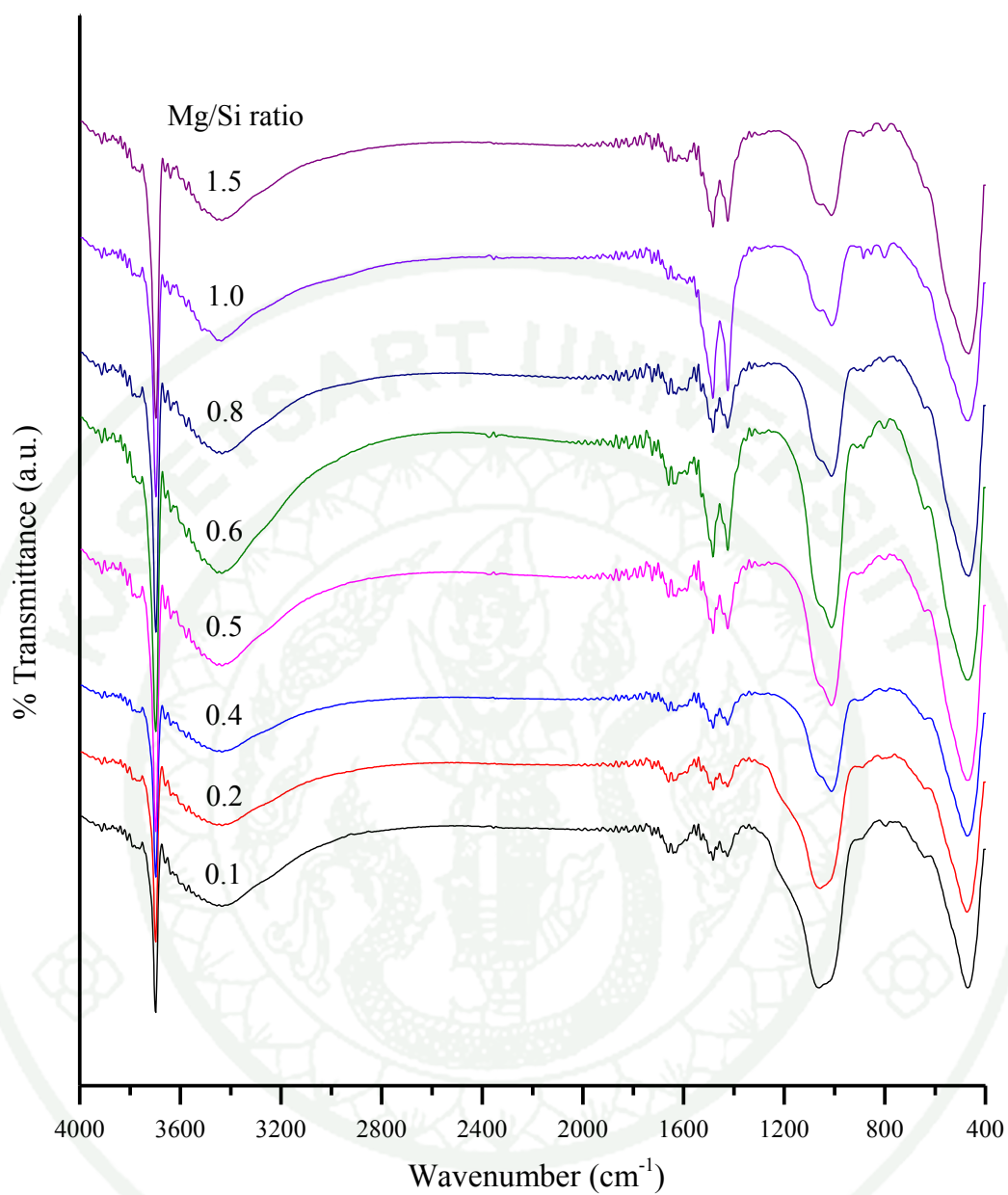
**Figure 40** FTIR spectra of M-S-H samples synthesized with initial Mg/Si ratio
between 0.1 and 1.5
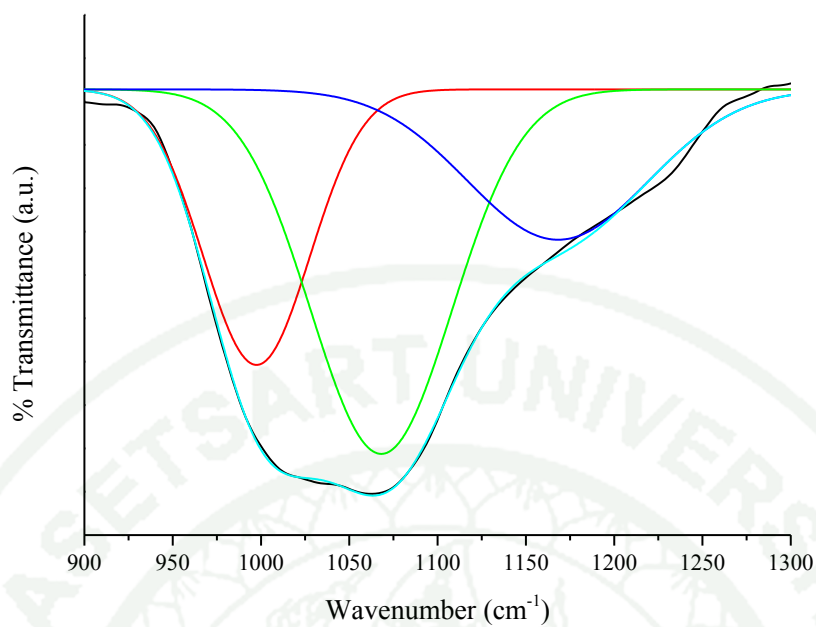
**Figure 41** Deconvoluted spectra of the synthesized M-S-H with the Mg/Si ratio at
0.1
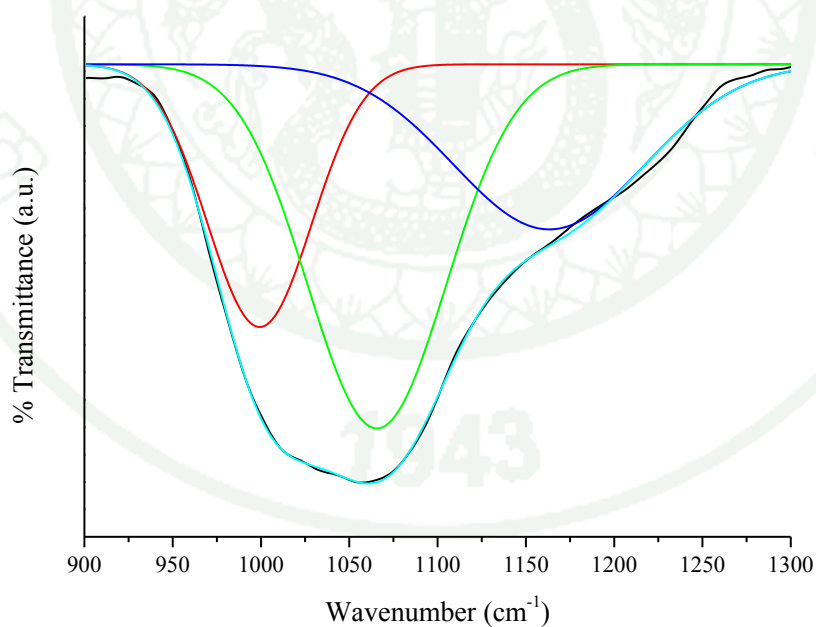


**Figure 42** Deconvoluted spectra of the synthesized M-S-H with the Mg/Si ratio at
0.2
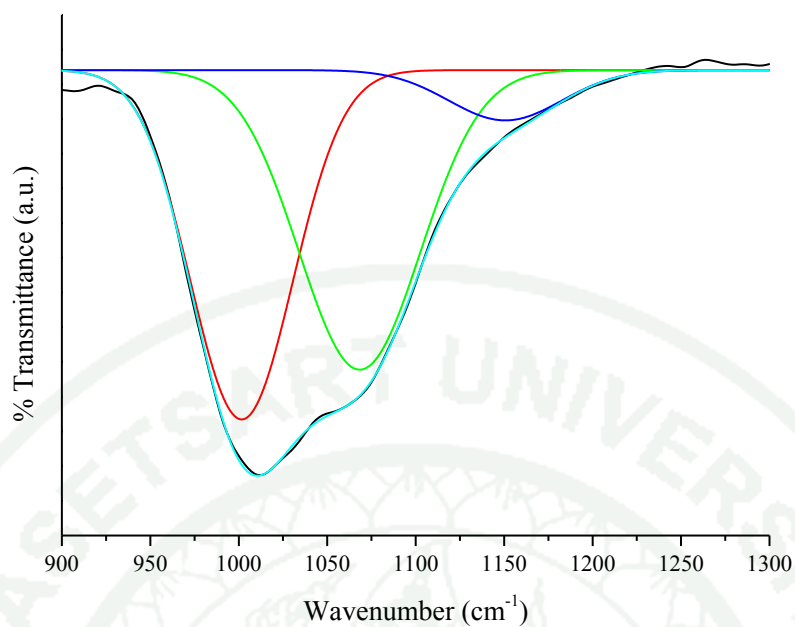
**Figure 43** Deconvoluted spectra of the synthesized M-S-H with the Mg/Si ratio at 0.4
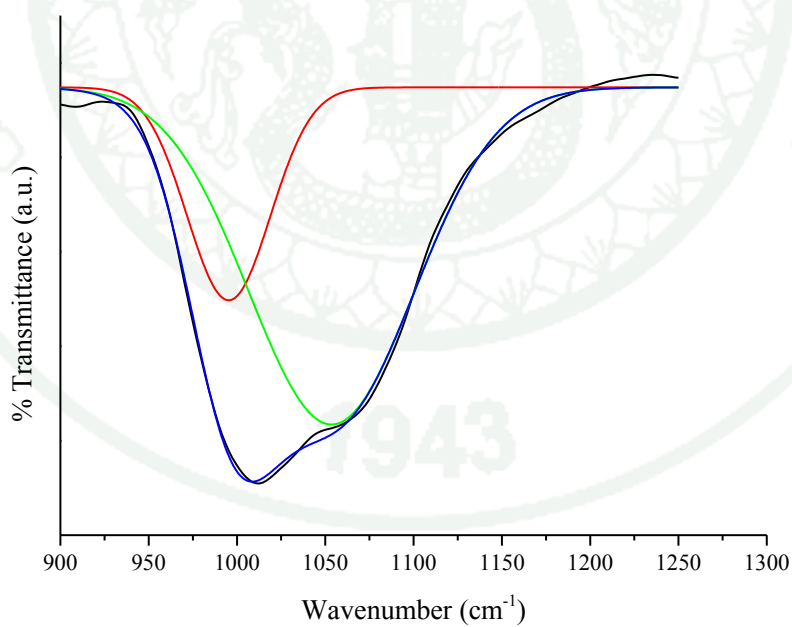


**Figure 44** Deconvoluted spectra of the synthesized M-S-H with the Mg/Si ratio at 0.5
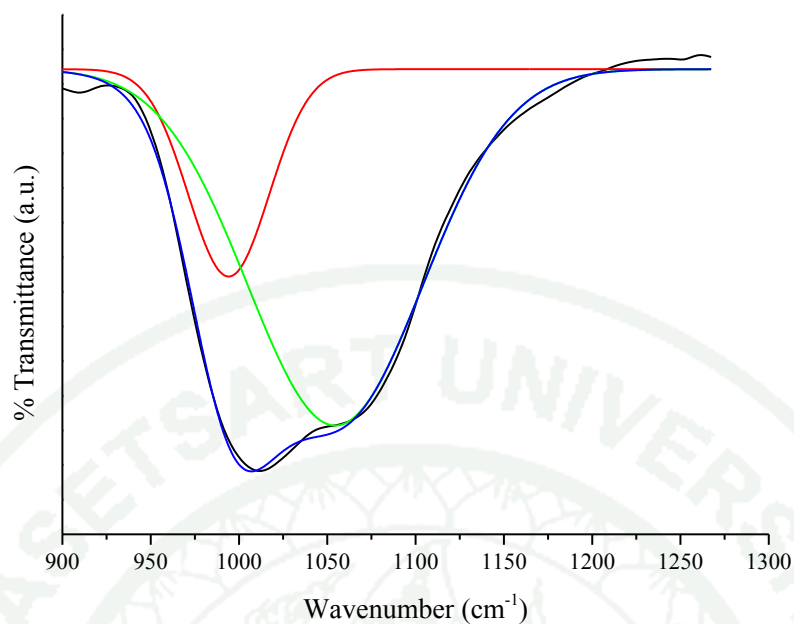
**Figure 45** Deconvoluted spectra of the synthesized M-S-H with the Mg/Si ratio at 0.6
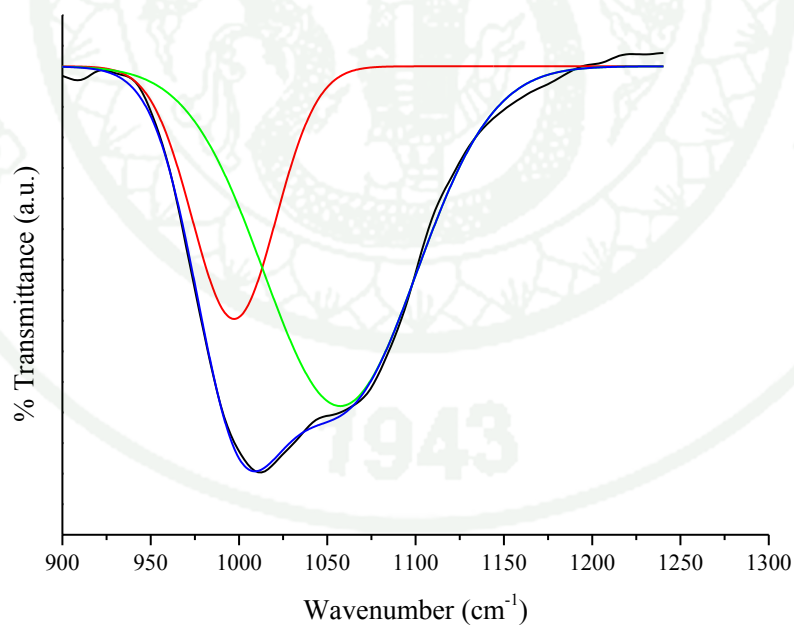


**Figure 46** Deconvoluted spectra of the synthesized M-S-H with the Mg/Si ratio at 0.8
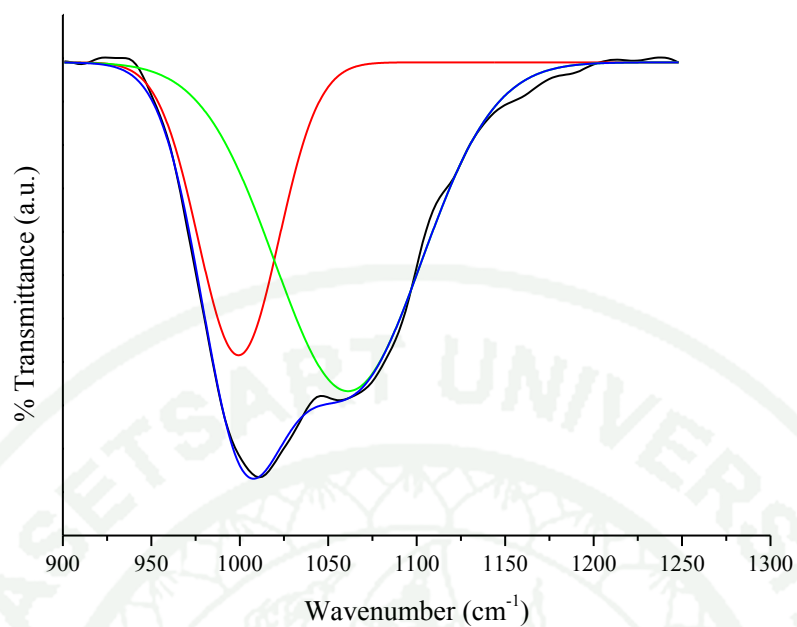
**Figure 47** Deconvoluted spectra of the synthesized M-S-H with the Mg/Si ratio at 1.0
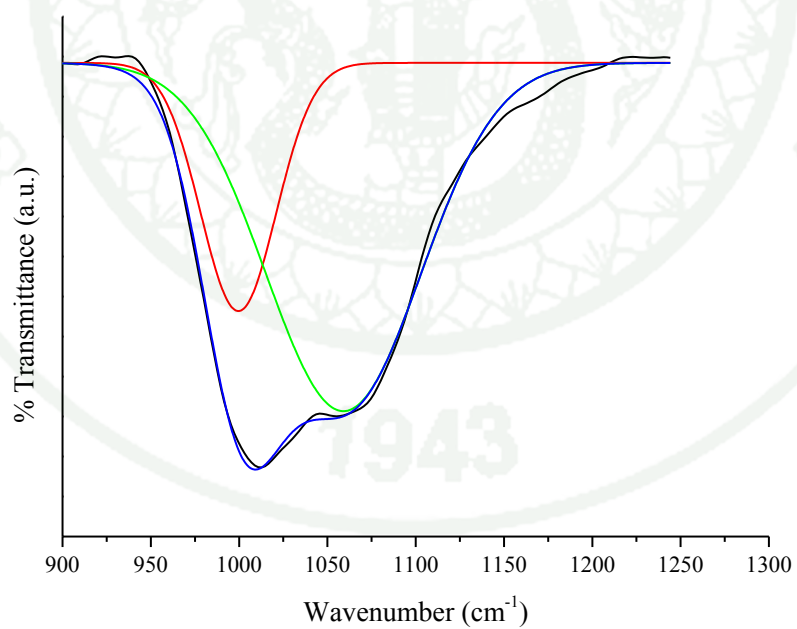


**Figure 48** Deconvoluted spectra of the synthesized M-S-H with the Mg/Si ratio at 1.5

**Table 9** Peak area from the deconvolution FTIR spectra of the synthesized
magnesium silicate hydrate (M-S-H) gel (Figure 41-48)

| Mg/Si ratio | Silicate species | | | |
|---|---|---|---|---|
| | $Q^1$ | $Q^2$ | $Q^3$ | $Q^4$ |
| 0.1 | | 0.30 | 0.45 | 0.24 |
| 0.2 | | 0.25 | 0.46 | 0.28 |
| 0.4 | | 0.46 | 0.47 | 0.07 |
| 0.5 | | 0.24 | 0.76 | |
| 0.6 | | 0.21 | 0.79 | |
| 0.8 | | 0.28 | 0.72 | |
| 1.0 | | 0.31 | 0.69 | |
| 1.5 | | 0.26 | 0.74 | |
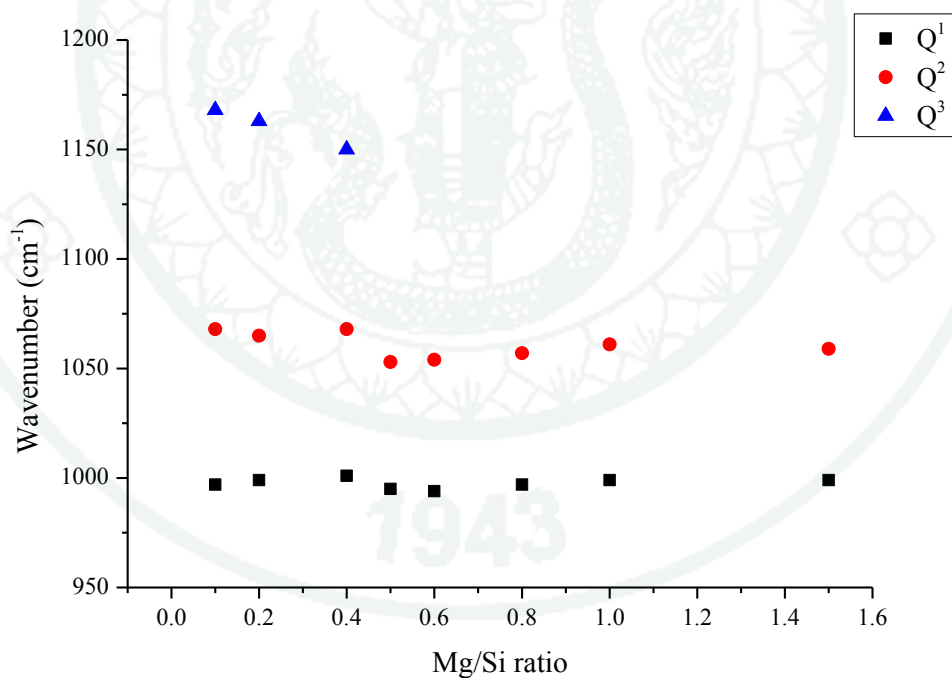


**Figure 49** Composition-dependent shift of the deconvoluted components of the
synthesized M-S-H sample with initial Mg/Si ratio between 0.1 and 1.5

Another sample was synthesized by mixing calcium and magnesium cations. The samples were synthesized using the same method as the C-S-H sample at Ca/Si ratio = 1.0 but replacing some of the calcium with magnesium ((Ca+Mg)/Si = 1.0) by using $Mg(OH)_2$ instead of $Ca(OH)_2$. The amount of magnesium 0, 25, 50 and 100% of the total amount of cation. The sample synthesized using 100% magnesium was the same as M-S-H sample at Mg/Si ratio = 1.0. All synthesized samples appeared as a white gel within 24 hours. Upon air drying, the gels turned white crumbly powder (Figure 50).
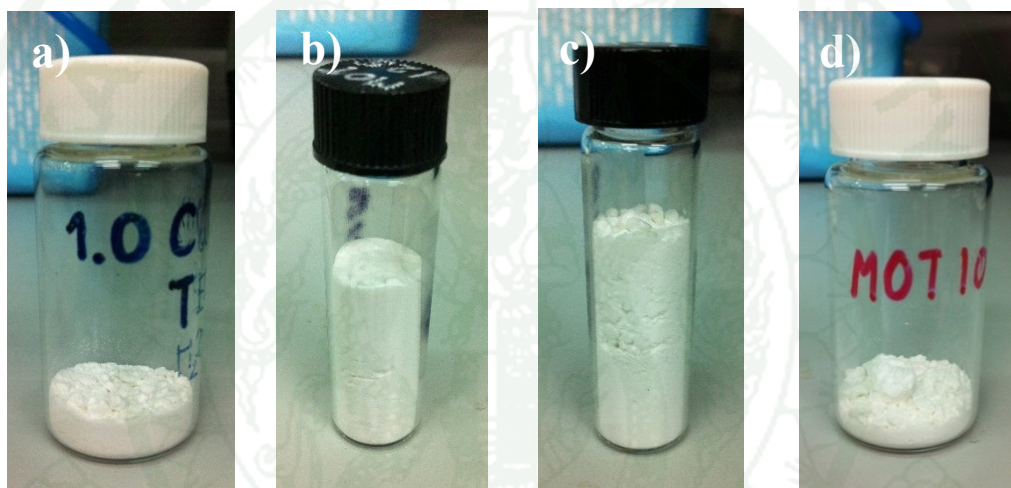


**Figure 50**  Images of samples synthesized with a) 0 (C-S-H), b) 25, c) 50 and b) 100% magnesium (M-S-H)

The synthesized samples were characterized by FTIR technique (Figure 51) and deconvolution method (Figure 52-53). The synthesized C-S-H sample with Ca/Si ratio at 1.0 (0% magnesium) showed the signal of $Q^3$, $Q^2$ and $Q^1$ silicate species at 1065, 956 and 846 cm$^{-1}$, respectively. It suggested that the $Q^2$ silicate species was the main structure. When increasing the magnesium from 0 to 25%, the synthesized samples showed the signals of $Q^4$, $Q^3$ and $Q^2$ silicate species and the $Q^3$ silicate species appeared to be the main structure. The $Q^2$ silicate species in this structure appeared two signals at 960 and 1000 cm$^{-1}$, corresponding the $Q^2$ silicate species of C-S-H and M-S-H, respectively. At magnesium 50%, FTIR spectrum showed the same signal with the

synthesized sample at magnesium 25%. In addition, the peak area of $Q^2$ signal of M-S-H increased when increasing magnesium. The different signals of $Q^2$ silicate species, occurring in the synthesized sample with magnesium showed the result of $Ca^{2+}$ and $Mg^{2+}$ ion reduced the negative charge of the silicate ions. The signal of $Q^4$ silicate species appeared in the sample synthesized with 25 and 50% magnesium because the decreasing of $Ca^{2+}$ is higher than the amount of added $Mg^{2+}$. The peak of carbonate (calcite) at 875 $cm^{-1}$ appeared in all samples, and synthesized sample from magnesium showed the peak of carbonate (aragonite) at 860 $cm^{-1}$. The synthesized M-S-H sample (100% magnesium) showed the signal of $Q^2$ silicate species as a main structure at 999 $cm^{-1}$ and also $Q^3$ silicate species at 1061 $cm^{-1}$. The addition of magnesium into the C-S-H sample indicated that the mixing peak of silicate species between C-S-H and M-S-H sample, and the increase of silicate polymerization (Figure 54).
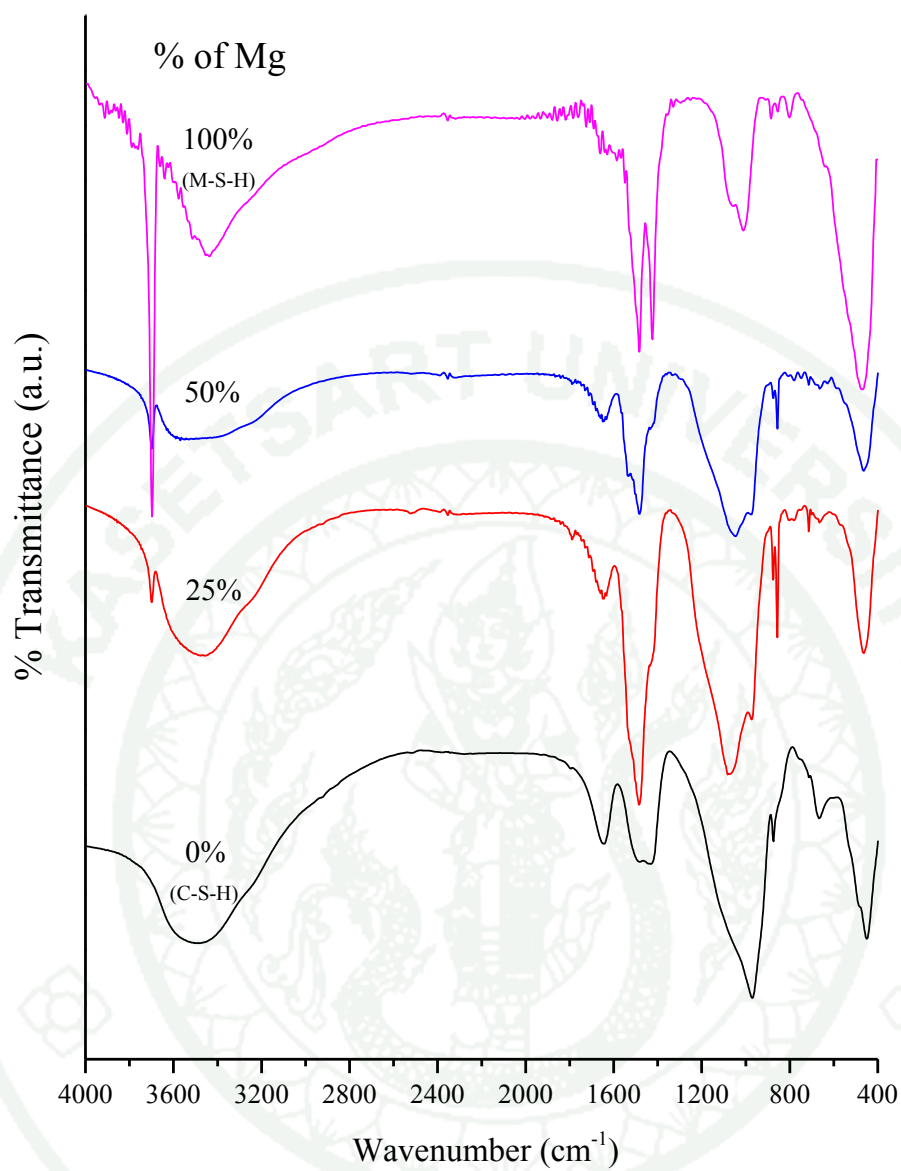
**Figure 51**  FTIR spectra of the C-S-H samples replacing Ca by using Mg from 0 to
100%
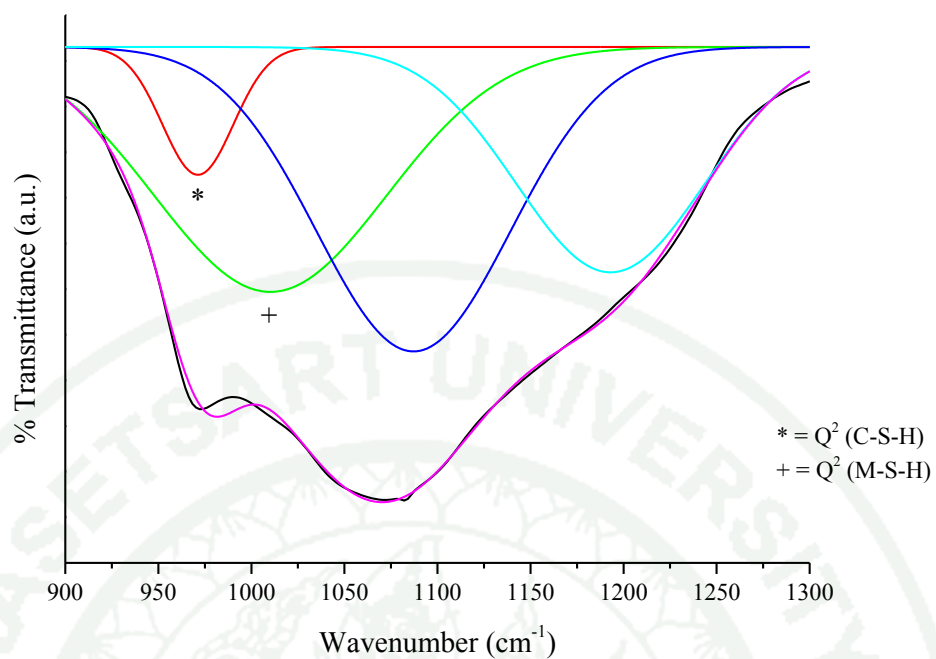
**Figure 52** Deconvoluted spectra of the C-S-H sample replacing Ca by using 25% Mg
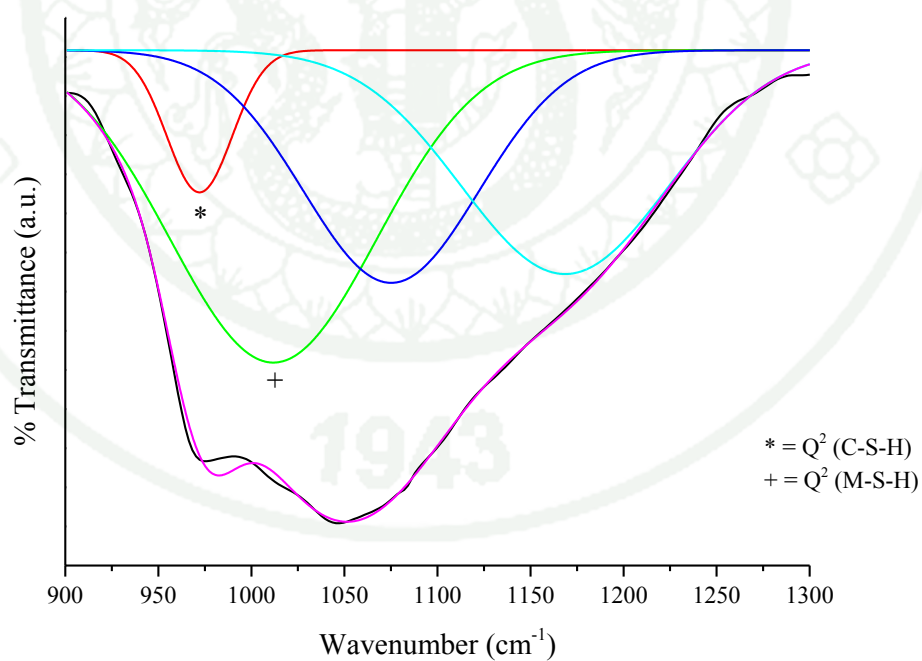


**Figure 53** Deconvoluted spectra of the C-S-H sample replacing Ca by using 50% Mg
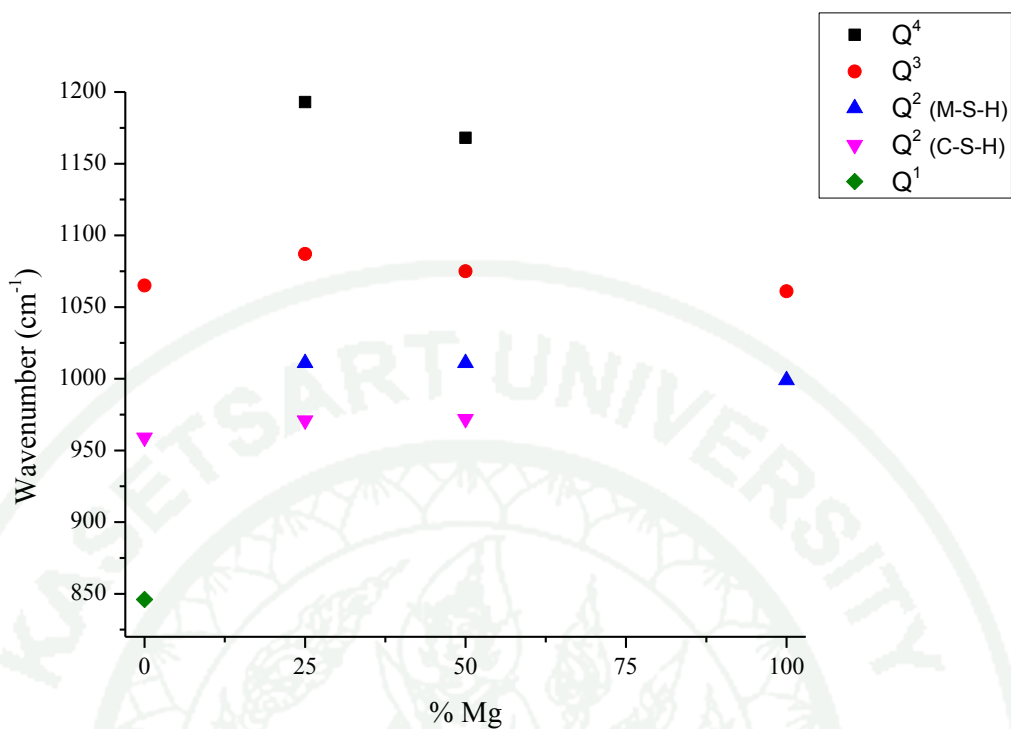
**Figure 54** Composition-dependent shift of the deconvoluted components of the synthesized C-S-H sample by replacing Ca with Mg

The cement powder was mixed with DI water and stirred at 600 rpm at room temperature for 3 hours. The sample was obtained and then dried in an oven at 40˚C for 24 hours (Figure 55). Its structure was characterized by FTIR technique.



**Figure 55** Image of hydrated cement

The spectrum of hydrated cement was shown in figure 56, and the deconvoluted spectrum was showed in figure 57. The asymmetric stretching of $CO_3^{2-}$ appeared in the absorption range at 1400-1500 $cm^{-1}$, and the sharp peak at 875 $cm^{-1}$ was due to the bending of $CO_3^{2-}$ (calcite). The molecular $H_2O$ showed the peak of H-O-H bending at 1640 $cm^{-1}$ and the broad band of O-H stretching at 3000-3670 $cm^{-1}$. In general, the absorption band of the hydrated cement resembled those of the synthesized C-S-H and M-S-H. The spectrum contained a characteristic set of silicate species at 800-1200 $cm^{-1}$, which could be assigned to the asymmetric and symmetric stretching of Si-O bond. The hydrated cement showed the peak of $Q^4$ silicate species at 1150 $cm^{-1}$, corresponding the $Q^4$ silicate species of synthesized sample at low cation. The absorption bands around 1030-1100 $cm^{-1}$ showed multiple peaks and could be assigned to the peak of $Q^3$ silicate species. Those peak corresponded to the $Q^3$ peak of C-S-H and M-S-H sample around 1040 and 1080 $cm^{-1}$, respectively. The peak between 970 and 1030 $cm^{-1}$ was due to Si-O stretching vibration of $Q^2$ silicate species, corresponding to the $Q^2$ silicate species peak of C-S-H and M-S-H sample at 970 and 1000 $cm^{-1}$, respectively.

The FTIR result suggested that the structure of the hydrated cement resembled those of C-S-H and M-S-H samples. The $Q^2$ and $Q^3$ silicate species appeared in the structure of hydrated cement, corresponding the silicate species in the structure of C-S-H sample. Besides, the Ca/Si ratio of C-S-H sample, occurring those peak was in the same range as Richardson (1999) reported. Furthermore, the hydrated cement showed the peak at 1006 $cm^{-1}$, corresponding the $Q^2$ silicate species of M-S-H sample. This corresponded to Brew and Glasser (2005), reporting that the hydrated cement has low magnesium (1-4%) in structure. The results of this project could predict the structure of hydrated cement by comparing with the structure of the synthesized samples. The precursors and additive used to synthesis the cement powder had an effect the structure and properties of cement therefore could not confirm the exact structure of cement. Next project, the other factors such as type of precursor and cations will be study for predict and control the structure and properties of cement.
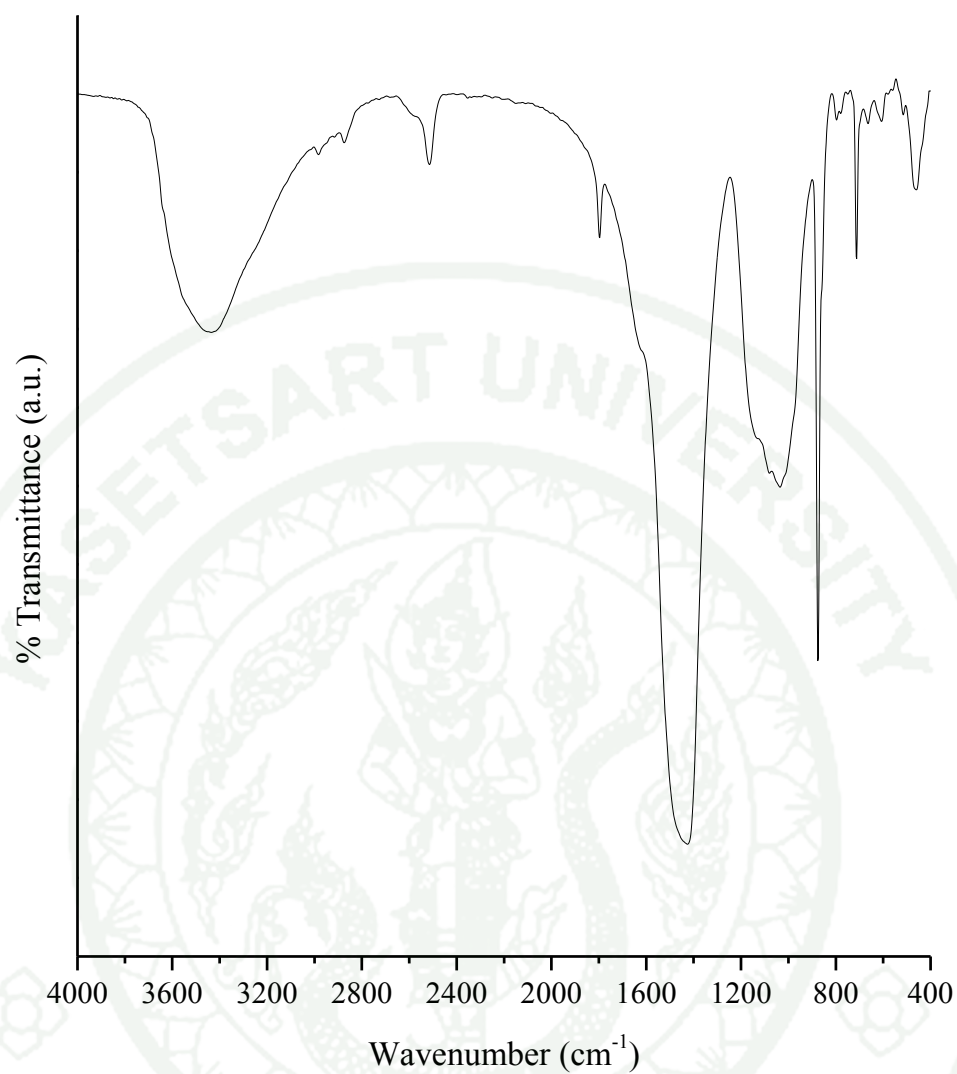
**Figure 56** FTIR spectrum of the hydrated cement
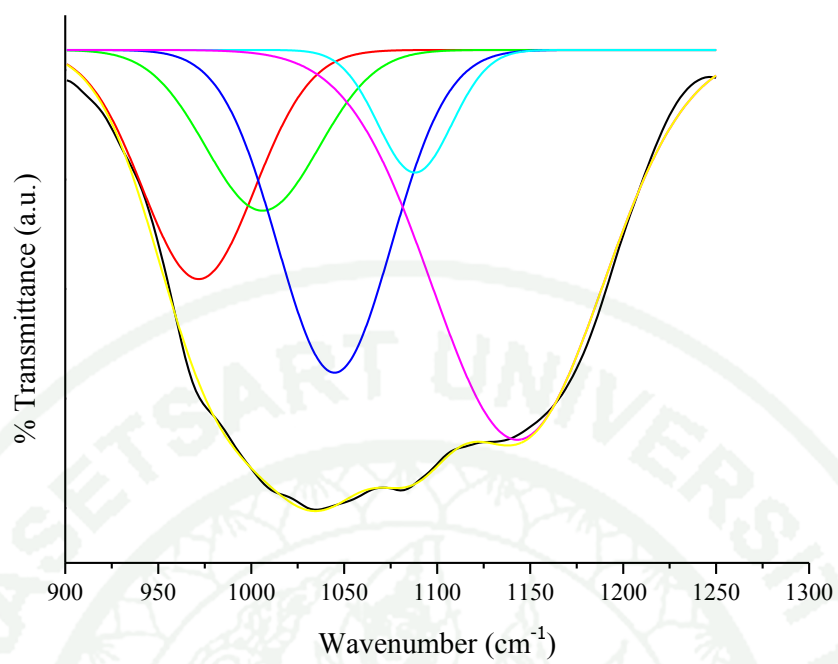
**Figure 57**  Deconvoluted spectra of the hydrated cement

# CONCLUSION

Calcium silicate hydrate (C-S-H) gel was synthesized successfully by using a simple method at room temperature. The influence of precursor and cation species on the structure of sample were investigated. The results from structural characterization using FTIR, XRD and $^{29}$Si MAS NMR suggested that the samples synthesized from TEOS was the C-S-H gel with the possessing different extent of silicate species as $Q^1$, $Q^2$, $Q^3$ and $Q^4$. The $Q^2$, $Q^3$ and $Q^4$ species could be observed at low Ca/Si ratio whereas the $Q^1$ appeared at high Ca/Si ratio. This was due to the effect of calcium ions which had an ability to partially reduce the negative charge of silicate ions. Furthermore, the silicon source also affected the C-S-H structure. The $Q^1$ silicate was observed in the sample derived from $Na_2SiO_3$ at low Ca/Si ratio.

Magnesium silicate hydrate (M-S-H) gel was synthesized in order to study the effect of cation species. The results indicated that magnesium ions showed the same effect as calcium ions on the silicate structure. The structure of M-S-H was similar to C-S-H. However, no $Q^1$ silicate species was observed at high Mg/Si ratio. Furthermore, mixed silicate species between C-S-H and M-S-H were observed in the sample synthesized by using mixed hydroxides of calcium and magnesium. Finally, FTIR results of hydrated cement suggested that the hydrated cement was partially composed of mixed C-S-H and M-S-H. This work presented the results that could be beneficial to understand the formation of silicate species and the structure of hydrated cement.

# LITERATURE CITED

Andersen, M.D., H.J. Jakobsen and J. Skibsted. 2003. Incorporation of aluminum in the calcium silicate hydrate (C-S-H) of hydrated Portland cements: A high-field $^{27}$Al and $^{29}$Si MAS NMR investigation. **Inorganic Chemistry** 42 (7): 2280-2287.

Al-Oweini, R. and H. Ei-Rassy. 2009. Synthesis and characterization by FTIR spectroscopy of silica aerogels prepared using several $Si(OR)_4$ and $R''Si(OR')_3$ precursors. **Journal of Molecular Structure** 919 (1-3): 140-145.

Brew, D.R.M. and F.P. Glasser. Synthesis and characterisation of magnesium silicate hydrate gels. **Cement and Concrete Research** 35 (1): 85-98.

Brinker, C.J. and G.W. Scherer. 1990. Sol-gel Science: The Physics and Chemistry of Sol-gel Processing. Academic Press. New York, USA. 915 pp.

Khouchafa, L., A. Hamoudia and P. Cordierb. 2009. Evidence of depolymerisation of amorphous silica at medium- and short- range order: XANES, NMR and CP-SEM contributions. **Journal of Hazardous Materials** 168 (2-3): 1188-1191.

Kirkpatrick, R.J., J.L. Yarger, P.F. McMillan, P. Yu and X. Cong. 1997. Raman Spectroscopy of C-S-H, Tobermorite, and Jennite. **Advanced Cement Based Materials** 5 (3-4): 93-99.

Lodeiro, I.G. and A.F. Jimenez. 2008. FTIR study of the sol-gel synthesis of cementitious gels: C-S-H and N-A-S-H. **Journal of Sol-Gel Science and Technology** 45 (1): 63-72.

Lodeiro, I.G., A.F. Jimenez, A. Palomo and D.E Macphee. 2010. Effect on fresh C-S-H gels of the simultaneous addition of alkali and aluminium. **Cement and Concrete Research** 40 (1): 27-32.

Lodeiro, I.G., D.E Macphee, A. Palomo and A.F. Jiménez. 2009. Effect of alkalis on fresh C-S-H gels. FTIR analysis. **Cement and Concrete Research** 39 (3): 147-153.

MacLaren, D.C. and M.A. White. 2003. Cement: Its Chemistry and Properties. **Journal of Chemical Education** 80 (6): 623-635.

Meiszterics, A., L. Rosta, H. Peterlik, J. Rohonczy, S. Kubuki, P. Henits and K. Sinko´. 2010. Effect on fresh Gel-Derived Calcium Silicate Systems. **The Journal of Physical Chemistry A** 114 (38): 10403-10411.

Minet, J., S. Abramson, B. Bresson, A. Franceschini, H.V. Dammea and N. Lequeux. 2006. Organic calcium silicate hydrate hybrids: a new approach to cement based nanocomposites. **Journal of Materials Chemistry** 16 (14): 1379-1383.

Pardal, X., I. Pochard and A. Nonat. 2009. Experimental study of Si-Al substitution in calcium-silicate-hydrate (C-S-H) prepared under equilibrium conditions. **Cement and Concrete Research** 39 (8): 637-643.

Dolado, J.S., M. Griebe and J. Hamaekers. 2007. A Molecular Dynamic Study of Cementitious Calcium Silicate Hydrate (C-S-H) Gels. **Journal of the American Ceramics Society** 90 (12): 3938-3942.

Richardson, I.G. 2008. The calcium silicate hydrates. **Cement and Concrete Research** 38 (2): 137-158.

Cong, X. and R.J. Kirkpatrick. 1996. ^{29}Si MAS NMR Study of the Structure of Calcium Silicate Hydrate. **Advanced Cement Based Materials** 3 (3-4): 144-156.

Taylor, H.F.W. 1986. Proposed structure for calcium silicate hydrate gel. **Journal of the American Ceramics Society** 69 (6): 464-467.

Richardson, I.G. 1999. The nature of C-S-H in hardened cements. **Cement and Concrete Research** 29 (8): 1131-1147.

Taylor, H.F.W. and J.W. Howison. 1956. Relationships between calcium silicates and clay minerals. **Clay Minerals** 3: 98-111.

Faucon, P., J.M. Delaye, J. Virlet, J.F. Jacquinot, and F. Adenot. 1997. Study of the structural properties of the C-S-H(I) by molecular dynamics simulation. **Cement and Concrete Research** 27 (10): 1581-1590.

Grutzeck, M., A. Benesi, and B. Fanning. 1989. Silicon-29 magic angle spinning nuclear magnetic resonance study of calcium silicate hydrates. **Journal of the American Ceramic Society** 72 (4): 665-668.

Lodeiro, I.G., A. Fernandez-Jimenez, I. Sobrados, J. Sanz, and A. Palomo. 2012. C-S-H gels: Interpretation of $^{29}$Si MAS-NMR spectra. **Journal of the American Ceramics Society** 95 (4): 1440-1446.

Schneider, J., M.A. Cincotto, and H. Panepucci. 2001. $^{29}$Si and $^{27}$Al high-resolution NMR characterization of calcium silicate hydrate phases in activated blastfurnace slag pastes. **Cement and Concrete Research** 31 (7): 993-1001.

Chen, J.J., J.J. Thomas, H.F.W. Taylor, and H.M. Jennings. 2004. Solubility and structure of calcium silicate hydrate. **Cement and Concrete Research** 34 (9): 1499-1519.

Musić, S., N.F. Vinceković and L. Sekovanić. 2011. Precipitation of amorphous $SiO_2$ particles and their properties. **Brazilian Journal of Chemical Engineering** 28 (1): 89-94.

Zhang, M. and J. Chang. 2010. Surfactant-assisted sonochemical synthesis of hollow calcium silicate hydrate (CSH) microspheres for drug delivery. **Ultrasonics Sonochemistry** 17 (5): 789-792.

Kim, J.J., E.M. Foley and M.M.R. Taha. 2013. Nano-mechanical characterization of synthetic calcium-silicate-hydrate (C-S-H) with varying $CaO/SiO_2$ mixture ratios. **Cement & Concrete Composites** 36: 65-70.

Yu, P., R.J. Kirkpatrick, B. Poe, P.F. McMillan and X. Cong. 1999. Structure of Calcium Silicate Hydrate (C-S-H): Near-, Mid-, and Far-Infrared Spectroscopy. **Journal of the American Ceramic Society** 82 (3): 742-48.

Surachai, T. and C. Arunruwiwat. 2013. Additive-Assisted Synthesis of Silica Gel with Large Pores. **Kasetsart Journal (Natural Science)** 47: 295-301.

Criado, M., A.F. Jimeˊnez and A. Palomo. Alkali activation of fly ash: Effect of the $SiO_2/Na_2O$ ratio Part I: FTIR study. **Microporous and Mesoporous Materials** 106 (1-3): 180-191.

Qomi1, M.J.A., K.J. Krakowiak, M. Bauchy, K.L. Stewart, R. Shahsavari1, D. Jagannathan, D.B. Brommer, A. Baronnet, M.J. Buehler, S. Yip, F.-J Ulm, K.J. Van Vliet and R.J-.M. Pellenq. Combinatorial molecular optimization of cement hydrates. **Nature Communications** 5 (4960).

Mostafa, N.Y., E.A. Kishar and S.A. Abo-El-Enein. FTIR study and cation exchange capacity of $Fe^{3+}$- and $Mg^{2+}$- substituted calcium silicate hydrates. **Journal of Alloys and Compounds** 473 (1–2): 538-542.
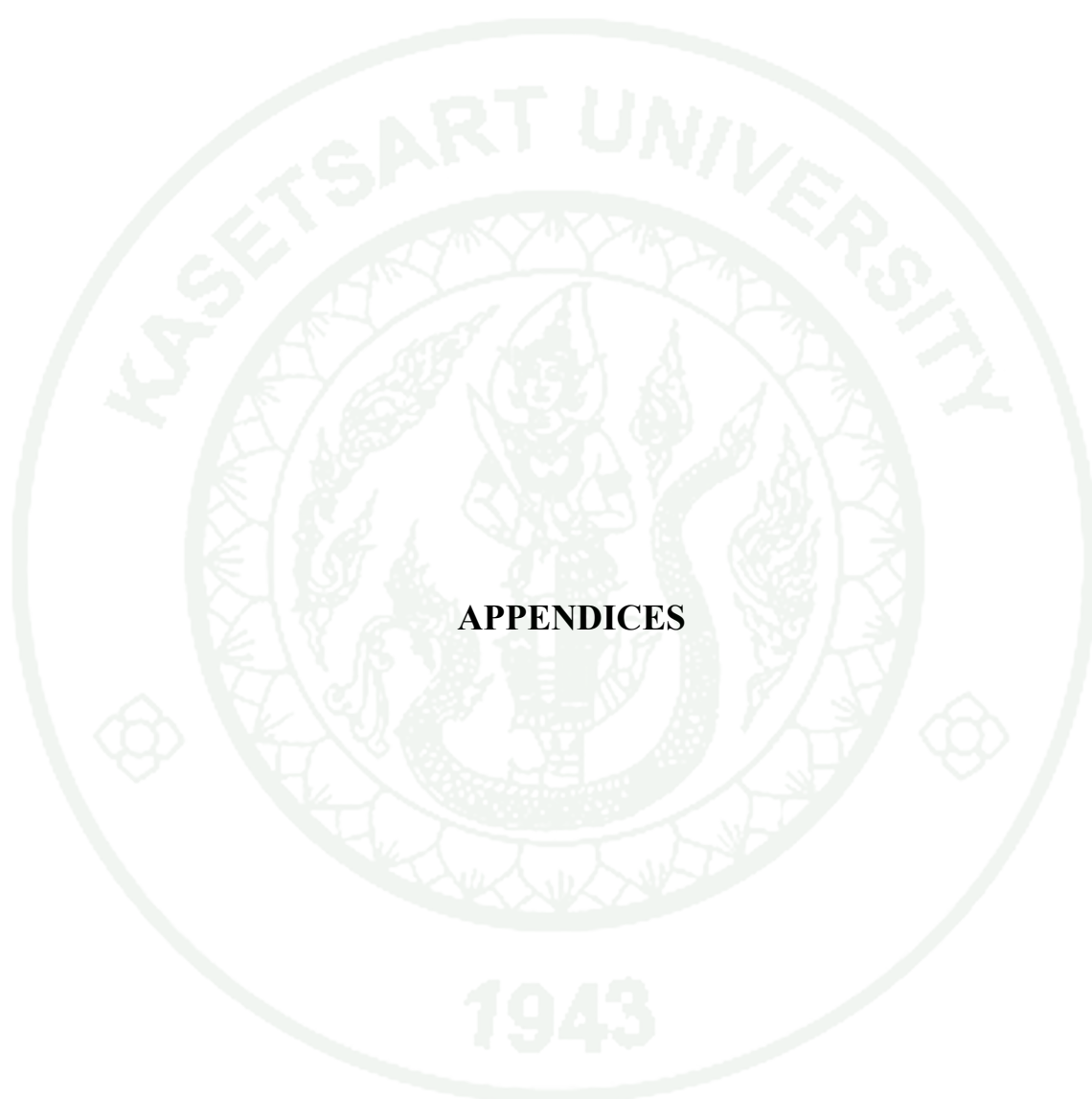
**APPENDICES**
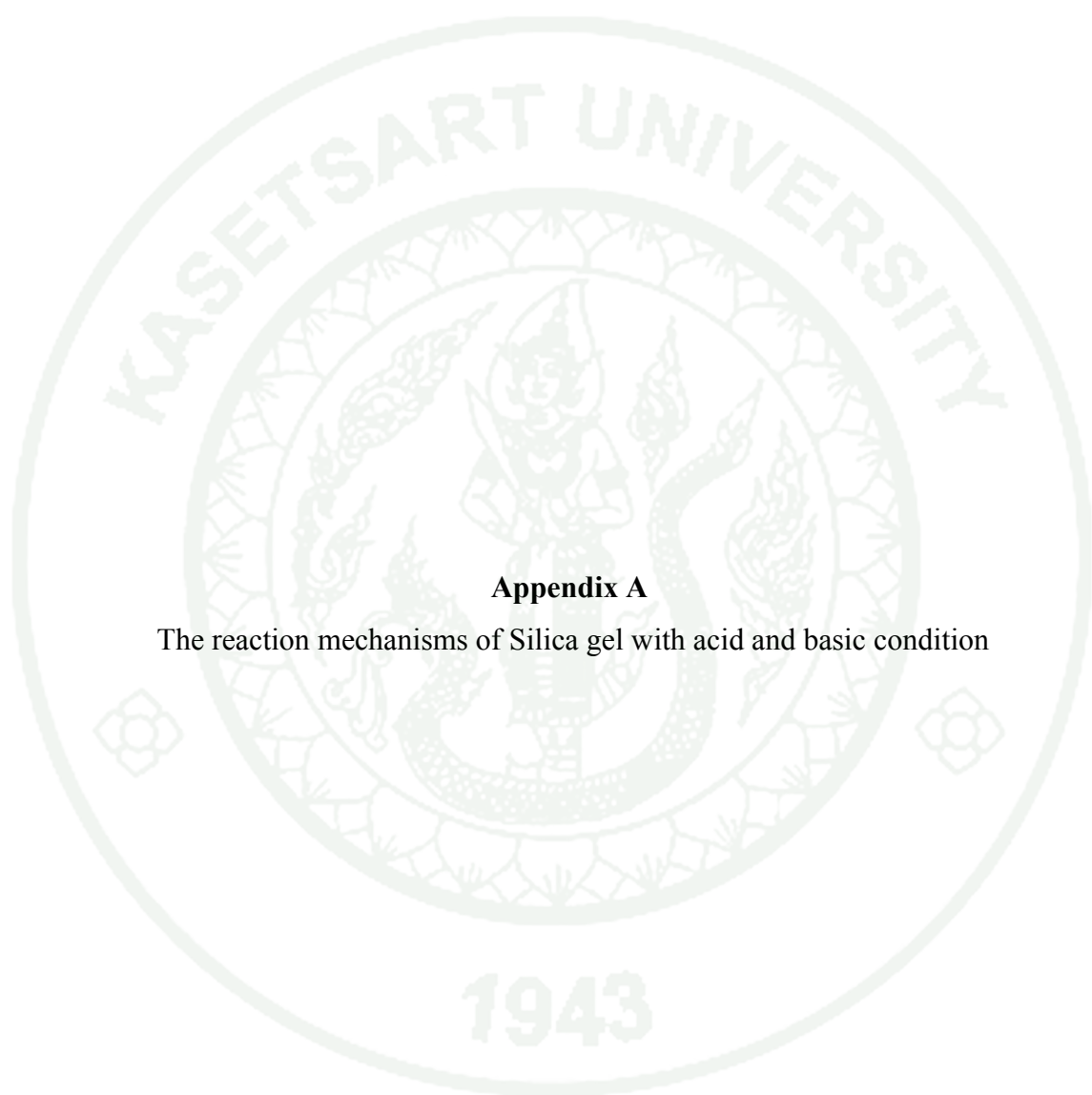
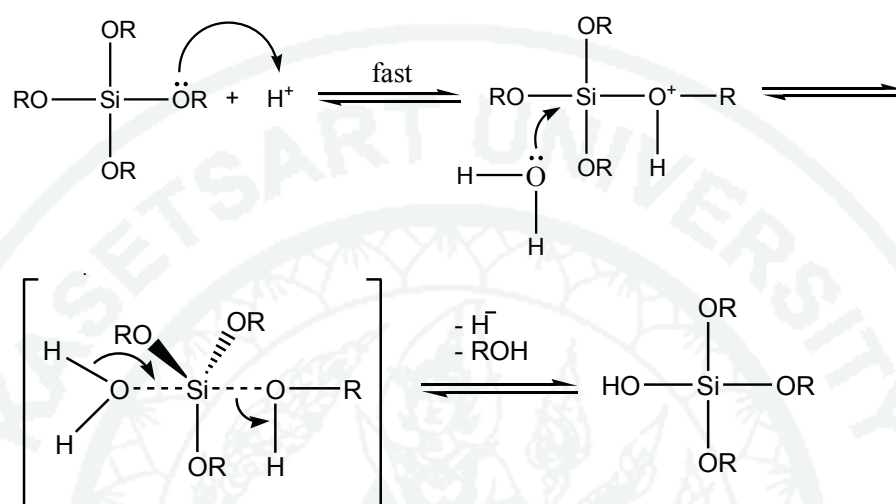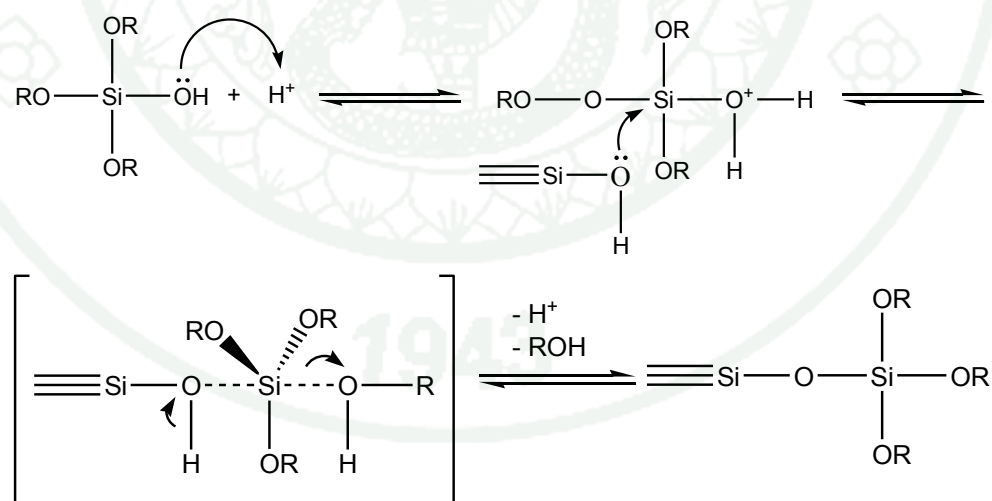**Appendix A**

The reaction mechanisms of Silica gel with acid and basic condition

**Acidic condition**

**Hydrolysis**
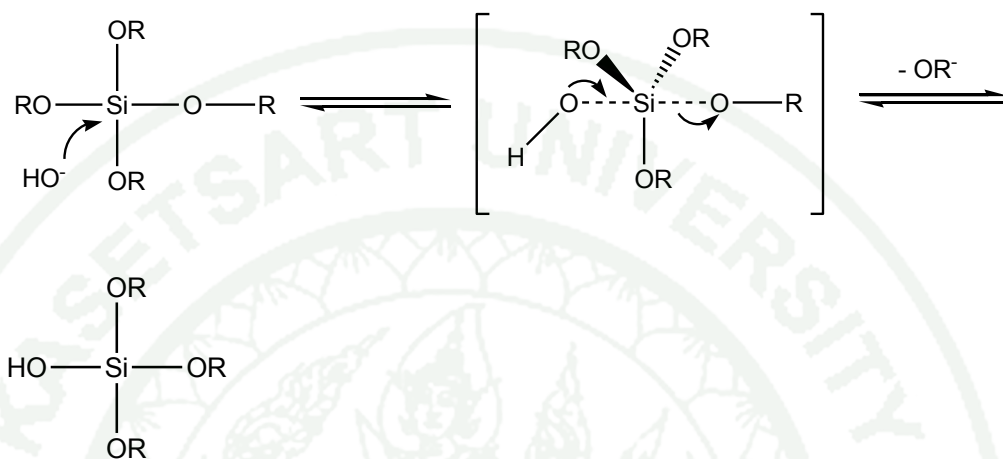


**Condensation**



**Appendix Figure A1** The reaction mechanisms of Silica gel with acid condition

**Basic condition**

**Hydrolysis**



**Condensation**
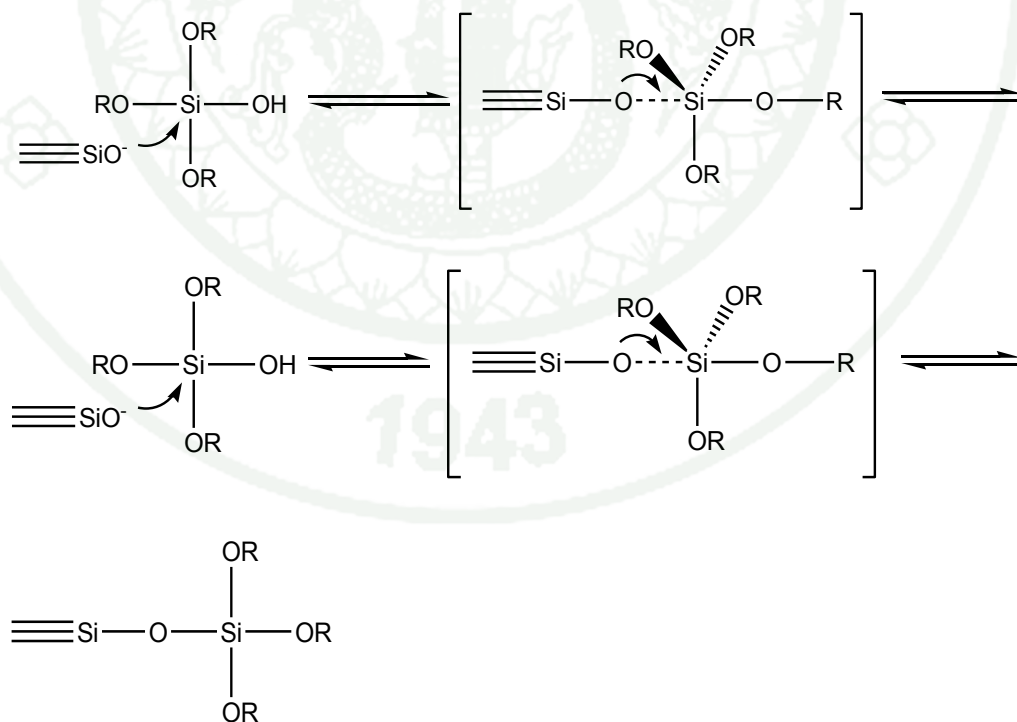


**Appendix Figure A2**  The reaction mechanisms of Silica gel with basic condition
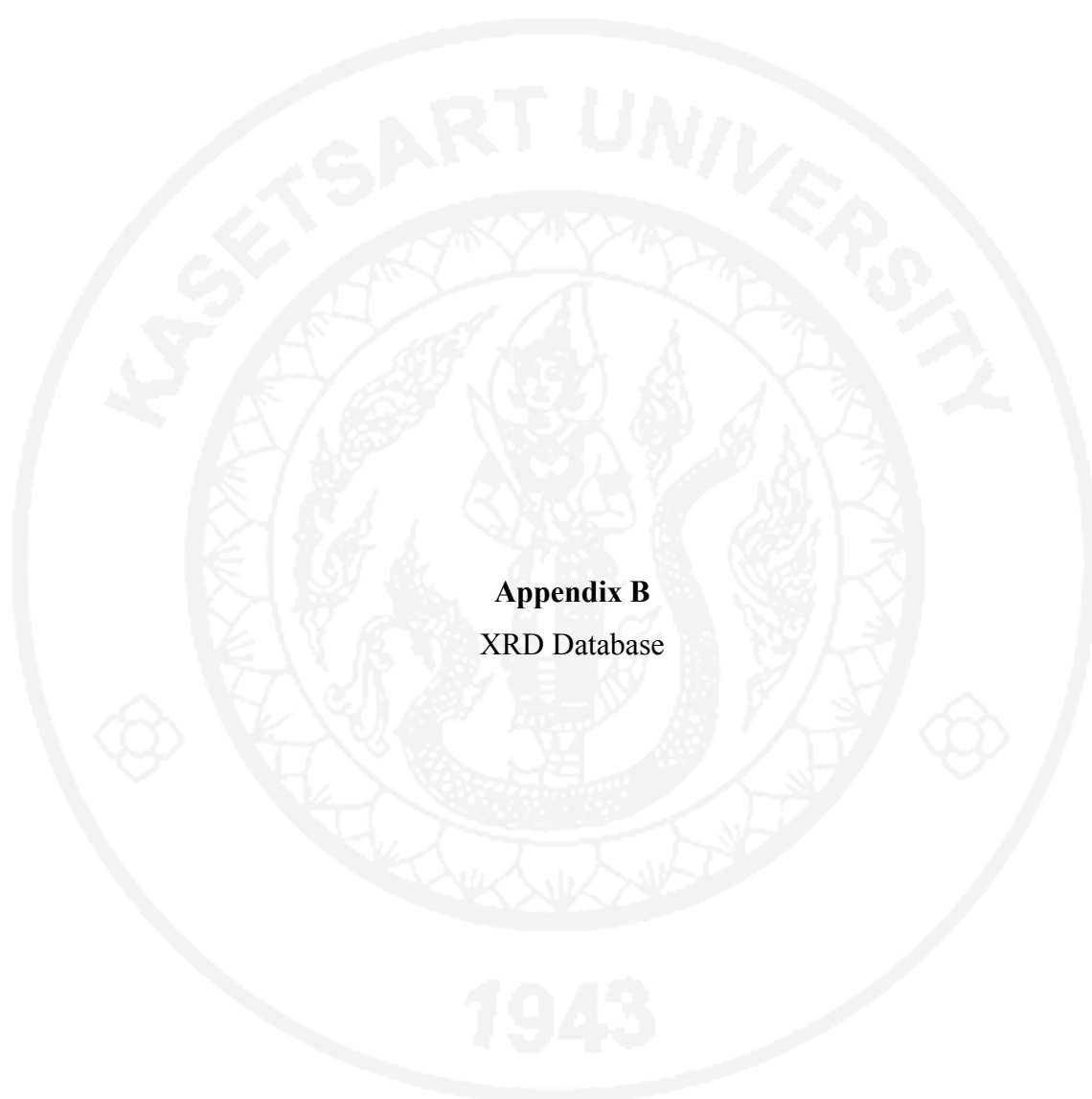
**Appendix B**
XRD Database

## Pattern: PDF 00-044-1481 Radiation: 1.54060 Quality: User modified

| Formula | Ca ( O H )2 |
|---|---|
| Name | Calcium Hydroxide |
| Name (mineral) | Portlandite, syn |
| Name (common) | |

| Lattice: | Hexagonal |
|---|---|
| S.G.: | P-3m1 (164) |

| Mol. weight = | 74.09 |
|---|---|
| Volume [CD] = | 54.87 |
| Dx = | |
| Dm = | |
| I/Icor = | 2.900 |

| a = | 3.58990 | alpha = | |
|---|---|---|---|
| b = | | beta = | |
| c = | 4.91600 | gamma = | |
| a/b = | 1.00000 | Z = | 1 |
| c/b = | 1.36940 | | |

Additional Patterns: Validated by a calculated pattern
Color: White
General Comments: Average relative standard deviation in intensity of the ten strongest reflections for three specimen mounts = 2.2%. Astringent
Sample Source or Locality: Sample obtained from Sigma Chemical Co
Unit Cell Data Source: Powder Diffraction

Primary Reference
Publication: ICDD Grant-in-Aid
Authors: Martin, K., McCarthy, G., North Dakota State University, Fargo, North Dakota, USA.

| Radiation: | CuKα1 | Filter: | M |
|---|---|---|---|
| Wavelength: | 1.54060 | d-spacing: | |
| SS/FOM: | 51.7 (0.0167,29) | | |

| d | 2θ | I | h | k | l |
|---|---|---|---|---|---|
| 4.92200 | 18.008 | 2330 | 0 | 0 | 1 |
| 3.11100 | 28.672 | 874 | 1 | 0 | 0 |
| 2.62700 | 34.102 | 3236 | 1 | 0 | 1 |
| 2.45800 | 36.527 | 32 | 0 | 0 | 2 |
| 1.92710 | 47.121 | 971 | 1 | 0 | 2 |
| 1.79540 | 50.813 | 1003 | 1 | 1 | 0 |
| 1.68640 | 54.358 | 453 | 1 | 1 | 1 |
| 1.63830 | 56.092 | 32 | 0 | 0 | 3 |
| 1.55410 | 59.426 | 97 | 2 | 0 | 0 |
| 1.48200 | 62.634 | 291 | 2 | 0 | 1 |
| 1.44890 | 64.233 | 227 | 1 | 1 | 2 |
| 1.44890 | 64.233 | 227 | 1 | 0 | 3 |
| 1.31350 | 71.811 | 194 | 2 | 0 | 2 |
| 1.22860 | 77.654 | 32 | 0 | 0 | 4 |
| 1.20980 | 79.095 | 65 | 1 | 1 | 3 |
| 1.17520 | 81.910 | 65 | 2 | 1 | 0 |
| 1.14290 | 84.751 | 162 | 2 | 1 | 1 |
| 1.14290 | 84.751 | 162 | 1 | 0 | 4 |
| 1.12740 | 86.197 | 65 | 2 | 0 | 3 |
| 1.06010 | 93.209 | 97 | 2 | 1 | 2 |
| 1.03630 | 96.030 | 65 | 3 | 0 | 0 |
| 1.01390 | 98.882 | 65 | 3 | 0 | 1 |
| 1.01390 | 98.882 | 65 | 1 | 1 | 4 |
| 0.98330 | 103.143 | 32 | 0 | 0 | 5 |
| 0.96410 | 106.066 | 32 | 2 | 0 | 4 |
| 0.95470 | 107.579 | 65 | 2 | 1 | 3 |
| 0.93739 | 110.521 | 32 | 1 | 0 | 5 |
| 0.89740 | 118.268 | 32 | 2 | 2 | 0 |

**Appendix Figure B1** XRD Database of calcium hydroxide (Ca(OH)$_2$)

**Pattern: PDF 01-072-1937    Radiation: 1.54060    Quality: User modified**

| Formula | Ca C O3 |
| Name | Calcium Carbonate |
| Name (mineral) | Calcite |
| Name (common) | |

| Lattice: | Rhombo.H.axes | Mol. weight = | 100.09 |
| S.G.: | R-3c (167) | Volume [CD] = | 368.93 |
| | | Dx = | 2.7 |
| | | Dm = | |
| | | I/Icor = | 3.230 |

| a = | 4.99400 | alpha = | |
| b = | | beta = | |
| c = | 17.08100 | gamma = | |
| a/b = | 1.00000 | Z = | 6 |
| c/b = | 3.42030 | | |

ANX: ABX3
Analysis: C1 Ca1 O3
Formula from original source: Ca (C O3)
ICSD Collection Code: 20179
Wyckoff Sequence: e b a(R3-CH)
Unit Cell Data Source: Single Crystal

Structure
Publication: Dokl. Akad. Nauk SSSR
Detail: volume 245, page 1099 (1979)
Authors: Borodin, V.L., Lutin, V.I., Ilyukhin, V.V., Belov, N.V.
Primary Reference
Publication: Calculated from ICSD using POWD-12++

| Radiation: | CuKα1 | Filter: | Not specified |
| Wavelength: | 1.54060 | d-spacing: | |
| SS/FOM: | 999.9 (0,30) | | |

| d | 2θ | I | h | k | l |
|---|---|---|---|---|---|
| 3.85840 | 23.032 | 1031 | 0 | 1 | 2 |
| 3.03867 | 29.369 | 10837 | 1 | 0 | 4 |
| 2.84683 | 31.398 | 206 | 0 | 0 | 6 |
| 2.49700 | 35.937 | 1562 | 1 | 1 | 0 |
| 2.28676 | 39.370 | 1985 | 1 | 1 | 3 |
| 2.09631 | 43.118 | 1681 | 2 | 0 | 2 |
| 1.92920 | 47.067 | 738 | 0 | 2 | 4 |
| 1.91453 | 47.450 | 2126 | 0 | 1 | 8 |
| 1.87722 | 48.452 | 2224 | 1 | 1 | 6 |
| 1.62724 | 56.508 | 358 | 2 | 1 | 1 |
| 1.60553 | 57.342 | 1020 | 1 | 2 | 2 |
| 1.58889 | 58.007 | 119 | 1 | 0 | 10 |
| 1.52664 | 60.606 | 597 | 2 | 1 | 4 |
| 1.51934 | 60.928 | 260 | 2 | 0 | 8 |
| 1.51098 | 61.301 | 271 | 1 | 1 | 9 |
| 1.47455 | 62.986 | 217 | 1 | 2 | 5 |
| 1.44164 | 64.596 | 673 | 3 | 0 | 0 |
| 1.42342 | 65.525 | 369 | 0 | 0 | 12 |
| 1.35809 | 69.110 | 119 | 2 | 1 | 7 |
| 1.34039 | 70.155 | 217 | 0 | 2 | 10 |
| 1.29795 | 72.808 | 315 | 1 | 2 | 8 |
| 1.28613 | 73.586 | 76 | 3 | 0 | 6 |
| 1.24850 | 76.192 | 130 | 2 | 2 | 0 |
| 1.23660 | 77.059 | 228 | 1 | 1 | 12 |
| 1.21952 | 78.343 | 11 | 2 | 2 | 3 |
| 1.19657 | 80.145 | 11 | 1 | 3 | 1 |
| 1.18786 | 80.854 | 54 | 3 | 1 | 2 |
| 1.18099 | 81.423 | 260 | 2 | 1 | 10 |
| 1.17424 | 81.991 | 33 | 0 | 1 | 14 |
| 1.15482 | 83.677 | 466 | 1 | 3 | 4 |
| 1.14338 | 84.707 | 217 | 2 | 2 | 6 |
| 1.13178 | 85.783 | 11 | 3 | 1 | 5 |
| 1.12583 | 86.346 | 43 | 1 | 2 | 11 |
| 1.07649 | 91.379 | 11 | 1 | 3 | 7 |
| 1.07267 | 91.798 | 11 | 0 | 4 | 2 |
| 1.06261 | 92.923 | 87 | 2 | 0 | 14 |
| 1.04816 | 94.599 | 282 | 4 | 0 | 4 |
| 1.04578 | 94.882 | 325 | 3 | 1 | 8 |
| 1.03645 | 96.011 | 152 | 1 | 1 | 15 |
| 1.03645 | 96.011 | 152 | 1 | 0 | 16 |
| 1.02411 | 97.557 | 22 | 2 | 1 | 13 |
| 1.01289 | 99.016 | 282 | 0 | 3 | 12 |
| 0.99054 | 102.093 | 33 | 3 | 2 | 1 |
| 0.98558 | 102.809 | 130 | 2 | 3 | 2 |
| 0.98164 | 103.387 | 43 | 1 | 3 | 10 |
| 0.97776 | 103.965 | 108 | 1 | 2 | 14 |
| 0.96646 | 105.695 | 108 | 3 | 2 | 4 |
| 0.96460 | 105.987 | 195 | 0 | 4 | 8 |
| 0.95727 | 107.160 | 54 | 0 | 2 | 16 |
| 0.95283 | 107.886 | 22 | 2 | 3 | 5 |
| 0.94928 | 108.478 | 11 | 0 | 0 | 18 |
| 0.94928 | 108.478 | 11 | 3 | 1 | 11 |
| 0.94378 | 109.410 | 195 | 4 | 1 | 0 |
| 0.93861 | 110.307 | 108 | 2 | 2 | 12 |
| 0.93107 | 111.650 | 11 | 4 | 1 | 3 |
| 0.91913 | 113.875 | 22 | 3 | 2 | 7 |
| 0.91358 | 114.952 | 11 | 4 | 0 | 10 |
| 0.89980 | 117.759 | 87 | 2 | 3 | 8 |
| 0.89583 | 118.604 | 87 | 1 | 4 | 6 |
| 0.89383 | 119.037 | 98 | 2 | 1 | 16 |
| 0.88705 | 120.543 | 98 | 1 | 1 | 18 |
| 0.86058 | 127.040 | 22 | 5 | 0 | 2 |
| 0.85796 | 127.748 | 87 | 3 | 2 | 10 |
| 0.85599 | 128.287 | 22 | 1 | 2 | 17 |
| 0.85536 | 128.462 | 33 | 3 | 1 | 14 |
| 0.84777 | 130.631 | 76 | 0 | 5 | 4 |
| 0.84506 | 131.437 | 11 | 4 | 1 | 9 |
| 0.84134 | 132.571 | 11 | 2 | 2 | 15 |
| 0.83787 | 133.664 | 87 | 0 | 1 | 20 |
| 0.83610 | 134.235 | 11 | 2 | 3 | 11 |
| 0.83233 | 135.479 | 43 | 3 | 3 | 0 |
| 0.82358 | 138.556 | 11 | 3 | 3 | 3 |
| 0.81640 | 141.307 | 11 | 2 | 4 | 1 |
| 0.81362 | 142.439 | 87 | 4 | 2 | 2 |
| 0.80920 | 144.324 | 11 | 0 | 4 | 14 |
| 0.80276 | 147.300 | 87 | 2 | 4 | 4 |

| d | 2θ | I | h | k | l |
|---|---|---|---|---|---|
| 0.80276 | 147.300 | 87 | 2 | 4 | 4 |
| 0.80170 | 147.824 | 65 | 5 | 0 | 8 |
| 0.79889 | 149.252 | 87 | 3 | 3 | 6 |

**Appendix Figure B2**   XRD Database of calcium carbonate (CaCO₃)

# CURRICULUM VITAE

**NAME**        : Mr. Chutrin  Arunruviwat

**BIRTH  DATE**   : February 21, 1989

**BIRTH  PLACE** : Nakhonpathom, Thailand

**EDUCATION**    : <u>**YEAR**</u>       <u>**INSTITUTE**</u>     <u>**DEGREE/DIPLOMA**</u>

| YEAR | INSTITUTE | DEGREE/DIPLOMA |
|---|---|---|
| 2007-2010 | Kasetsart Univ. | B.Sc. (Chemistry) |
| 2011-Present | Kasetsart Univ. | M.S. (Chemistry) |

**POSITION/TITLE**  :     Postgraduated student

**WORK PLACE**      :     Faculty of science, Kasetsart University

**SCHOLARSHIP**     :     - The National Research University Project of Thailand (NRU)

        - Kasetsart University Research and DeverlopmentInstitute (KURDI)

**PUBLICATION**     :     S. Thachepan and C. Arunruwiwat, "*Additive-Assisted Synthesis of Silica Gel with Large Pores*", Kasetsart J. (Nat. Sci.), Vol. 47, 2013, pp. 295-301